Digitized by Arya Samaj Foundation Chennai and eGangotri

ma Foundation Chenn

Pure

Seneca

Digitized by Arya Samaj Foundation Chennai and eGangotri

CC-0. In Public Domain. Gurukul Kangri Collection, Haridwar

Digitized by Arya Samaj Foundation Chennai and eGangotri

Stock Verification-2024

CC-0. In Public Domain. Gurukul Kangri Collection, Haridwar

Digitized by Arya Samaj Foundation Chennai and eGangotri

CC-0. In Public Domain. Gurukul Kangri Collection, Haridwar

Digitized by Arya Samaj Foundation Chennai and eGangotri

# BULLETIN OF PURE AND APPLIED SCIENCES

ISSN-0970-6569

(An International Research Journal of Physics)

SEC. - D
PHYSICS

Volume - 28-D
No.1 (Jan. - June)
2009

Prof. Durga P. Ojha
Convenor, Editorial Board

CC-0. In Public Domain. Gurukul Kangri Collection, Haridwar

www.bpas.in

Digitized by Arya Samaj Foundation Chennai and eGangotri

CC-0. In Public Domain. Gurukul Kangri Collection, Haridwar

13179

Digitized by Arya Samaj Foundation Chennai and eGangotri


# Bulletin of Pure and Applied Sciences

Vol.28D- Physics (No.1) January- June 2009


Contents


**Satyendra Nath Tiwari and Sachchida Nand Shukla**
QUALITATIVE ANALYSIS OF SMALL SIGNAL MODIFIED DARLINGTON PAIR AND TRIPLE DARLINGTON AMPLIFIERS. 1-11

**Dhirendra Kumar, Prakash Nayak and Lalan jha**
THEORETICAL STUDY OF MULTI-BAND MICROSTRIP ANTENNA. 13-19

**Kumar Balwant Singh**
STUDY OF VARIATION OF SELECTIVITY OF MICROSTRIPLINE WITH STRIP GEOMETRY AND OPERATING FREQUENCY. 21-28

**G.Wellington Fernando and S. Alfred Cecil Raj**
PREPARATION AND CHARACTERISATION OF LITHIUM DOPED AND NICKEL – DOPED $Co_3O_4$ FILMS. 29-41

**Madan jee, Manish Kumar Bhatt, Sunil Kumar Mishra, Sanjiv Kumar, Vikas Kumar, and Ashok Kumar Singh**
SCATTERING OF ELECTRONS BY EQUILIBRIUM PHONONS IN A TWO SUBBAND QUASI TWO DIMENSIONAL ELECTRON GAS IN A QUANTISING MAGNETIC FIELD. 43-46

**Ashok Kumar Singh, Janardan Choudhari, Ashok Kumar, Dilip Kumar Verma, and Manoj Ranjan**
THE INFLUENCE OF TEMPERATURE AND THE FILLING OF STATES ON THE CONDUCTIVITY OF A VARIABLE RANGE HOPPING SYSTEM WITH AN EXPONENTIAL DISTRIBUTION OF LOCALIZED STATE ENERGIES. 47-51

**S. Thangapandian, V. Arumugam and A.N. Kannappan**
MOLECULAR INTERACTION IN TERNARY LIQUID MIXTURES - AN ULTRASONIC STUDY. 53-58

**Ketki A. Mistry, I.B.Patel and Priyanka Rustagi**
GROWTH STUDY OF NaCl,NaCl+NaBr AND NaBr CRYSTALS GROWN BY SOLUTION EVAPORATION METHOD AT AMBIENT TEMPERATURE. 59-65

**C. Y. Lo**
PRECESSION FORMULAS FOR GRAVITY PROBE-B AND ITS COMPLEMENTARY EXPERIMENTS OF LOCAL LIGHT SPEEDS . 67-85


Central Library
Gurukul Kangri University
Haridwar-249404 (U.A.)


*Address for communication :*
**Dr. A. K. Sharma , *Editor –in-chief* , 387-RPS- DDA Flats, Mansarover Park, Post Box No.-9043,Shahdara, Delhi- 110032, India (Phone : 011-22138726, Mobile-9212200909**

Emails : editorbulletin@yahoo.co.in , ajaykumarsharma1955@yahoo.com ,bpaseditor@gmail.com ,ajay_research@hotmail.com , ajay_shrm@yahoo.com , editordrsharma@rediffmail.com



ISSN-0970-6569 Website : www.bpas.in


CC-0. In Public Domain. Gurukul Kangri Collection, Haridwar

Digitized by Arya Samaj Foundation Chennai and eGangotri

ISSN-0970-6559

# BULLETIN OF PURE AND APPLIED SCIENCES

Volume-28D(Physics) No.1(JANUARY – JUNE) 2009

## EDITORIAL BOARD

Convenor(Hon.) Prof. Dr. Durga P. Ojha ,Postgraduate Department of Physics
Andhra Loyala College (Autonomous),Vjyajwada (AP)-520008 ,India

### Members

Prof. R.N.P.Choudhary, Dept. of Physics, Indian Institute of Technology,Kharagpur-721303
Prof. S.H.Pawar, Dept. of Physics, Shivaji University, Kolhapur-416004
Prof. K.L.Alawadhi, Dept. of Physics, Punjabi University,Patiala-147002
Prof. Lalan Jha ,Dept. of Physics, L.N.Mithila University, Darbhanga-846004
Prof. D.L.Sharma, Dept. of Physics, Punjab Ag. University, Ludhiana-141004
Prof. S.C.Mehrotra, Dept. of Physics, Dr.B.A.M. University,Aurangabad-431004
Prof. T.V.Ramakrishna Rao, Dept. of Physics, S.K.University, Anantapur-515003
Prof. S. Umapathy,School of Physics, Madurai Kamaraj University, Madurai-625021
Prof. S.K.Narayandass, Dept. of Physics, Bharathiar University,Coimbatorte-641046
Prof. V.R.K.Murthy,Dept. of Physics,Indian Institute of Technology,Chennai-600036
Prof. T.Sankarappa,Dept. of Physics, Gulbarga University, Gulbarga-585106
Prof. Z.H.Zaidi, Former Vice chancellor,M.J.P.Rohilkhand University, Bareilly-243006
Prof. B.Hanumanaiah,Dept. of Physics,Indian Institute of Technology,Bangalore-560012
Prof. A.K.Deb,Dept. of Physics, University of Chittagong,Chittagong-4331, Bangladesh
Prof .Sarabettin EREL,Dept. of Physics, Fac. of Sc.,University of Kirikale,71450 Kirikkale, Turkey
Prof. Florentin Smarandache, University of New Mexico, Gallup,NM 87301, USA
Prof. A.O.Boyo,Dept. of Physics,Lagos State University,Ojo,Lagos State,Nigeria
Prof. Bekir GURBULAK, Ataturk University,Fen-Edebiyat Fak.,Fizik Bolumu, 25240 7ERZYRUM,Turkey
Prof. H.O.Boyo, Dept. of Applied Physics,Fukuoka University,8-19-1,Nanakuma,Joham-ku, Fukuoka,Japan
Prof. C.Y.Lo,Applied and Pure Research Institute, 17 Newcastle Drive, Nashua,NH 03060, USA
Email: c_y_lo@yahoo.com
Prof. Temur Z. Kalanov, Home of Physical Problems, Pisatelskaya 61,700200,Tashkent,Uzbekistan , Email.
Tzk_uz@yahoo.com, t.z.kalanov@mail.ru, t.z.Kalanov@rambler.ru
(Research Papers may be submitted through above Professors on online only )

**Bulletin of Pure and Applied Sciences** is devoted to the International advancement of organized knowledge on all aspect of Science. It provides a forum for comments by publishing original research contributions, scientific surveys, case studies, book reviews and letters to the Editor-in-chief.

**Bulletin of Pure and Applied Sciences** is issued six monthly, i.e. in June and December of each year. The Editor-in-chief/Managing Editor/Editorial Board, etc , assume no responsibility for the statements and opinions advanced by the contributors. The editorial staff in its work of examining papers, received for possible publication, is assisted in an honorary capacity, by a large number of distinguished scientists working in various parts of the world.

**Bulletin of Pure and Applied Sciences** is copy righted. Manuscripts published in this Bulletin should not be reproduced without the written permission of the Editor-in-chief.,2009.

**Annual Subscription Rates**

India Rs.1000 US $ 60 U.K. £ 30

CC-0. In Public Domain. Gurukul Kangri Collection, Haridwar

Digitized by Arya Samaj Foundation Chennai and eGangotri


# Bulletin of Pure and Applied Sciences

Vol.28D- Physics (No.2) July- December 2009


## Contents


C. Y. Lo
DETECTION OF THE GRAVITATIONAL WAVE WITH THE LIGO AND EINSTEIN'S THEORETICAL ERRORS ON MEASUREMENTS. 87-103

M. Iyanar, J. Thomas Joseph Prakash , C. Muthamizhchelvan and S. Ponnusamy
GROWTH AND CHARACTERIZATION OF TETRA (THIOUREA) POTASSIUM CHLORIDE (TTPC) A SEMIORGANIC NLO MATERIAL. 105-115

Anant Ranjan, Abhishek Kumar, Janardan Chaudhary, Asim Kumar and Madan jee
THE EFFECT OF BYCHKOV - RASHBA SPIN-ORBIT COUPLING IN THE OPTICAL TRANSITION SPECTRA AND ENERGY LEVELS OF PARABOLIC DOTS. 117-120

A. Alfred Cecil Raj, A. Sinthiya, Samuel Robinson Jebas and S.R. Wheeter
SYNTHESIS AND CHARACTERIZATION OF TETRAKIS (2-AMINOPYRIDINE – κN¹) – DICHLORIDOCOPPER (II) MONOHYDRATE 121-125

Jetki A. Mistry, Priyanka Rustagi and I.B.Patel
STUDY OF HARDNESS OF NaF, NaCl & NaF+NaCl CRYSTALS GROWN BY SOLUTION EVAPORATION METHOD AT AMBIENT TEMPERATURE. 127-136

Amita Sharma, Maqbool Hussain, Girijesh Sharma, Ashwambhar Roy and Veena Kumari
STUDY OF THE CHANGE OF THE SPIN WAVE SPECTRUM WITH DECREASING LATTICE CONSTANT BY DENSITY FUNCTIONAL THEORY. 137-140


Central Library Gurukul Kangri University Haridwar-249404. (U.A.)


Address for communication :
Dr. A. K. Sharma , *Editor –in-chief* , 115-RPS- DDA Flats, Mansarover Park, Post Box No.-9043,Shahdara, Delhi- 110032, India (Phone : 011-22138726, Mobile-9212200909

Emails : editorbulletin@yahoo.co.in , ajaykumarsharma1955@yahoo.com ,bpaseditor@gmail.com , research@hotmail.com , ajay_shrm@yahoo.com , editordrsharma@rediffmail.com



ISSN-0970-6569

Website : www.bpas.in


CC-0. In Public Domain. Gurukul Kangri Collection, Haridwar

Digitized by Arya Samaj Foundation Chennai and eGangotri


# BULLETIN OF PURE AND APPLIED SCIENCES

VOLUME – 28 D (Physics) No. 2 (July- December) 2009



## EDITORIAL BOARD

**Convenor (Hon.):** Prof. Durga P.Ojha, P.G.Dept. of Physics,Andhra Loyala College(Autonomous),Vijayawada-520008,India

### *MEMBERS*

Prof. R.N.P.Choudhary, Dept. of Physics, Indian Institute of Technology,Kharagpur-721303,India
Prof. S.H.Pawar, Dept. of Physics, Shivaji University, Kolhapur-416004,India
Prof. K.L.Alawadhi, Dept. of Physics, Punjabi University,Patiala-147002,India
Prof. Lalan Jha ,Dept. of Physics, L.N.Mithila University, Darbhanga-846004,India
Prof. D.L.Sharma, Dept. of Physics, Punjab Ag. University, Ludhiana-141004,India
Prof. S.C.Mehrotra, Dept. of Physics, Dr.B.A.M. University,Aurangabad-431004,India
Prof. T.V.Ramakrishna Rao, Dept. of Physics, S.K.University, Anantapur-515003,India
Prof. S. Umapathy,School of Physics, Madurai Kamaraj University, Madurai-625021,India
Prof. S..K.Narayandass, Dept. of Physics, Bharathiar University,Coimbatorte-641046,India
Prof. V.R.K.Murthy,Dept. of Physics,Indian Institute of Technology,Chennai-600036,India
Prof. S.C.Ingle,Dept. of Physics,L.T.Technology,Nagpur University,Nagpur-440001,India
Prof. B.Hanumanaiah,Dept. of Physics,Indian Institute of Technology,Bangalore-560012,India
Prof. A.K.Deb,Dept. of Physics, University of Chittagong,Chittagong-4331, Bangladesh
Prof .Sarabettin EREL,Dept. of Physics, Fac. of Sc.,University of Kirikale,71450 Kirikkale, Turkey
Prof. Florentin Smarandache, University of New Mexico, Gallup,NM 87301, USA
Prof. A.O.Boyo,Dept. of Physics,Lagos State University,Ojo,Lagos State,Nigeria
Prof. Bekir GURBULAK, Ataturk University,Fen-Edebiyat Fak.,Fizik Bolumu, 25240 ERZYRUM,Turkey
Prof. H.O.Boyo, Dept. of Applied Physics,Fukuoka University,8-19-1,Nanakuma,Johamku, Fukuoka,Japan
Dmitri Rabounski, Sirenevi boulevard 69–1–65, Moscow 105484, Russia.

**(Research papers may be submitted through the above Professors)**


**Bulletin of Pure & Applied Sciences** is devoted to the international advancement of organized knowledge on all aspects of Science. It provides a forum for comments by publishing original research contributions, scientific survey, case studies, book review and letter to the Editor-in-Chief.

**Bulletin of Pure & Applied Sciences** is issued six monthly, i.e. June and December of every year. The Editor-in-Chief/Managing Editor/Editorial Board etc. assumes no responsibility for the statements and opinions advanced by the contributors. The editorial staff in its work of examining papers, received for possible publication is assisted, in an honorary capacity, by a large number of distinguished scientist working in various parts of the world.

**Bulletin of Pure & Applied Science** is copy-righted. Manuscripts published in the Bulletin should not be reproduced without the written permission of the Editor-in-Chief.


## *Annual Subscription Rate*

India Rs. 1000 U.S. $ 60 U.K. £ 30


CC-0. In Public Domain. Gurukul Kangri Collection, Haridwar

ISSN-0970-6569
Bulletin of Pure and Applied Sciences. Vol. 28D (No.1) 2009. P.1-11
Digitized by Arya Samaj Foundation Chennai and eGangotri

# QUALITATIVE ANALYSIS OF SMALL SIGNAL MODIFIED DARLINGTON PAIR AND TRIPLE DARLINGTON AMPLIFIERS

**Satyendra Nath Tiwari and Sachchida Nand Shukla**
Department of Physics and Electronics,
Dr. R. M. L. Avadh University, Faizabad - 224001, U.P., India.

**ABSTRACT**

Modification in Darlington pair amplifier and Triple Darlington amplifiers is proposed. An extra biasing resistance $R_D$ is added in modified amplifiers and position of bypass capacitor $C_E$ is changed in Triple Darlington amplifier. This produces higher voltage gain than conventional Darlington pair amplifier. One of the proposed amplifiers removes the consequences of conventional Darlington pair amplifier at higher frequencies. In modified Triple Darlington amplifier, maximum voltage gain remains unaffected for any change in emitter resistance $R_E$. Proposed amplifiers may be useful for amplification of small signals in mid frequency range and beneficial for various analog communication applications.

**Key words:** Small Signal amplifiers, Darlington Amplifiers, Basic Electronic Circuits

## INTRODUCTION

Now a day, coupling of active devices is becoming advantageous to get the desired level of amplification for numerous application oriented electronic circuits. Till now many popular and useful circuits have been designed by coupling of BJTs, FETs and PN diodes(Rebert and Louis 2002,Zherebstov 1988,David 2002,Grob 1986,Motayed *et al* 2001). Amplification of weak as well as medium range signals through BJT and its coupled version (e.g. Darlington pair, Differential Amplifier, Current Mirror etc.) has been observed as an important phenomenon of electronics and communication. The most popular BJT amplifier recognized in audible frequency range is the high-fidelity Common Emitter RC coupled amplifier, which produces enlarged output at the same frequency of input(Motayed *et al* 2001). Adding one more transistor in the CE amplifier in form of Darlington pair, produces another interesting BJT amplifier circuit that significantly underlines the importance of coupled junction devices(David 2002). The current gain of the joint unit of composite transistor in Darlington pair becomes equal to the product of the current gains of the individual transistors (typically a few thousand). The input resistance of Darlington pair amplifier circuit is much higher and out put resistance is lower than that of a single-stage Emitter Follower (Grob 1986). However, a major drawback in its performance stems from its frequency response. At higher frequency its response is much worse than that of a single transistor emitter follower on the cost of improved

**E-mail of corresponding author:** sachida_shukla@yahoo.co.in
CC-0. In Public Domain. Gurukul Kangri Collection, Haridwar

Digitized by Arya Samaj Foundation Chennai and eGangotri


gain (Grob 1986,Sayed *et al* 2002,Motayed and Mohammad 2001). A number of books and research papers are available to explain the usefulness of Darlington pair amplifier but the efforts are still continued to develop its modified versions (Rebert and Louis 2002,Grob 1986,Sayed *et al* 2002,Motayed and Mohammad 2001,Tiwari *et al* 2008).

Comparatively less work has also been carried out for Triple Darlington amplifiers (Chris and Robert 1989,Tiwari *et al* 2009) due to a fact that the frequency response of a conventional Triple Darlington amplifier is much worse than that of a conventional Darlington pair amplifier at mid and high range frequencies.

In the present manuscript, we started with a conventional Darlington pair amplifier and obtained two modified amplifier circuits of distinct behaviour. One of the modified amplifiers is found to produce consistent voltage gain in mid frequency range and effectively reduces the consequences of conventional Darlington pair amplifier at higher frequencies. Similarly, the other modified amplifier produces high voltage gain in mid frequency range and suppresses the problems at high frequencies to a significant level. Finally, we made a comparative qualitative analysis of all the three amplifiers and received some unseen results.

## EXPERIMENTAL CIRCUITS

In present work, we selected a commonly used CC/CE Darlington pair amplifier of figure-1 as reference circuit. We further obtained two modified amplifier circuits as shown in figure 2 and 3. Adding an extra biasing resistance $R_D$ between emitter of transistor Q1 and ground configures the modified Darlington pair amplifier of figure-2. The modified Triple Darlington amplifier of figure-3 is obtained by adding one more BJT (of same parameters) in the transistor pair of reference amplifier (figure-1) and placing an extra biasing resistance $R_D$ in parallel with emitter bypass capacitor $C_E$ between emitter of transistor Q2 and ground.

To configure the amplifier circuits of figures 1, 2 and 3, we selected transistor Q2N2222 (an n-p-n BJT with $\beta$=255.9) as an active device. Similarly, $R_S$=500Ω, $R_1$=47KΩ, $R_2$=5KΩ, $R_C$=10KΩ, $R_E$=2KΩ, $R_D$=1KΩ, $R_L$=10KΩ, $C_1$=1μF, $C_2$=1μF and $C_E$=10μF are introduced as passive biasing elements in the selected amplifier circuits. All the amplifiers are biased with +15V DC power supply. Respective observations were made by feeding the circuit with 1V AC input signal source from which a distortion free 1mV AC signal at 1KHz frequency is drawn as input for amplification purpose. All the observations are accomplished through PSpice simulation software(Rashid,2004) (Student version 9.2).


CC-0. In Public Domain. Gurukul Kangri Collection, Haridwar

Digitized by Arya Samaj Foundation Chennai and eGangotri

# QUALITATIVE ANALYSIS OF SMALL SIGNAL MODIFIED DARLINGTON PAIR AND TRIPLE DARLINGTON AMPLIFIERS

## OBSERVATIONS AND DISCUSSIONS

Variation of voltage gain as a function of frequency for all the three amplifiers in form of frequency response curves is depicted in figure-4. Frequency response curves are clearly indicating that the reference amplifier of figure-1 performs with a maximum voltage gain of 16.98 and 99 KHz bandwidth, while the amplifier in figure-2 produces a maximum voltage gain of 20.56 and 2809 KHz bandwidth. Similarly, amplifier of figure-3 produces a maximum voltage gain of 30.56 and 104.44 KHz bandwidth. The depicted response curves are obtained for the biasing elements as indicated in figures 1, 2 and 3.

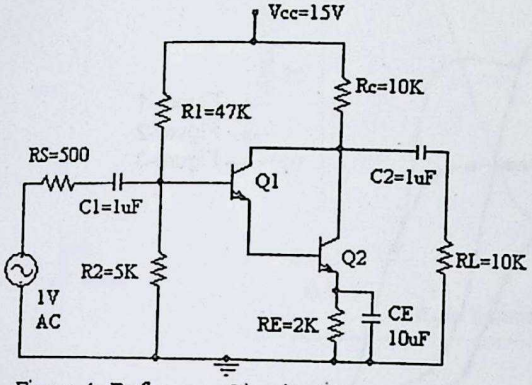


Figure-1: Reference Circuit (Conventional Darlington Pair Amplifier)

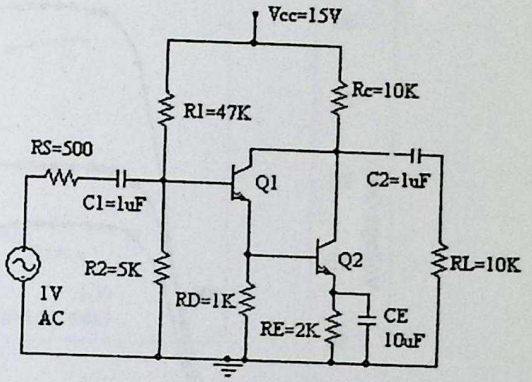


Figure-2: Modified Darlington Pair Amplifier

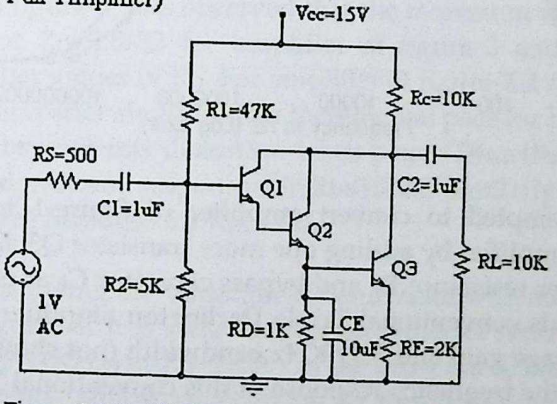


Figure-3: Modified Triple Darlington Amplifier


CC-0. Panini Kanya Maha Vidyalaya Collection. Gurukul Kangri Collection, Haridwar

Digitized by Arya Samaj Foundation Chennai and eGangotri



The frequency response of figure-4 is clearly suggesting that due to the inclusion of added resistance $R_D$, the gain and bandwidth both are enhancing to a significant level(Tiwari *et al* 2008) for the amplifier of figure-2. Similarly, connecting the R-C network of emitter resistance $R_E$ and bypass capacitor $C_E$ at emitter end of Q2 is perhaps responsible for significantly high voltage gain of amplifier(Tiwari *et al* 2009) of figure-3. Thus, the amplifier configuration suggested in figure 2, effectively removes the consequences of a conventional Darlington pair amplifier (of figure-1) at higher frequencies and both the modified amplifiers are found to produces high voltage gain.

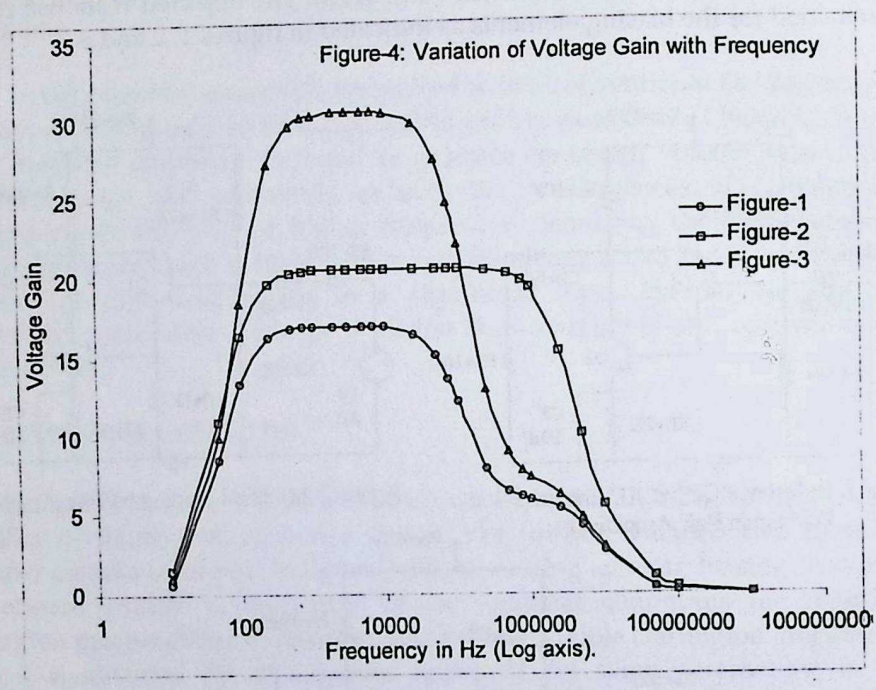


We also attempted to convert amplifier of figure-1 into conventional Triple Darlington amplifier by adding one more transistor Q3 and placing the R-C network of emitter resistance $R_E$ and bypass capacitor $C_E$ at emitter end of Q3. We observed for this conventional Triple Darlington amplifier that it produces 3.35 maximum voltage gain and 3.39 KHz bandwidth (not shown in figure). It is also observed that the frequency response of this conventional Triple Darlington amplifier is poorer than conventional Darlington pair amplifier of figure-1 at higher frequencies.

We again modified the circuit of figure-3. This time $R_D$ is connected at emitter end of Q1 and $C_E$ is connected across $R_E$ at emitter end of Q3 (circuit is not shown). With this modification we observed a severe reduction in maximum

CC-0. In Public Domain. Gurukul Kangri Collection, Haridwar

Digitized by Arya Samaj Foundation Chennai and eGangotri


voltage gain to a value of 4.32 but a significant enhancement in bandwidth to a value of 5959.96 KHz (not shown in figure).

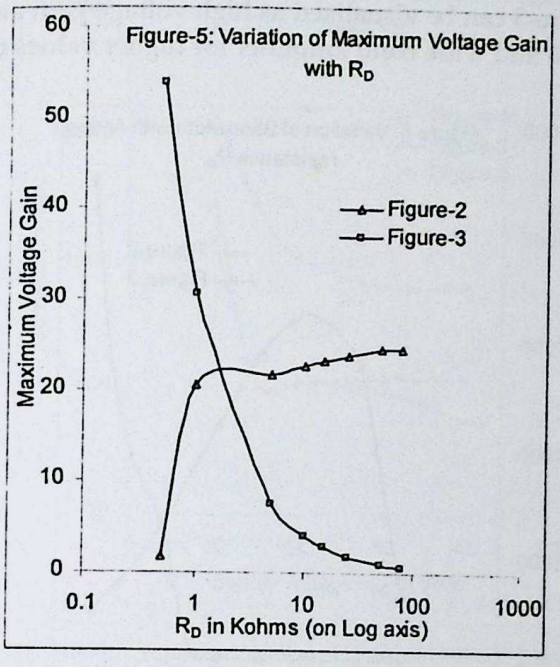


The variation of maximum voltage gain as a function of added resistance $R_D$ is shown in figure-5. It is observed that the maximum voltage gain has a peak value (53.72) at $R_D$=0.5KΩ for amplifier of figure 3 and thereafter decreases rapidly for higher values of $R_D$. For amplifier of figure-2 it rapidly increases up to $R_D$=1KΩ and thereafter shows a slow incremental pace for higher values of $R_D$ up to 80 KΩ and beyond this distortion takes place. Thus the amplifier of figure-3 produces the significant response for $R_D \leq 15K\Omega$. Similarly amplifier of figure-2 produces a useful response for $R_D \geq 1K\Omega$.

Graphs showing the variation of bandwidth with added resistance $R_D$ are indicated in figures-6. It is clear that for amplifier of figure-2, bandwidth has a maximum (3239.91KHz) at $R_D$=2KΩ. On the other hand, bandwidth for amplifier of figure-3 remains almost constant up to $R_D$=15 KΩ after which it increased rapidly to 4519.96 KHz value at $R_D$ = 80KΩ and beyond this distortion in output waveform takes place.

Figures 5 and 6 are clearly suggesting that the proposed amplifier of figure-3 show a high voltage gain of 30.56 with 104.44 KHz bandwidth at 1K value of $R_D$. It is observed that at higher values of $R_D$, the maximum gain is


CC-0. In Public Domain. Gurukul Kangri Vishwavidyalaya, Haridwar

Digitized by Arya Samaj Foundation Chennai and eGangotri


reduced significantly (at 80K of $R_D$ gain is 0.64) but bandwidth becomes very high (at 80K of $R_D$ bandwidth is 4519.96 KHz). It is also observed that the functional range for amplifier of figure-3 is 0.5 KΩ ≤ $R_D$ ≤ 80 KΩ of $R_D$ and beyond this resistance range distortion in frequency response takes place. Thus, the amplifier of figure-3 can be visualized as high voltage gain amplifier at lower values of $R_D$ (≤15KΩ) and wide band amplifier for higher values of $R_D$ (≥25KΩ).

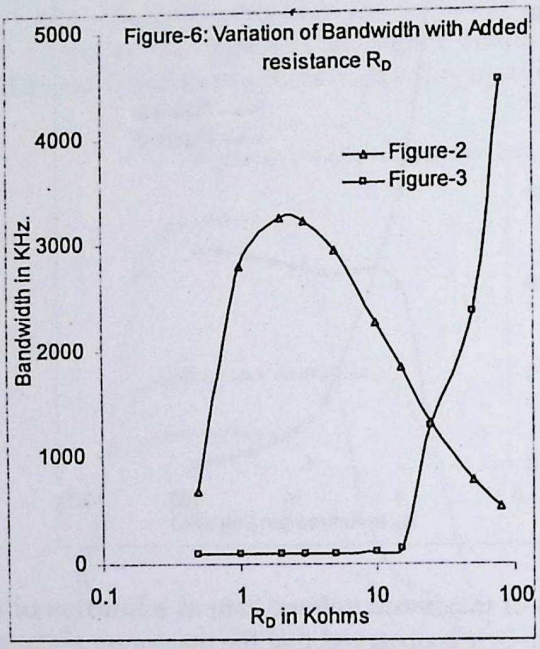


Variation of bandwidth as a function of DC supply voltage $V_{CC}$ is depicted in figures 7. From figure-7, we observed that the bandwidth is maximum at $V_{CC}$ = 10V for all the three amplifiers and thereafter successively decreases with increasing supply voltage. It is also observed that all the three amplifiers work properly for 10V ≤ $V_{CC}$ ≤ 40V voltage range of DC supply voltage and beyond this, distortion in frequency response is reported.

It is clear from figure-8 that maximum gain has a nonlinear rising tendency for increasing values of DC supply voltage $V_{CC}$ for all the three amplifier circuits to a certain point. For amplifier of figure-1, maximum voltage gain rapidly rises to 15V value of $V_{CC}$ and thereafter it shows a steady increasing tendency at higher values of $V_{CC}$ with a maxim at 40V of $V_{CC}$. The amplifier of figure-2 shows an optimum performance at 20V of $V_{CC}$, with maximum voltage gain. For amplifier of figure-3 there are two transition points for maximum gain on $V_{CC}$ scale. The maximum gain rapidly rises to 15V $V_{CC}$ value, after which the rising pace gets affected and after 40V of $V_{CC}$ it falls down rapidly.


CC-0. In Public Domain. Gurukul Kangri Collection, Haridwar

Digitized by Arya Samaj Foundation Chennai and eGangotri



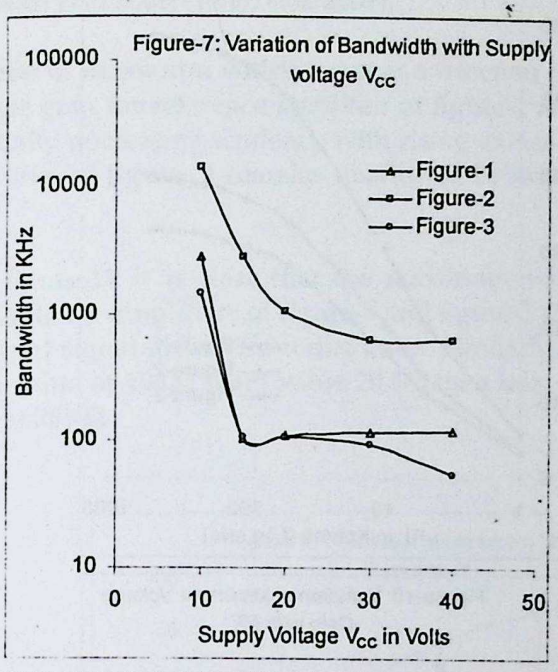


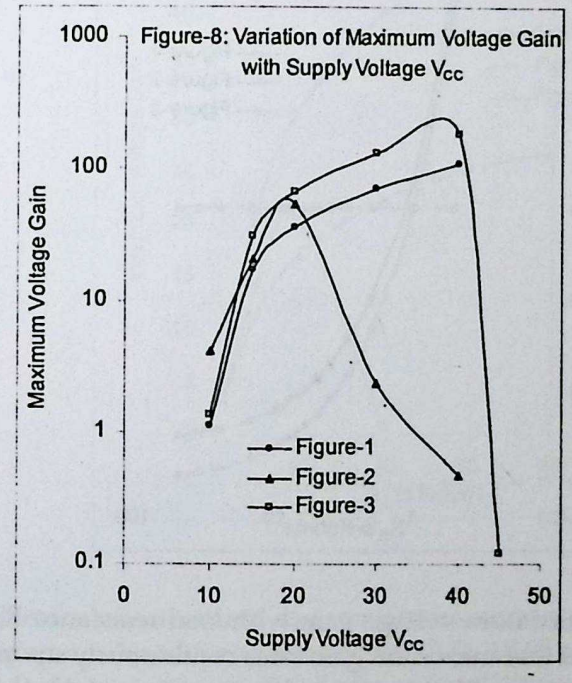



CC-0. In Public Domain. Gurukul Kangri Collection, Haridwar

Digitized by Arya Samaj Foundation Chennai and eGangotri


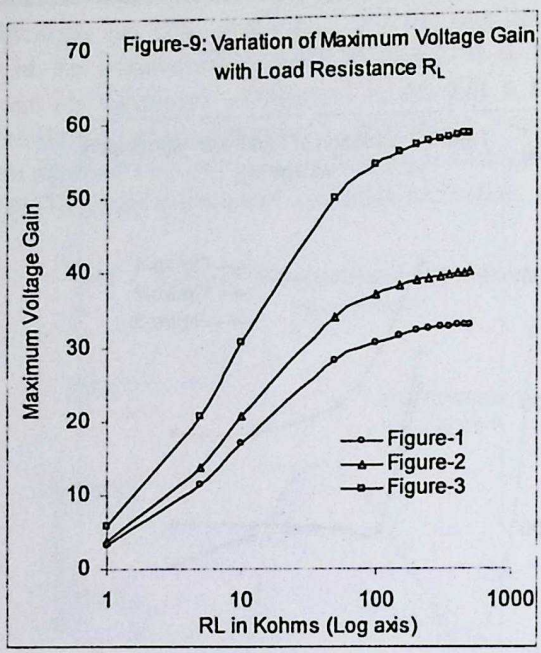


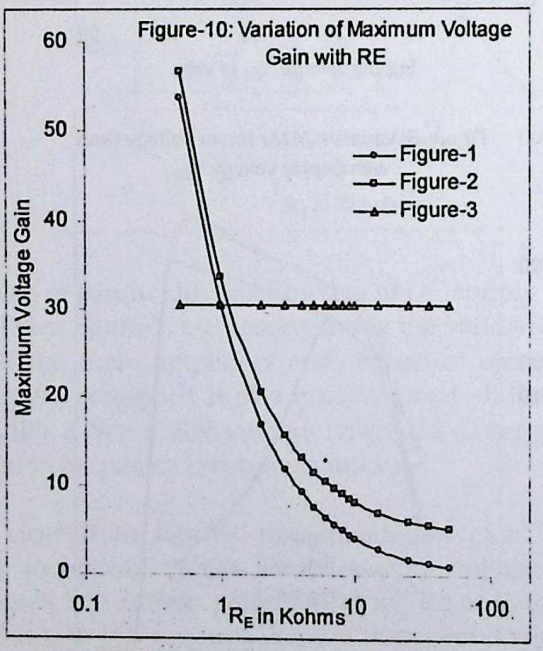


Variation of maximum voltage gain with load resistance $R_L$ is plotted in figure-9. We observed that maximum gain rises continuously up to 100KΩ value of $R_L$ for all the three amplifiers and tend to a sustained level for higher $R_L$ values. It is also found that the basic nature (rising and saturation) of the voltage


CC-0. In Public Domain. Gurukul Kangri Collection, Haridwar

Digitized by Arya Samaj Foundation Chennai and eGangotri


gain curves are similar and well in accordance of the usual behaviour of CE amplifier (Tiwari *et al* 2008,Tiwari *et al* 2009).

Variation of maximum voltage gain as a function of $R_E$ is traced in figure-10. The voltage gain for reference amplifier of figure-1 and amplifier of figure-2 has exponentially decreasing tendency with rising values of $R_E$ while the voltage gain for amplifier of figure- 3 remains unaffected by any change in the value of $R_E$.

From figure-11 it is clear that the maximum voltage gain successively increases with $R_C$ for amplifiers of figure-1 and figure-3 till 40KΩ after which the amplified output signal suffers from distortion. Similarly, for amplifier of figure-2 it rises to a value of 10KΩ (gain value 20.56) then falls down rapidly to a gain value of 0.59 at 20KΩ.

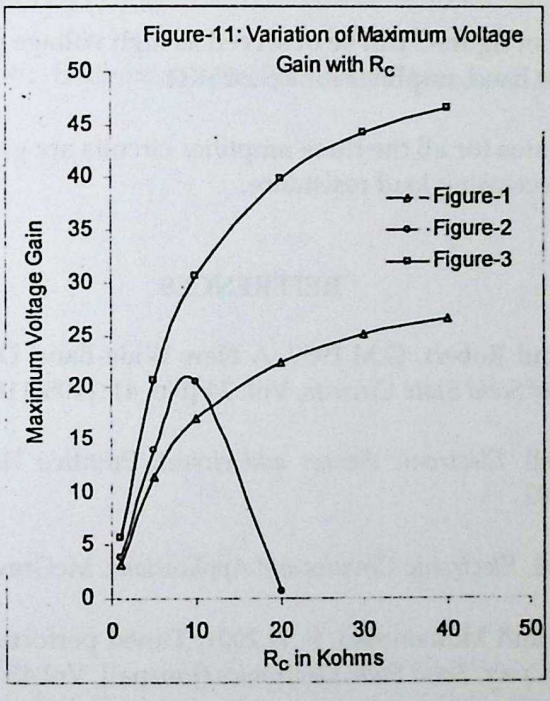


We have also measured the maximum current gain for all the three circuits of figures 1, 2 and 3 and found them 8.51, 10.03 and 15.31 respectively at $R_L$=10KΩ (not shown in figure). Similarly, at $R_L$ =3KΩ the respective current gain values for circuits of figure 1, 2 and 3 are 13.21, 15.59 and 23.94 (not shown in


CC-0. In Public Domain. Gurukul Kangri Collection, Haridwar

Digitized by Arya Samaj Foundation Chennai and eGangotri


figure). Thus, decreasing the load resistance, the current gain increases for all the three circuits under discussion.

## CONCLUSIONS

Thus, the amplifier configuration suggested in figure-2 and 3 effectively removes the consequences of a conventional Darlington pair amplifier at higher frequencies with significant high voltage gain.

The emitter resistance $R_E$ significantly affects the maximum voltage gain and bandwidth of Darlington pair amplifiers of figure-1 and 2 but maximum voltage gain and bandwidth remains unaffected for any change in emitter resistance $R_E$ for amplifier of figure-3.

Amplifier of figure-2 and 3 can be visualized as a high voltage gain amplifier in mid frequency range for the biasing parameters depicted in respective circuit diagrams.

Amplifier of figure-3 can be observed as high voltage gain amplifier for $R_D \leq 25K\Omega$ but wide band amplifier for $R_D \geq 25K\Omega$.

Current gains for all the three amplifier circuits are greater than unity and increases with decreasing load resistance.

## REFERENCES

1. Chris, T.A. and Robert, G.M.1989. A New Wide-Band Darlington Amplifier, *IEEE Journal of Solid State Circuits*, Vol. 24 (No. 4) :1105-1109.

2. David, A. Bell. *Electronic devices and circuit*, Prentice Hall of India, 3rd ed., P.687-717, 2002

3. Grob, Bernard. *Electronic Circuits and Applications*, McGraw Hill, P. 47-48, 1986

4. Motayed, A. and Mohammad, S. N.2001. Tuned performance of small signal BJT Darligton pair, *Solid State Electronics* (Journal), Vol.45 : 369-371.

5. Motayed, Browne, T. E., Onuorah, A. I. and Mohammad, S.N.2001. Experimental studies of frequency response and related properties of small signal bipolar junction transistor amplifier, *Solid State Electronics* (Journal), Vol. 45 : 325-333.


CC-0. In Public Domain. Gurukul Kangri Collection, Haridwar

Digitized by Arya Samaj Foundation Chennai and eGangotri


6. Rashid, M.H.. *Introduction to PSpice Using OrCAD for Circuits and Electronics*, Pearson Education, 3rd Ed. P. 255-300, 2004

7. Rebert L. Boylestad and Louis Nashelsky. *Electronic Devices and Circuit Theory*, Pearson Education Asia, 3rd ed.P. 389-396,461-483, 627-633, 2002

8. Sayed ElAhl, A.M.H., Fahmi, M.M.E., and Mohammad, S.N.,2002. Qualitative analysis of high frequency performance of modified Darlington pair, *Solid State Electronics* (Journal), Vol. 46 : 593-595.

9. Tiwari, S.N., Dwivedi, A.K. and Shukla, S.N.2008.Qualitative Analysis of Modified Darlington Amplifier, *Ultra Scientist of Physical Sciences*, Vol.20 (No.3): 625-629.

10. Tiwari, S.N., Pandey, B. and Shukla, S.N., 2009.Qualitative Analysis of Two distinct Wide Band Triple Darlington Amplifiers, *Ultra Scientist of Physical Sciences*, Vol.21 (No.1) :117-120.

11. Zherebstov, I., *Basic Electronics*, Mir Publishers, Moscow, 1st ed., P. 46-48, 1988.


CC-0. In Public Domain. Gurukul Kangri Collection, Haridwar

Digitized by Arya Samaj Foundation Chennai and eGangotri

CC-0. In Public Domain. Gurukul Kangri Collection, Haridwar

ISSN-0970-6569
Bulletin of Pure and Applied Sciences Vol.28D(No.1)2009 P.13-19
Digitized by Arya Samaj Foundation Chennai and eGangotri

# THEORETICAL STUDY OF MULTI-BAND MICROSTRIP ANTENNA

**Dhirendra Kumar*, Prakash Nayak** and Lalan jha*****
* Department of Physics, Mithila Janta Inter College, Madhubani-847211 (Bihar)

**ABSTRACT**

In the present paper on the basis of concept of inserting slot arrays following a known antenna distribution a theoretical study of a multi-wideband microstrip-patch anteena has been made. The design of anteena included the insertion of rectangular slots following a Chebyshev distribution around a central rectangular slot in addition to a triangular slot. These slots engraved in rectangular and triangular patch are joined together and fed by one probe feed. A close agreement was found when theoretical results were compared with simulated results.

**Key words** : Microstrip antennas, Multifrequency antennas, Wideband antennas.

## INTRODUCTION

With the growing demand of modern wireless communication there has been significant surge in researches leading to novel design and application of various type of antenna. To achieve various functionalities, such as dual frequency operation, dual band circular polarised performance polarisation diversity with only one patch and a single feed a reconfigurable patch antenna with switchable slots (PASS) was proposed (Sittironnarit and Ali,2002). For wireless local area network applications a dual wideband folded microstrip patch antenna was introduced (Yang and Rahmat-Samii,2003). For the design of dual-band microstrip antenna a cavity-model based simulation tools, along with genetic optimization algorithm was presented in Ozlem *et al* (2003). Multiple slots in the patch, or multiple shorting strips between the patch and the ground plane have been used. Acceptable antenna operation over the desired frequency band was then achieved by optimization of the position of the slots and performance of shorting strips via a genetic optimization algorithm. Using similar approach a single low-profile printed anteena which provided dual-band operation by having loading from two-step slots embedded close to radiating edge was presented in Khairul *et al* (2003) . It has been suggested in Khairul *et al* (2003) that the ratio of the two frequencies can be well controlled by the aspect ratio of the step-loading dimension.

** P.G. Department of Physics, R.K.College, Madhubani-847211 (Bihar)
***University Department of Physics, L.N.M.University, Darbhanga-846004 (Bihar)
CC-0. In Public Domain. Gurukul Kangri Collection, Haridwar

Digitized by Arya Samaj Foundation Chennai and eGangotri

In this paper a multi-band antenna design approach based on inserting rectangular slots, following a Chebyshev distribution, in addition to a triangular slots into the patch, which represents a combination of a rectangular and isosceles-triangular patch have been presented. The sample antenna was simulated and compared with theoretical results. There was good agreement between the theoretical and simulated results.

## ANTENNA GEOMETRY AND RADIATION PATTERN OF THE PROBLEM

The proposed antenna geometry is based on joining a rectangular patch and a triangular patch, in order to increase the radiation area, as shown in Figure 1. The structure is fed by a 50Ω coaxial probe. The radiation pattern of the proposed structure with this feeding technique is determined by adding the fields radiated by the rectangular patch to those radiated by the triangular patch. The substrate used in the formulation process was of thickness $h$ = 0.32 cm. The far electric fields of the rectangular patch were given in Balanis,(1997) as

$$E_\theta = \frac{Ke^{-jk_0 r}}{r}\cos(k_0 h\sqrt{\varepsilon_r}\cos\theta)\,\frac{\sin\left(\frac{\pi W}{\lambda_0}\sin\theta\sin\varphi\right)\cos\left(\frac{\pi L}{\lambda_0}\sin\theta\cos\varphi\right)\cos\varphi}{\sin\theta\sin\varphi}. \quad (1)$$

$$E_\varphi = \frac{-Ke^{-jk_0 r}}{r}\cos(k_0 h\sqrt{\varepsilon_r}\cos\theta)\,\frac{\sin\left(\frac{\pi W}{\lambda_0}\sin\theta\sin\varphi\right)\cos\left(\frac{\pi L}{\lambda_0}\sin\theta\cos\varphi\right)\cos\theta}{\sin\theta s}. \quad (2)$$

In Equations (1) and (2), $k$o is the wavenumber, $\lambda$o is the wave-length, $\varepsilon r$ is the dielectric permittivity, and $W$ and $L$ are the width and the length dimensions of the rectangular patch, respectively. The far electric fields radiated from an equilateral triangle were given in Lee *et al* (1988) as

$$E_\theta = -j\omega\eta_0\,(F_x\cos\theta\cos\varphi + F_y\cos\theta\sin\varphi), \quad (3)$$

$$E_\varphi = -j\omega\eta_0\,(-F_x\sin\varphi + F_y\cos\varphi), \quad (4)$$

In Equations (3) and (4), $\eta$o = 120$\pi$ Ω, and the terms $Fx$ and $Fy$ are the electric potential components. These were given in detail in Lee *et al* (1988) ,


CC-0. In Public Domain. Gurukul Kangri Collection, Haridwar

Digitized by Arya Samaj Foundation Chennai and eGangotri


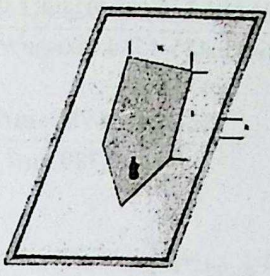

**Figure 1 : A rectangle added to an equilateral triangle patch, fed by a probe.**

By specifying the lowest-order mode, TM010, for approximating the rectangular dimensions to a length, $L$, of 4 cm and width, $W$, of 3 cm, and for an equilateral triangle 3 cm on a side, for an operating frequency, $f_0$, of 3.24 GHz, Equations (1) and (2) become

$$E_\theta = \frac{Ke^{-jk_0 r}}{r} \cos(0.322\cos\theta) \frac{\sin(0.9448\sin\theta\sin\varphi)\cos(0.7086\sin\theta\cos\varphi)}{\sin\theta\sin\varphi} \cos\theta, \quad (5)$$

$$E_\varphi = \frac{Ke^{-jk_0 r}}{r} \cos(0.322\cos\theta) \frac{\sin(0.9448\sin\theta\cos\varphi)\cos(0.707\sin\theta\cos\varphi)}{\sin\theta} \cos\theta, \quad (6)$$

It is clear from Equation (5) that for $\varphi = 0^o$ and $\varphi = 90^o$, both components of the electric field vanish, due to the terms $\sin\varphi$ and $\cos\varphi$, respectively, Moreover, for $\varphi = 90^o$, Equation (6) becomes

$$E_\varphi = \frac{Ke^{-jk_0 r}}{r} \cos(0.322\cos\theta) \frac{\sin(0.9448\sin\theta)}{\sin\theta} \cos\theta \quad (7)$$

For an equilateral triangular patch, the $\varphi$ components of the electric field are given by the product of the terms $A$ and $C$, given by


CC-0. In Public Domain. Gurukul Kangri Collection, Haridwar

Digitized by Arya Samaj Foundation Chennai and eGangotri

$$A = \left\{ \frac{2J(139.6258 + J39.1789\sin\theta)\,[\sin(1.01789\sin\theta)]}{6498.455 - 1534.986\sin^2\theta} + \frac{2J\cos(1.01789\sin\theta) - 2J}{39.1789\sin\theta} \right\}. \quad (8)$$

$$C = -J\omega\eta_0 \left[(4\pi r)^{-1}\varepsilon_0 h e^{-jk_0 r}\right] e^{J39.1789\sin\theta\cos\varphi}\, 2J\omega\mu C_{01} \quad (9)$$

$C_{01}$ is constant defined in Lee *et al* (1988) . The total electric field of the new structure is obtained by adding the electric field radiated from the rectangular patch, defined in Equation (7), to that of the triangular patch, derived in Equations (8) and (9). A comparison between calculated and simulated results is shown in Figure 2 (a & b).

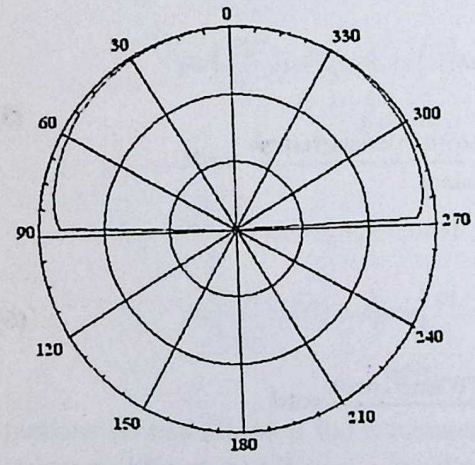


*Figure 2a. The simulated electric field, to be compared to Fig. 2b.*

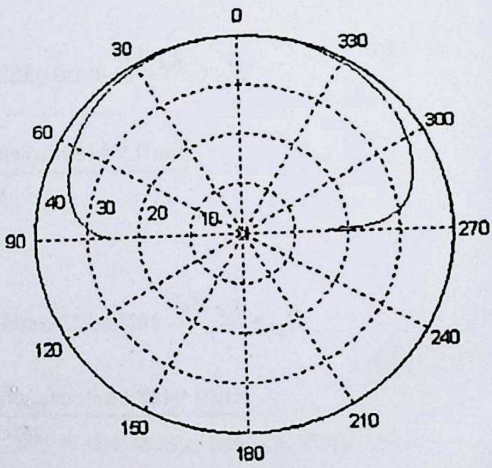


*Figure 2b. The calculated electric field, to compared to Fig. 2a.*

The $S_{11}$ parameter of a simple rectangular patch of dimensions similar to those of structure in Figure 1 was compared to the $S_{11}$ parameter of the combined structure to prove that joining a triangular and a rectangular patch increases the radiation area and provides a multi-resonating anteena. Comparison shown in Fig. 3 clearly establishes dual-band operation of the new structure.


CC-0. In Public Domain. Gurukul Kangri Collection, Haridwar

Digitized by Arya Samaj Foundation Chennai and eGangotri



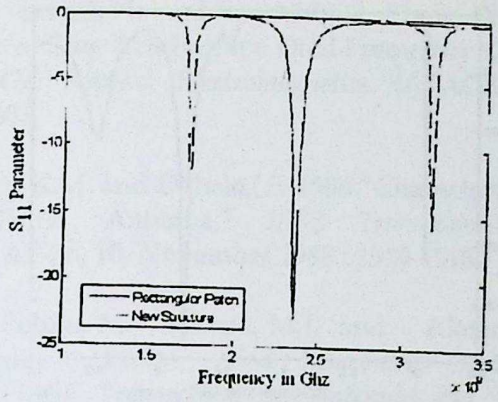


**Figure 3 : The $S_{11}$ parameter of a simple rectangular patch, and the $S_{11}$ parameter of the structure shown in Fig. 1.**

## FURTHER ANTENNA STRUCTURE AND RESULTS

The basic structure of the proposed antenna, shown in Figure 4, consists of three layers. The lower layer, which constitutes the ground plane, covers all the substrate and has a width of 6 cm and a length of 15 cm. The middle substrate, which is Polyflon Norclad, has a dielectric constant $\varepsilon r$ = 2.55 and a height of 0.32cm. The upper layer, which is the patch, consists of a rectangle with a width of 3 cm and a length of 4 cm, joined with an isosceles triangle having the same area as the rectangular patch and a base of 3 cm and a height $h$ = 8cm. Inside the rectangular patch, ten rectangular slots, following a Chebyshev distribution around a central rectangular slot, were inserted. On the basis of parametric study and optimization carried out it was concluded that moving the feed deeper into the structure and putting it closer to the triangular slot made the functioning of the triangular slot more effective and gave the total response. The $S_{11}$ parameter of the new antenna structure shown in Fig. 5 clearly exhibits GSM 900 MHz wide band operation in addition to operation at 2.8 GHz and 3.5 GHz.

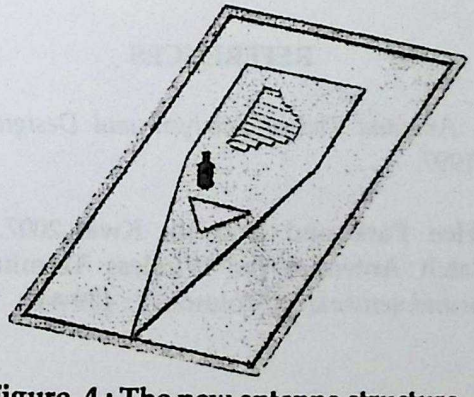

**Figure 4 : The new antenna structure**


CC-0. In Public Domain. Gurukul Kangri Collection, Haridwar

Digitized by Arya Samaj Foundation Chennai and eGangotri


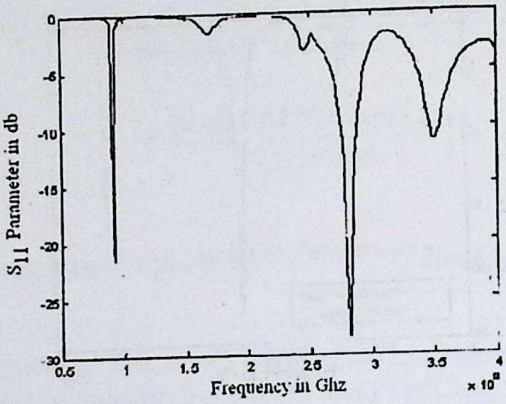


**Figure 5 : The $S_{11}$ parameter of the new antenna structure.**

## CONCLUSION

A new multi-band antenna design has been presented. The design consists of joining a rectangular and a triangular patch together in one patch, and inserting several forms of slots. The new idea behind this design also includes the insertion of rectangular slots following a Chebyshev distribution around a central rectangular slot, in addition to a triangular slot inserted into the triangle, which has the same area as the rectangular patch. The concept of inserting slot arrays following a known antenna-array distribution has proven to give remarkable functionality to an antenna. It causes it to be highly radiating in different frequency ranges, using only one single feed, represented by a 50Ω.

The antenna has many applications, such as GSM, GPS, Wi-Fi, WiMax, video wireless communication, and Bluetooth applications, in one single instrument, using this type of antenna.

## REFERENCES

1. Balanis, C.A. *Antenna Theory Analysis and Design, Second Edition,* New York, Wiley, 1997.

2. Dong - Hee Park and Yoonsik Kwak.2007. "Design Multi-Band Microstrip Patch Antennas for Wireless Terminals" *Future generation communication and networking,* Volume. 1 : 439-441.

CC-0. In Public Domain. Gurukul Kangri Collection, Haridwar

Digitized by Arya Samaj Foundation Chennai and eGangotri


3. Khairul, M., Ismail, H. and Esa, M.2003. "Low Profile Printed Antenna With A Pair of Step Loading for Dual-Frequency Operation," *Asia Pacific Conference On Applied Electromagnetics* (APACE 2003), Shah Alam, Malaysia, 2003.

4. Lee,K.F., Luk, K.M. and Dahele,J.S. 1988."Characteristics of the Equilateral Triangular Patch Antenna," *IEEE Transactions on Antennas and Propagation*, AP-36, 10, November 1988 : 1510-1518.

5. Ozlem, O., Selma, M., Aksun, M.I. and Alatan, L.2003. "Design of Dual-Frequency Probe Fed Microstrip Antennas with Genetic Algorithm," *IEEE Transactions on Antennas and Propagation*, AP-51, 8, August 2003 : 1947-1954.

6. Sittironnarit ,T. and Ali,M. 2002."Analysis and Design of a Dual-Band Folded Microstrip Patch Antenna for Handheld Device Application", *IEEE Southeast Conference Proceedings*, 2002 : 255-258.

7. Yang,F. and Rahmat-Samii,Y. 2003. "A Compact Dual Band Circularly Polarized Antenna Design For Mars Rover Mission," IEEE International Symposium on Antennas and Propagation, *Digest*, 3, June 22-27, 2003 : 858-861.


CC-0. In Public Domain. Gurukul Kangri Collection, Haridwar

Digitized by Arya Samaj Foundation Chennai and eGangotri

CC-0. In Public Domain. Gurukul Kangri Collection, Haridwar

Digitized by Arya Samaj Foundation Chennai and eGangotri

ISSN-0970-6569
Bulletin of Pure and Applied Sciences. Vol.28D(No.1)2009:P.21-28

# STUDY OF VARIATION OF SELECTIVITY OF MICROSTRIPLINE WITH STRIP GEOMETRY AND OPERATING FREQUENCY

**Kumar Balwant Singh**
Department of Physics, Govt. Polytechnic,Darbhanga-846004, India
E-mail: kbsphysics@yahoo.co.in

**ABSTRACT**

In this paper, characteristic impedance, Phase velocity, Attenuation constant and Selectivity, which are important parameters to be discussed. The metallic and dielectric loss has been also calculated for the study of selectivity of microstriplines with fused quartz as substrate and its variation with strip width and operating frequency-using computer added technique. The calculation of selectivity of the microstripline structure keeping strip width and permittivity fixed has been carried out for different frequencies. In the growing edge of computer and information technology the communication system has shrinked to a miniaturized size, lightweight and less expansive. It is due to advent of microwave integrated circuit (MIC's), which gave birth to planar microwave transmission structure. Microstripline structure appears to be the most convenient and easy to fabricate. This furnishes very useful information for designing microstrip line coupler and resonators of high selectivity.

**Key words** : Stripline, Microstripline, MIC's, CPW, Selectivity, Attenuation Constant,

## 1. INTRODUCTION

The increasing importance of miniature planar microwave integrated circuits has renewed interest on the part of microwave circuit's designers in the various form of planar strip transmission line such as stripline, microstripline, slotline, coplanar stripline and coplanar waveguide (CPW) etc. Out of these microstriplines appears to be most simple, convenient, inexpensive and easy to fabricate. Due to openness of the structure radiation, conductor and dielectric losses need to be minimized to insure the fields to be confined near the metal strip. Use of dielectric substrate of suitable permittivity and low loss tangent is necessary. Also electromagnetic field lines extend in the space above the strip, the microstrip structure becomes a mixed dielectric transmission line. This needs effective permittivity to be taken into account.

The microstripline consists of a narrow "strip" conductor of width (W) and thickness (t) separated from a conducting ground plane by an intervening supporting dielectric substrate of thickness and width much greater than the

CC-0. In Public Domain. Gurukul Kangri Collection, Haridwar

Digitized by Arya Samaj Foundation Chennai and eGangotri


strip width. For maximum circuit size reduction, the dielectric constant of substrates now being used is of the order of two or higher. But due to smaller loss tangent or low dissipation factor fused quartz like substrate is preferably used.

F or design purpose it is necessary to study the characteristic parameters of the stripline and different losses occurred in this structure during the propagation of electromagnetic waves through the structure. The TEM-mode of the propagation is considered in the lower Giga hertz range of frequency. This study provides and easy method for the calculation of the selectivity of the microstriplines using different width of the conductor strip.

The study of selectivity of microstriplines has not received much attention in recent years. This restricts our attention to the study of variation of selectivity with strip width and operating frequency. This will furnish useful information for design of the microstriplines of given characteristic impedance operative at given frequency, microstriplines couplers and resonators of high selectivity.

## 2. BRIEFS OF MICROSTRIPLINE

This was realized with a planar form of single wire transmission line over a ground plane, called microstrip (Vendelin *et al* 1990). Microstrip employs a flat strip conductor suspended above a ground plane by a low-loss dielectric material. The size of the circuit can be reduced through judicious use of a dielectric constant some 2-10 times that of free space (or air), with a penalty that the existence of two different dielectric constants (below and above strip) makes the circuit difficult to analyze in closed form (and also introduces a variability of propagation velocity with frequency that can be a limitation on some applications). Microstripline is an inhomogeneous structure. It consists of a narrow conductor strip one side of it a dielectric substrate and the other side being completely metalized to serve as a ground plane as shown in Fig- (1). Though the structure is open and suffers from radiation, metallic and dielectric losses, fused quartz substrate with copper conductor is used to minimize the losses. The microwave energy propagates both in the dielectric substrate below the metal strip and in the air region above. Fraction of power flows outside the substrate depending on the width of the metal strip. So, effective dielectric constant is considered instead of considering relative dielectric constant. The field configuration distribution is shown in Fig- (2). In the lower Giga hertz range of frequency TEM-mode of propagation of microwave is considered as proposed by Wheelar (1965).


CC-0. In Public Domain. Gurukul Kangri Collection, Haridwar

Digitized by Arya Samaj Foundation Chennai and eGangotri

# STUDY OF VARIATION OF SELECTIVITY OF MICROSTRIPLINE WITH STRIP GEOMETRY AND OPERATING FREQUENCY

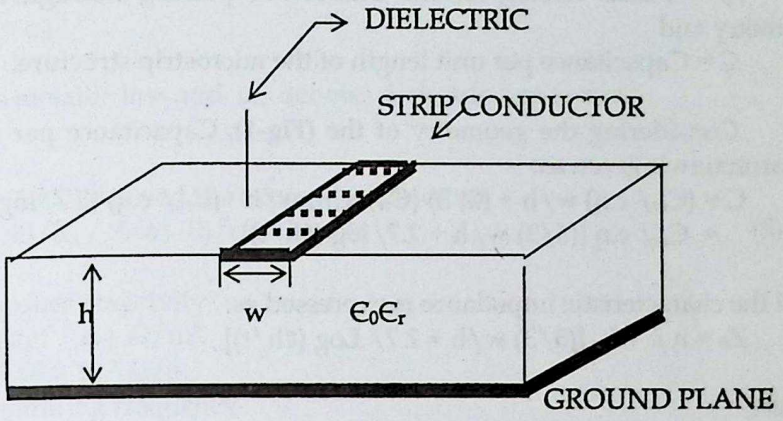


**Fig 1: Microstrip line**

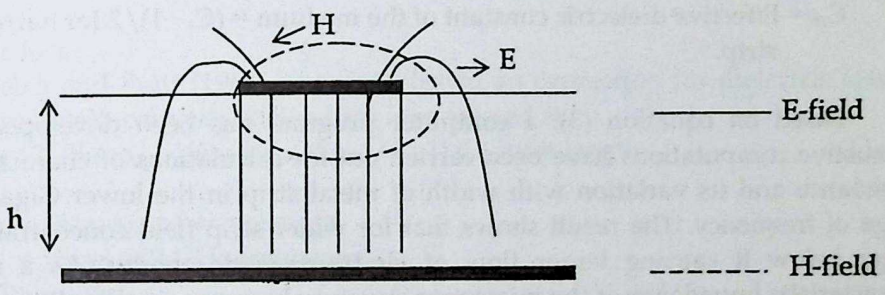


**Fig 2: Microstrip Field configuration**

## 3. CHARACTERISTIC IMPEDANCE

For the study of selectivity of microstriplines (Selvester ,1968) it is necessary to study the characteristic impedance and its dependence on the geometry of the microstriplines using Wheelar's conformal transformation technique, which converts the microstrip geometry into parallel plate geometry (Singh and Sah,2000,Kaul,1992,Singh and Sah,2003). The knowledge of capacitance provides the knowledge of characteristic impedance of the microstrip geometry using formula


CC-0. In Public Domain. Gurukul Kangri Collection, Haridwar

Digitized by Arya Samaj Foundation Chennai and eGangotri


$$Z_0 = 1/V_pC \quad (1)$$

Where

$V_p$ = Phase velocity of the microwave passing through the microstrip geometry and

C = Capacitance per unit length of the microstrip structure.

Considering the geometry of the (Fig-1); Capacitance per unit length of the structure is given as:

$$C = (\epsilon_{re}/\ c.\eta)\ w/h + (2/3)\ (\epsilon_{re}/\ c.\eta)\ w/h + (\epsilon_{re}/\ c.\eta)\ \{2.7/\log\ (4h/t)\}$$
$$= \epsilon_{re}/\ c.\eta\ [(5/3)\ w/h + 2.7/\log\ (4h/t)] \quad (2)$$

And the characteristic impedance is expressed as:

$$Z_0 = \eta\ /\ \sqrt{\epsilon_{re}}\ [(5/3)\ w/h + 2.7/\ \text{Log}\ (4h/t)] \quad (3)$$

Where,

h = height of dielectric substrate

w = width of the metal strip.

t = thickness of the metal strip.

$\eta$ = Free space impedance = 377 Ω

$\epsilon_{re}$ = Effective dielectric constant of the medium = $(\epsilon_r + 1)/2$ for narrow strip.

Based on equation (3), a computer program has been developed and exhaustive computations have been carried out for calculations of characteristic impedance and its variation with width of metal strip in the lower Giga hertz range of frequency. The result shows that for wider strip field concentration is larger below it causing larger flow of electromagnetic energy. As a result, characteristic impedance of the microstrip structure becomes smaller. But reverse is the case with narrow metal strip. This provides useful information for the design of the microstrip structure of good selectivity.

## 4. SELECTIVITY

The selectivity or figure of merit of microstriplines is very significant characteristic need to be studied for the design of microstrip structure and its usefulness in couplers, circulators, resonators, antenna and coupled cavities of high selectivity. The selectivity depends on the losses taking place inside the structure during the flow of microwave energy. There are too important losses in this structure:

(i) Metallic loss

(ii) Dielectric loss


CC-0. In Public Domain. Gurukul Kangri Collection, Haridwar

Digitized by Arya Samaj Foundation Chennai and eGangotri



Assuming these losses per unit length to be small, the term attenuation factor α is used to represent this loss. Here α is written as:

$$\alpha = \alpha_c + \alpha_d \quad (4)$$

Where,

$\alpha_c$ denotes metallic loss and $\alpha_d$ denotes dielectric loss factor.

**Metallic loss**

Pucel *et al* (1968) derived the expression for $\alpha_c$ as;

$$\alpha_c = 8.68 (R_S / Z_0 w) \text{ dB/unit length} \quad (5)$$

Where,

$R_S$ = Surface resistivity

$= \sqrt{(\pi \mu f / \sigma_c)}\ \Omega/m^2$

$= 11.58 \times 10^{-3}\ \Omega/m^2$

f = operating frequency

= 2 GHz

$\alpha_c = 1.7\ \mu\Omega$ for Cu.

$\mu = 15.57 \times 10^{-7}$ H /m for Cu

Putting different values of w and $Z_0$, $\alpha_c$ has been calculated.

**Dielectric loss**

Welch and Pratt (1966) have established an expression for dielectric loss, further used by Pucel *et al* (1968) which is expressed as;

$$\alpha_d = (27.3 \tan\delta / \lambda_0)(\epsilon_r / \sqrt{\epsilon_{re}})(\epsilon_{re} - 1/\epsilon_r - 1) \text{ dB/unit length} \quad (6)$$

Where,

$\lambda_0$ = Free space wavelength

= 15 cm at 2 GHz frequency.

$\epsilon_r = 3.75$

$\tan\delta = 10^{-4}$ for fused quartz

$\epsilon_{re}$ = Effective dielectric constant of the medium used.

$= (\epsilon_{re}+1)/2$ for narrow strip.

Calculating these losses selectivity can be studied. A simple formula for the selectivity of the microstrip line has been given by Delinger (1971) and Schneider (1969) and expressed as;

$$\text{Selectivity} = S = 27.3 / \alpha \lambda_g \quad (7)$$

Where, $\lambda_g$ = guide wavelength of microstrip line.

This shows that selectivity of microstrip line is the inverse of total loss factor and guide wavelength. With the help of equation (4) total loss factor has been calculated and using equation (7) selectivity has been obtained. Further exhaustive computations have been carried out for obtaining selectivity for



CC-0. In Public Domain. Gurukul Kangri Collection, Haridwar

Digitized by Arya Samaj Foundation Chennai and eGangotri


different strip width and different frequency. The variation of total loss factor with strip geometry is shown in Fig- (3).

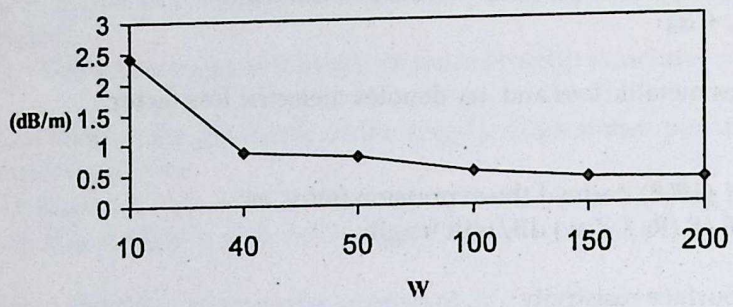


**Fig.3: Variation of W with strip width**

The selectivity has been plotted against strip width and operating frequency is shows in Fig-(4) & (5).

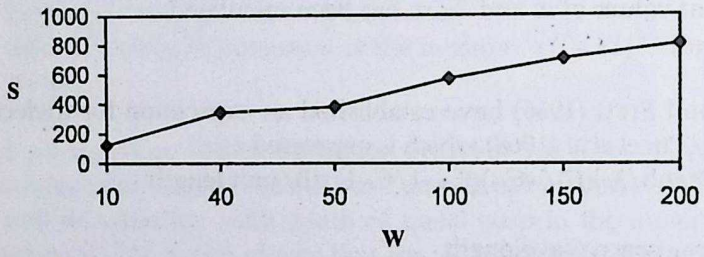


**Fig.4: Variation of selectivity with strip width**

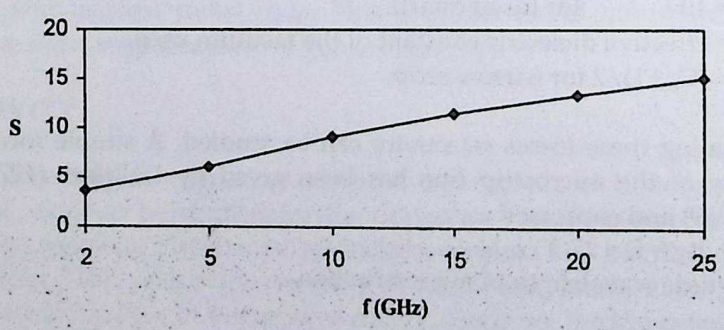


**Fig-5: Variation of selectivity with operating frequency**


CC-0. In Public Domain. Gurukul Kangri Collection, Haridwar

Digitized by Arya Samaj Foundation Chennai and eGangotri

## STUDY OF VARIATION OF SELECTIVITY OF MICROSTRIPLINE WITH STRIP GEOMETRY AND OPERATING FREQUENCY

### 5. RESULT AND DISCUSSION

Variation of total loss factor with width of metal strip reveals that with increase of width total loss decreases sharply showing concentration of more and more energy below the strip in the dielectric medium. Also, guide wavelength shows a slight decrease with increase of width of metal strip. Further variation of selectivity of microstrip line shows a sharp increase in selectivity with increase of metal strip width. The calculations of selectivity of the structure keeping strip width and permittivity fixed have been carried out for different frequencies. The result has been plotted keeping frequency on X-axis and selectivity on Y-axis shown in Fig- (5). This shows that selectivity increases with increase of frequency. The rate of increase is almost the same in the lower GHz frequency range but becomes abnormal high in higher GHz frequency range of frequency dispersion effect is higher. Thus, selectivity is smaller for narrow strip and larger for wide strip. The selectivity of microstrip using Copper strip and fused quartz dielectric substrate has been experimentally obtained by Van *et al* (1970), which shows good agreement with the present results.

### 6. CONCLUSION

This concludes that wider metal strip is more useful for larger flow of power through the structure with smaller dissipation. But dispersion effect is smaller in lower GHz frequency range than the higher GHz range of frequency. For higher selectivity or figure of merit and higher storing ability higher frequency, higher relative permittivity and wider metal strip are more useful. This study helps a designer to design and fabricate a practical microstrip transmission structure, which will be used in coupler, filter, and oscillator and antenna circuits. This work has the scope for future work also.

### ACKNOWLEDGEMENT

The author wish to thank Dr. H.L.Sah, Ex. H.O.D. Deptt. Of Electronics, B.R.A.Bihar University, Muzaffarpur and Dr. S.K.Kaul, I.I.T. Delhi, for the guidance and inspiration.

### REFERENCES

1. Denlinger, E.J. 1971."A frequency Dependent Solution for Microstrip Transmission Lines", *IEEE Tran. MTT*, Vol. 19: 30-39.


CC-0. In Public Domain. Gurukul Kangri Collection, Haridwar

Digitized by Arya Samaj Foundation Chennai and eGangotri



2. Kaul,S.K. "Strip line transmission for MIC's", *Wiley Publication*, New Delhi, 1992.

3. Pucel,R.A. *et al.*,1968. "Losses in Microstrip", *IEEE MTT*, Vol. 16, 342-350, 1968.

4. Schneider, M.V. 1969."Dielectric loss in integrated Microwave circuits", *Bell system, Technical Journal*, Vol.48: 2325-2332.

5. Selvester,P.1968."TEM wave properties of microstrip transmission lines and of coupled pair of microstrip lines", IEEE *Trans. Microwave Theory Technique*, Vol.16:1021-1027.

6. Singh,K.B. and Sah,H.L.2000."Investigation of Characteristics of Microstrip directional coupler", *J. of Institute of Engineers, India* ,Vol.80: 36-42, March 2000.

7. Singh,K.B. and Sah ,H.L.2003."Study of variation of selectivity of microstripline with strip width" *NSAML*, 143-146, 2003.

8. Vendelin, G., Pavio, A., and Rohde, U., " Microwave circuit Design using Linear and Nonlinear Technique, J. Wiley,P. 37-44, 1990.

9. Wheeler, H.A.1965."Transmission line properties of parallel strip separated by dielectric sheet"; *IEEE, Tr. MTT*-13:172-185.

10. Welch,J.D. and Pratt,H.J.1966. "Losses in Microstrip Transmission System for MIC", *NEREM, Ree*, Vol.8, 100-101.

11. Van , J.H.C. *et al.* "Properties of microstriplines on fused quartz", *IEEE- Tr. MTT*, pp. 113-115, Sep. 1970.


CC-0. In Public Domain. Gurukul Kangri Collection, Haridwar

ISSN-0970-6569
Bulletin of Pure and Applied Sciences Vol.28D(No.1)2009:P.29-41
Digitized by Arya Samaj Foundation Chennai and eGangotri

# PREPARATION AND CHARACTERISATION OF LITHIUM – DOPED AND NICKEL – DOPED $Co_3O_4$ FILMS

**G.Wellington Fernando and S. Alfred Cecil Raj**
Dept. of Physics, St. Joseph's College (Autonomous), Tiruchirappalli (TN),India

**ABSTRACT**

A Novel material of Lithium – doped and Nickel – doped $Co_3O_4$ thin films has been successfully prepared and The deposited films were annealed as mentioned in the case of lithium – doped films and made ready for characterisation. The Li – doped and Ni – doped $Co_3O_4$ have been characterized by different instrumentation techniques like XRD pattern , thickness measurement , SEM, Optical behaviour , Electrical resistivity . The Absorption for 0.0025M Li doped $Co_3O_4$ is higher than the pure $Co_3O_4$, while for other concentrations absorption decreases with the increases in molarity in concentration of the dopant. Same trend is observed for Ni doped $Co_3O_4$ also.

**Key words:** Thin Films, Characterization methods, Optical behaviour, Electrical resistivity, XRD Pattern.

## 1. INTRODUCTION

Lithium – doped cobalt oxide film has attracted special attention in the context of its application in rechargeable lithium – ion batteries (Thacteracy *et al*,1983,Shysukun *et al* ,1993,Braussely *et al*,1995,Byourand and Jarascom ,1992,Debmas and Saadoune 1992 ) Lithium – doped $Co_3O_4$ has been studied by Rasiya and Treasury (1983). Also Nickel – doped $Co_3O_4$ has been reported as having a high performance when used as an electrode for oxygen reduction and water electrolysis (King 1978,Augelo and Jaseva 1977,Augelo *et al* 1991, Gennero de Ehialvo 1993). Studies on the physical chemical and electro chemical catalytic properties of complex oxides with the special structure, particularly $Co_3O_4$ and Nickel – doped $Co_3O_4$ and Nickel – doped $Co_3O_4$ have received considerable attention ( Boggio *et al* 1987,Trasathi 1984, Vartires *et al* 1987,Iwakura *et al* 1981, Carugati *et al* 1983, Pirovano and Trasattit 1984, Burke and Mccarthy 1988) as they are low cost, easily available, reasonably stable and catalytically active materials. In this Paper, the preparation and characterization of both Lithium – doped and nickel – doped $Co_3O_4$ thin films are described.

## 2. PREPARATION OF THIN FILMS

### A) Lithium – doped thin films

In order to prepare the precursor required for preparing thin film 0.237 gms of cobalt chloride $CoCl_2\ 6H_2O$ is mixed with 50ml of double distilled water.

Corresponding author: *S. Alfred Cecil Raj, Dean of Sciences, St. Joseph's College, Tiruchirappalli – 620 002. Tamilnadu,.India, Ph : 0431 – 4226438 (O), Fax: 0431 – 2701501
CC-0. In Public Domain. Gurukul Kangri Collection, Haridwar

Digitized by Arya Samaj Foundation Chennai and eGangotri


Appropriate amount of Lithium chloride is added in order make a Lithium doped $Co_3O_4$ thin film.

0.0025 M of Lithium doped : $42.40 \times 0.0025 \times \frac{50}{1000} = 0.053$ gm

0.005 M of Lithium doped : $42.40 \times 0.005 \times \frac{50}{1000} = 0.106$ gm

0.0075 M of Lithium doped : $42.40 \times 0.0075 \times \frac{50}{1000} = 0.159$ gm

0.001 M of Lithium doped : $42.40 \times 0.01 \times \frac{50}{1000} = 0.212$ gm

The resulting precursor is well-stirred and kept ready for deposition of the film by spray pyrolysis technique.

**B. Nickel – doped $Co_3O_4$ films**

0.237 gms of cobalt chloride is added to 50ml of doubly distilled water in order to prepare 0.02m of cobalt chloride precursor appropriate amount of nickel chloride is added to prepare the precursor required to deposit nickel – doped $Co_3O_4$ this films.

0.0025 M of Nickel doped: $237.71 \times 0.0025 \times \frac{50}{1000} = 0.0297$ gm

0.005 M of Nickel doped : $237.71 \times 0.005 \times \frac{50}{1000} = 0.0594$ gm

0.0075 M of Nickel doped : $237.71 \times 0.0075 \times \frac{50}{1000} = 0.0891$ gm

0.01 M of Nickel doped : $237.71 \times 0.01 \times \frac{50}{1000} = 0.1189$ gm

This resulting aqueous solution is well – stirred and is used to deposit spray pyrolysed films of nickel – doped $Co_3O_4$ this films.

## 3. DEPOSITION OF FILMS

The prepared aqueous solution of cobalt chloride and lithium chloride, when sprayed over the hot substrates, fine droplets of solution thermally decompose after falling over the surface of hot substrates. The carrier gas tube is supplied with purified air through a gas flow mater. The solution flow rate is maintained at 3ml / min. The pressure of the carrier gas is maintained at 12kg / $cm^2$ glass slides of (75mm x 25mm x 1.45mm) are thoroughly cleared in chromic acid and degreased they were thoroughly cleaned in distilled water and then dried in a hot air oven before spraying was done. The thermo – couple monitored


CC-0. In Public Domain. Gurukul Kangri Collection, Haridwar

Digitized by Arya Samaj Foundation Chennai and eGangotri



substrate temperature was maintained at 573K. The spraying was done for 50 s and another 50 s was allowed between successive spraying. The film was annealed after the spraying was over. The film was raised to a temperature 673K and maintained for 2 hours. Then it is cooled to room temperature. This was repeated three times. After annealing the films were ready for characterisation.

The nickel - doped $Co_3O_4$ thin films were deposited in the identical parametric condition the glass slides were of the size 75mm x 25mm x 1.45mm. The substrate temperature was 673K and the solution flow rate was 3ml / min. The carrier gas has a pressure 12kg / $cm^2$. The deposited films were annealed as mentioned in the case of lithium - doped films and made ready for characterisation.

## 4. RESULTS AND ANALYSIS

### 4.1 Thickness measurement

**A) Lithium - doped $Co_3O_4$ film**

With the help of the KEROY single pan balance the weight of each coated substrate was taken in air and in water. Knowing the surface area of each substrate the following values were obtained as shown in Table 1.

**Table 1 :** Thickness of Lithium - doped $Co_3O_4$ films for various molar weights

| Molar Weight (M) | 0.0025 | 0.005 | 0.0075 | 0.01 |
|---|---|---|---|---|
| Thickness (μm) | 85.00 | 93.16 | 85.34 | 92.72 |

**B. Nickel - doped $CO_3O_4$ film**

Table 2 shows values were obtained for the thickness of nickel - doped film with different molarity concentrations.

**Table 2 :** Thickness of Nickel - doped $Co_3O_4$ films for various molar weights

| Molar Weight (M) | 0.0025 | 0.005 | 0.0075 | 0.01 |
|---|---|---|---|---|
| Thickness (μm) | 85.23 | 76.11 | 91.43 | 98.01 |


CC-0. In Public Domain. Gurukul Kangri Collection, Haridwar

Digitized by Arya Samaj Foundation Chennai and eGangotri


## 4.2 XRD patterns

### A) Lithium – doped $Co_3O_4$ film

Fig 1 displays the XRD diagram of lithium – doped $Co_3O_4$ this film. The peaks are not much different from that of undoped $Co_3O_4$ film except that they are slightly shifted to the left. This does not show any additional peak. This pattern shows that lithium is very well doped into the $Co_3O_4$ host material.

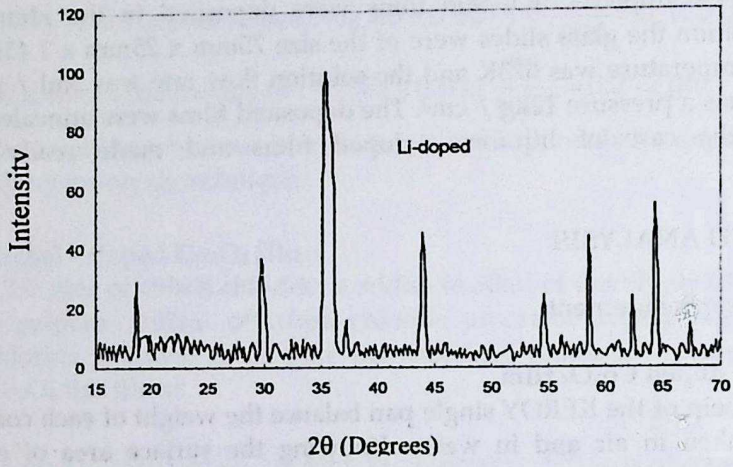


Fig 1 : XRD Pattern of lithium-doped $Co_3O_4$ film

### B. Nickel – doped $Co_3O_4$ film

The nickel – doped $Co_3O_4$ film produces an XRD pattern as shown in the Fig 2. The intensity of the peak is less than that of undoped $Co_3O_4$ film. Here too no other additional peak appear, showing that the nickel – dopant is well doped into the $Co_3O_4$ host material.

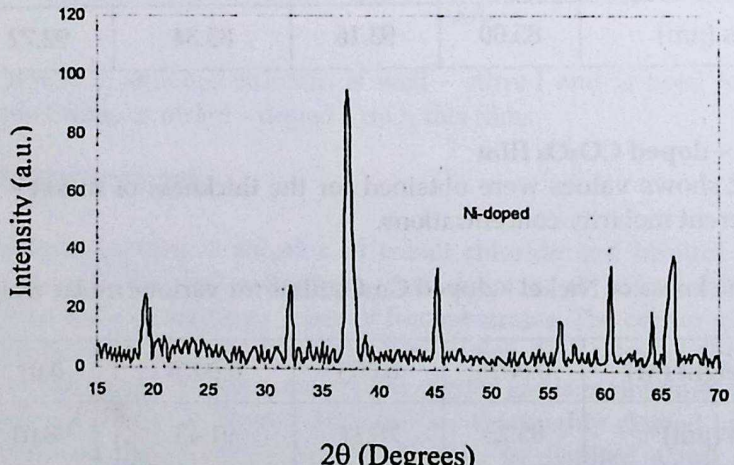


Fig 2 : XRD Pattern of nickel-doped $Co_3O_4$ film


CC-0. In Public Domain. Gurukul Kangri Collection, Haridwar

Digitized by Arya Samaj Foundation Chennai and eGangotri

## 4.3 SEM

### A) Lithium – doped $Co_3O_4$ film

The scanning electron micrograph of the lithium doped film is shown in Fig 3. The film has uniform surface morphology. Doping with lithium results in the appearance of well – shaped crystallites. The morphology showed porous structure with uneven surface

**Fig 3 :** SEM image of lithium doped $Co_3O_4$ film

### B. Nickel – doped $Co_3O_4$ film

The surface morphology of the spray – deposited nickel – doped $Co_3O_4$ thin film is shown in Fig. 4. The SEM shows the nanocrystalline grains with some overgrown clusters. This overgrowth can be explained on the basis of nucleation and coalescence process. Initially green nano grains may have increased their size by further deposition and come closer to each other.

**Fig. 4 :** SEM image of nickel – doped $Co_3O_4$ film

## 4.5 OPTICAL BEHAVIOUR

### A) Lithium – doped $Co_3O_4$ film

**Direct transition**

From Figures 6 to 9 the plots of $(\alpha h\nu)^2$ Vs $(h\nu)$ is displayed. In order to confirm the nature of theoretical transition in the sample the optical data were analysed using classical relation :


CC-0. In Public Domain. Gurukul Kangri Collection, Haridwar

Digitized by Arya Samaj Foundation Chennai and eGangotri


$$\alpha = \frac{\alpha_0 (h\nu - E_g)^n}{h\nu} \qquad (1)$$

where $\alpha_0$ is a constant, and on a constant depending on the kind of optical transition that prevails specifically n is ½ for the transition having direct.

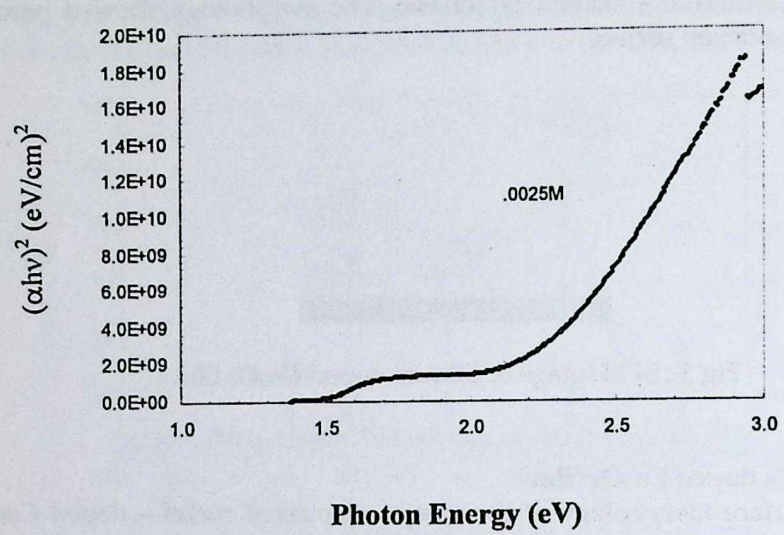


Fig. 6 : Plot of $(\alpha h\nu)^2$ Vs hν of 0.0025 M lithium-doped $Co_3O_4$ film

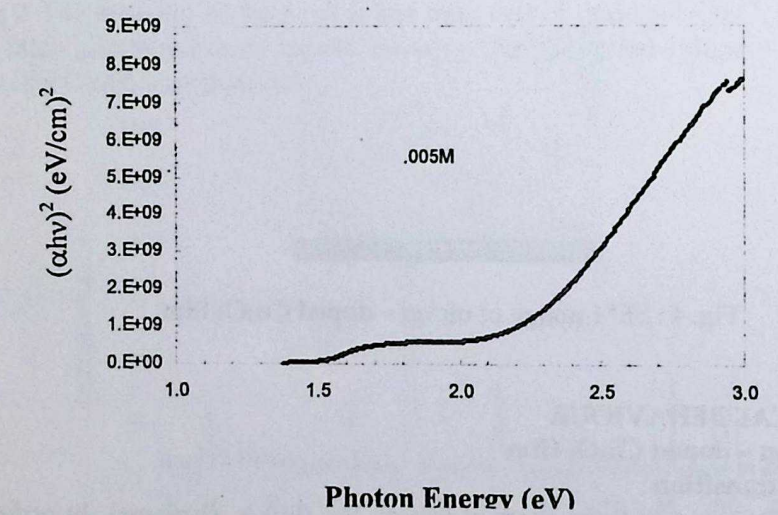


Fig. 7 : Plot of $(\alpha h\nu)^2$ Vs hν of 0.005 M lithium-doped $Co_3O_4$ film


CC-0. In Public Domain. Gurukul Kangri Collection, Haridwar

Digitized by Arya Samaj Foundation Chennai and eGangotri



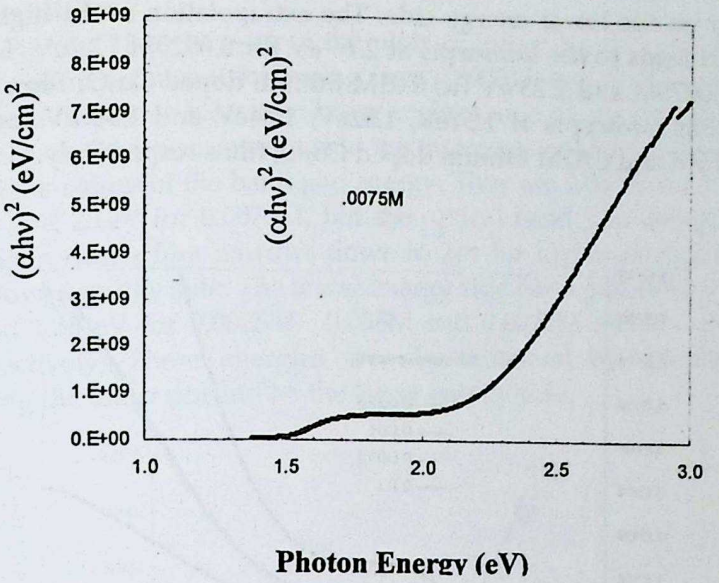


Fig. 8 : Plot of $(\alpha h\nu)^2$ Vs $h\nu$ of 0.0075 M lithium-doped $Co_3O_4$ film

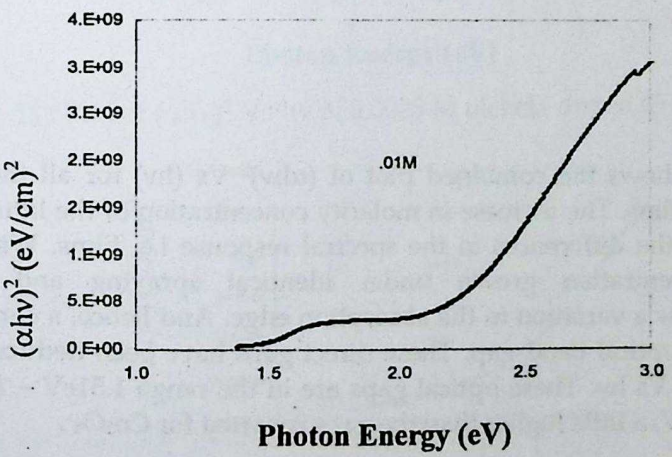


Fig. 9 : Plot of $(\alpha h\nu)^2$ Vs $h\nu$ of 0.01M lithium-doped $Co_3O_4$ film


CC-0. In Public Domain. Gurukul Kangri Collection, Haridwar

Digitized by Arya Samaj Foundation Chennai and eGangotri


The plot consists of two straight basic region are on the higher energy side and the other on the lower energy side. The extrapolation at the higher side of the linear part leads to the intercepts at 2.16 eV for 0.0025M, 2.2eV for 0.005M, 2.22 eV for 0.0075M and 2.23 eV fro 0.01M lithium doped $Co_3O_4$ film. The lower energy side has intercepts at 1.51eV, 1.52eV, 1.54eV and 1.56 eV for 0.0025M, 0.005M, 0.0075M and 0.01M lithium doped $Co_3O_4$ films respectively.

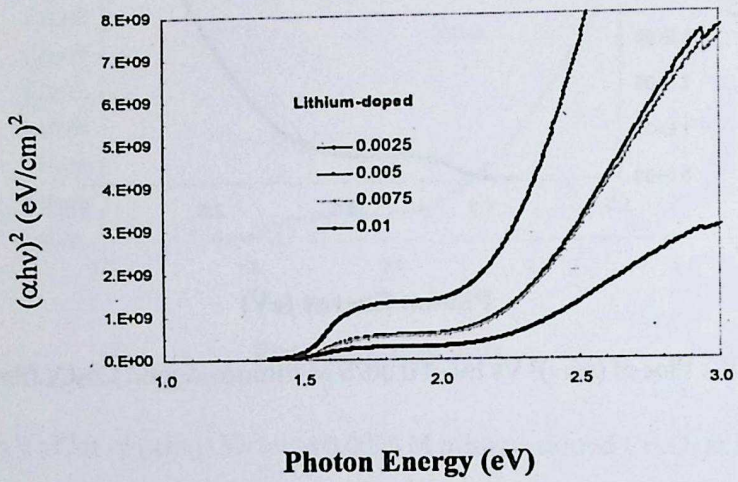


Fig. 10 : Combined plot of $(\alpha h\nu)^2$ Vs $h\nu$ of lithium-doped $Co_3O_4$ films

Fig 10 shows the combined plot of $(\alpha h\nu)^2$ Vs $(h\nu)$ for all the lithium – doped $Co_3O_4$ films. The increase in molarity concentration of the lithium dopant is reflected in the differences in the spectral response i.e. films. With different molarity concentration grown under identical spraying and deposition conditions show a variation in the absorption edge. And hence, a corresponding change in the optical band gap. These direct gaps have been deduced from the plots of $(\alpha h\nu)^2$ Vs $h\nu$. These optical gaps are in the range 1.51eV – 1.56eV and 2.16eV – 2.23 eV, a little higher than the gaps reported for $Co_3O_4$ .

These observations suggest that it is possible to control the optical properties of spray – pyrolysed lithium – doped $Co_3O_4$ film by changing molarity concentration of the lithium – dopant.

CC-0. In Public Domain. Panini Kanya Maha Vidyalaya Collection. Haridwar

Digitized by Arya Samaj Foundation Chennai and eGangotri

**B. Nickel – doped $Co_3O_4$ films**

**Direct transition**

The Figures 11 to 14 portray the plots of $(\alpha h\nu)^2$ Vs $(h\nu)$ for the film with the dopant molarity constant increasing from 0.0025M. to 0.01M , Like the other samples, these films also have two linear regions, one on the higher energy side and the other on the lower energy side the intercepts got by extrapolating these region give the values of the band gap energy. They are 2.06 eV for 0.0025M, 2.08 for 0.005M and 2.1eV for 0.0075M, but the optical band gap energy for 0.01M nickel – doped $Co_3O_4$ film narrows down to 2ev for higher energy side and 1.3 eV for the lower energy side. The lower energy side band gap energy are 1.32 eV, 1.35 eV and 1.38 eV for 0.0025M, 0.005M and 0.0075M nickel – doped $Co_3O_4$ films respectively. These energies are also obtained by intercepts got by extrapolating the linear portion on the lower energy side.

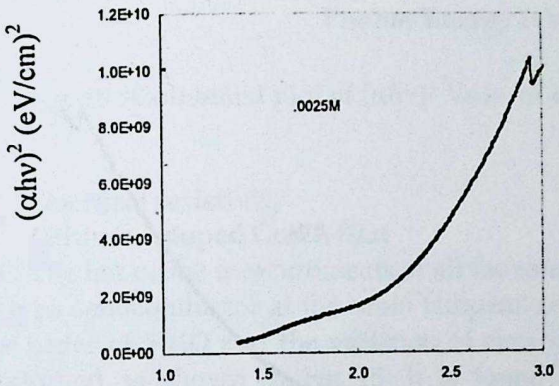


**Fig. 11 :** Plot of $(\alpha h\nu)^2$ Vs $h\nu$ of 0.0025 M nickel - doped $Co_3O_4$ film

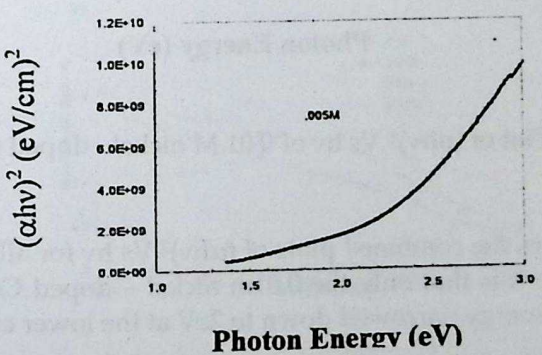


**Fig. 12 :** Plot of $(\alpha h\nu)^2$ Vs $h\nu$ of 0.005 M nickel - doped $Co_3O_4$ film


CC-0. In Public Domain. Gurukul Kangri Collection, Haridwar

Digitized by Arya Samaj Foundation Chennai and eGangotri

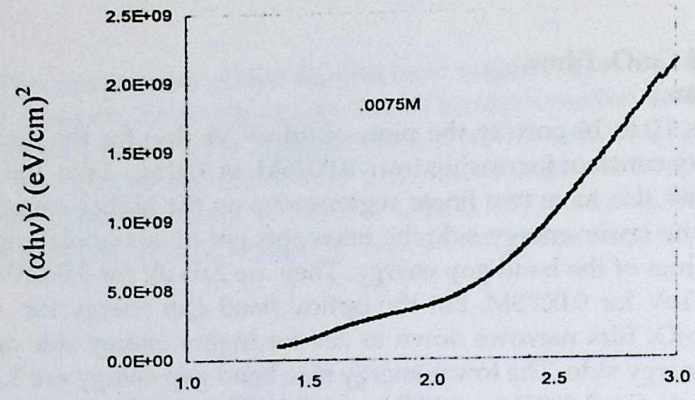


**Fig .13** : Plot of $(\alpha h\nu)^2$ Vs hν of 0.0075 M nickel - doped $Co_3O_4$ film

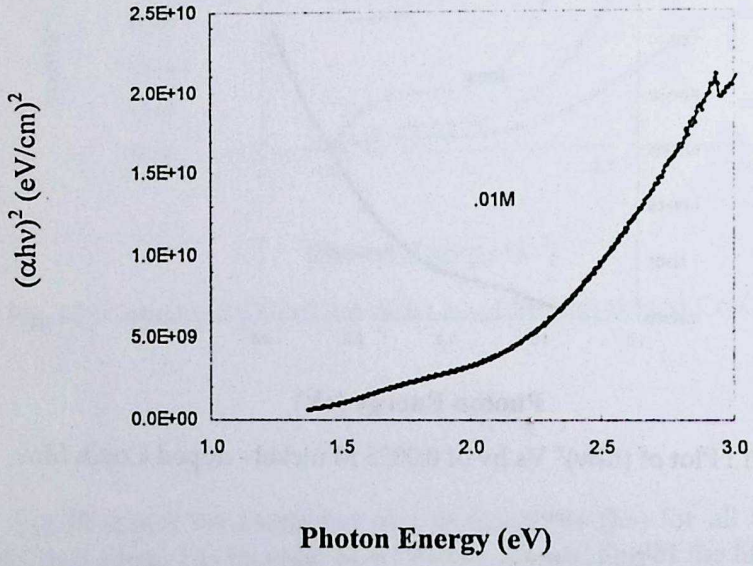


**Fig. 14 :** Plot of $(\alpha h\nu)^2$ Vs hν of 0.01 M nickel - doped $Co_3O_4$ film

Fig 15 shows the combined plots of $(\alpha h\nu)^2$ Vs hν for all the nickel – doped $Co_3O_4$ films. Here it is that only the 0.01m nickel – doped $CO_3O_4$ films gets the optical band gap energy narrowed down to 2eV at the lower energy side.


CC-0. In Public Domain. Gurukul Kangri Collection, Haridwar

Digitized by Arya Samaj Foundation Chennai and eGangotri


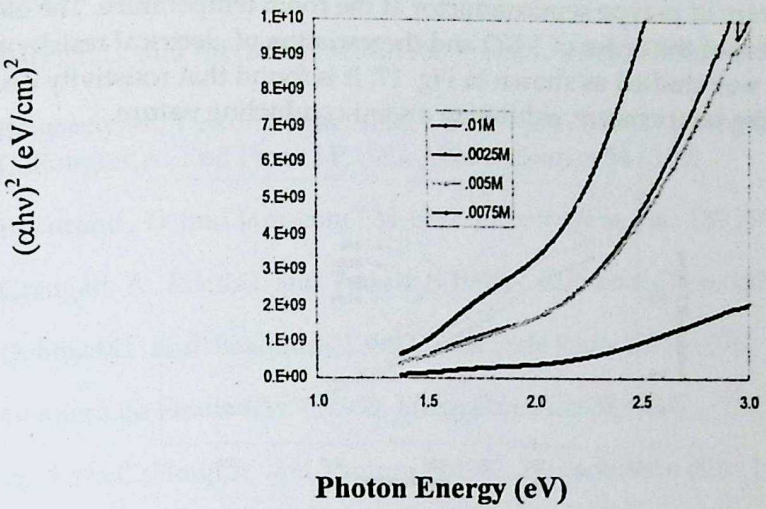


Fig. 15 : Combined plot of $(\alpha h\nu)^2$ Vs hν of nickel - doped $Co_3O_4$ film

## 4.6 Electrical resistivity

### A) Lithium – doped $Co_3O_4$ film

The hot probe measurements of all the samples show that these films were of p-type semiconductor at the room temperature. The electrical resistivity were of the order of 3 KΩ and the variation of electrical resistivity with temperature was studied as shown in Fig 16. It is found that resistivity decreases with increasing temperature, exhibiting a semi-conducting nature. For 0.0075M, there is slight hump at 420K.

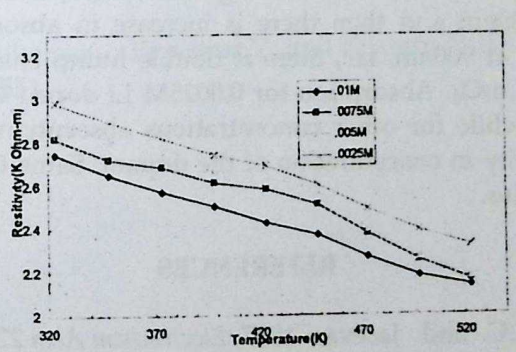


Fig 16 : Plot of resistivity Vs temperature of the lithium - doped film of different molarity concentrations.


CC-0. In Public Domain. Gurukul Kangri Collection, Haridwar

Digitized by Arya Samaj Foundation Chennai and eGangotri


**B) Nickel – doped $Co_3O_4$ films**

The hot probe measurements of all the nickel doped samples show that these films were of p-type semiconductor at the room temperature. The electrical resistivity were of the order of 1 KΩ and the variation of electrical resistivity with temperature was studied as shown in Fig. 17. It is found that resistivity decreases with increasing temperature, exhibiting a semi-conducting nature.

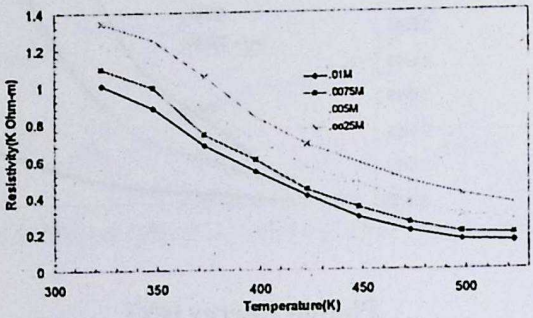


**Fig 17 :** Plot of resistivity Vs temperature of the nickel – doped $Co_3O_4$ films

## CONCLUSION

The XRD pattern of Li – doped and Ni – doped $Co_3O_4$ have shown no difference to the host matrix, which reveals that the incorporation Li / Ni into $Co_3O_4$ did not change the structure of $Co_3O_4$. Thus no new compound was formed i.e., Li / Ni very well doped into the host matrix. But the surface morphology shows that uneven over grown cluster surface. Absorption spectra of Li doped $Co_3O_4$ with different molarity concentration studied in the range 400nm to 900 nm shows that there is a greater absorption at 400 nm while at decreases upto 600nm and then there is increase in absorption upto 750 nm followed by drop at 900nm, i.e., there is double hump characteristic similar to that of undoped $Co_3O_4$. Absorption for 0.0025M Li doped $Co_3O_4$ is higher than the pure $Co_3O_4$, while for other concentrations absorption decreases with the increases in molarity in concentration of the dopant. Same trend is observed for Ni doped $Co_3O_4$ also.

## REFERENCES

1. Augelo,A.C.C. and Jaseva,S.1977. *Electrochem Acta* 22: 31.

2. Augelo,A.C.D., Gouzaleze,E.R. and Aveca,L.A. 1991. *Int. J.Hydrogen Energy* ,16 : 1.


CC-0. In Public Domain. Gurukul Kangri Collection, Haridwar

Digitized by Arya Samaj Foundation Chennai and eGangotri


3. Boggio, R.,Carugati,A. and Trasatti,S. 1987. *J. Appl Electrochem* 17 : 828.

4. Burke,L.D. and Mccarthy, M.M.1988.*J. Electro chem., Chem, Soc* 135 : 1175.

5. Braussely,M., Perton,F., Bieusan,P., Bodet,J.M. Labat,J., Lecerf,A., Delmas, C.,Rougier,A., and Peres,J.P.1995. *J.Power Sources* 54 : 109.

6. Byourand , D. and Jarascom,J.M.1992. *J.Electrochem, Joc.* 139 : 937.

7. Carugati, A., Locti,G. and Trasatti,S.1983. *J. Eletraand Chem*, 143: 419.

8. Debmas,C. and Saadoune,I.1992. *Solid State Jonics* 53-56 : 370.

9. Gennero de Ehialvo,M.R..1993. *Electrochin Acta* 38 : 2247.

10. Iwakura,C.,Houji,A. and Tamura,H.1981. *Electachim An* d26 : 1319.

11. King,E.J. 1978. *A.C.C. Tresung Electrochem, Acta* 19 : 485.

12. Pirovano,C. and Trasattit,S.1984. *J. Electroanal Chem.* 180 :171.

13. Rasiya,P. and Tseung,A.C.C.1983. *J.Electrochem. Soc* 130 : 365.

14. SHysuku,T., Urda,A.,Nagayana,M., Wakoshi,Y.I. and Komori,H.1993. *Electrochem, Acta* 38 : 1159.

15. Thacteracy ,M.M., David,W.F. and Brace,P.G.,1983. *Mater. Res. Bull* 18 : 461.

16. Trasathi,S.1984. *Electrochim Acta* 29 : 1503.

17. Vartires,I., Mihelss,A., Popescur,V. and Spataru,N.1987. *Revure Rounaine de Chinie* 32 : 551.


CC-0. In Public Domain. Gurukul Kangri Collection, Haridwar

Digitized by Arya Samaj Foundation Chennai and eGangotri

CC-0. In Public Domain. Gurukul Kangri Collection, Haridwar

ISSN-0970-6569
Bulletin of Pure and Applied Sciences Vol.28D(No.1)2009 P.43 -46
Digitized by Arya Samaj Foundation Chennai and eGangotri

# SCATTERING OF ELECTRONS BY EQUILIBRIUM PHONONS IN A TWO SUBBAND QUASI TWO DIMENSIONAL ELECTRON GAS IN A QUANTISING MAGNETIC FIELD

**Madan jee, Manish Kumar Bhatt, Sunil Kumar Mishra, Sanjiv Kumar, Vikas Kumar, and Ashok Kumar Singh*.**
University Department of Physics, B.R.A. Bihar University,
Muzaffarpur( Bihar), India.

**ABSTRACT**

We have studied the scattering of electrons by equilibrium phonons in a two subband quasi two dimensional electron gas in a quantising magnetic field. This has been studied in connection with the integer quantum Hall effect. The electron-phonon coupling constant is nearly equal to magnetic field, the phonon induced longitudinal conductivity at high enough magnetic fields may be comparable with impurity induced longitudinal conductivity. A resonant enhancement of the conductivity was found due to interaction of two Landau levels.

**Key words :** Scattering, Phonon, Conductivity, Quantum Hall effect, Impurity, Concentration.

## INTRODUCTION

Benedict *et al* (1999) made a detailed analysis of the acoustic phonon emission and absorption spectra in two dimensional electron systems has been carried out in connection with phonon absorption spectroscopy, which is used to investigate electronic states in both integer and fractional quantum Hall effects. Fal'ko and Challis (1993) showed that at a certain stage of suppression of the one phonon transitions dominate the electron relaxation rate. However in a two subband system the electron relaxation rate can still be due to the one-phonon transition occurring between Landau levels of different size quantization subbands. Maksym (1992) investigated an oscillatory behavior of the electron lifetime was found in a two-sub band system. Apalkov and Portrioi (2002) studied the electron-phonon scattering and they neglected the effects related to the Coulomb interaction between the electrons. These effects significantly change the result at low temperatures. The two dimensional case of transition was considered by Ablyazov *et al* (1991), where the electron scattering occurred on a random potentials of impurities. At $B \neq 0$ the Fermi surface is obtained. Usually, the donor supply of the electrons into the two dimensional layer is not sufficient to achieve filling of the second size quantization subband. However a significant increase in the concentration can be achieved by illuminating the sample with photons of energy close to the band gap of GaAs. The photo excited electrons come either from the Dx centers in the AlGaAs layer or from the valence band of

* H.N.K. Inter College Ara, Bihar, India.
CC-0. In Public Domain. Gurukul Kangri Collection, Haridwar

Digitized by Arya Samaj Foundation Chennai and eGangotri



the bulk GaAs producing a charge separation at the interface was observed by Lang (1986) and Kastalsky (1984). The two dimensional electron concentration can be tuned within a large range using the method of continuous photo excitation - showed by Kukushkin *et al* (1989). Population of the second sub band of size quantization in a magnetic filed has been observed by Turberfield *et al* (1990) in an experiment related to magneto-optical studies of the integer and fractional quantum Hall effects. Gusev *et al* (2003) showed that the disorder mediated magneto conductivity is noticeably smaller in wide parabolic quantum wells, which represent the best system for observation of the said effect. The enhancement of electron-phonon scattering near the Landau level intersection is possibly responsible for some features observed in magneto thermal conductivity of highly oriented pyrolitic graphite was investigated by Ocana *et al* (2003) and Ulrich and Esquinazi (2004).

## RESULTS AND DISCUSSION

The largest possible value of longitudinal conductivity $\sigma xx$ is obtained for the crossing of the Landau levels with smallest possible numbers i.e. $l$=1 and $l'$=0 and belonging to the two lowest subbands of size quantization. Graph 1 shows the dependence of $\sigma xx$ on the magnetic field B in the vicinity of an interaction of two Landau levels in parabolic quantum well. The magnetic field corresponding to the intersection of the levels in that of the minimum on the graph. The two maxima appear at magnetic fields close to those at which the electron-phonon scattering rate is maximum. The distance between the Landau levels at the maxium of $\sigma xx$ is of the order $T_\lambda = \hbar s \backslash \lambda$. Graph-2 shows the comparison of different contributions of $\sigma xx$. At a small value of quantum well width a, the deformation potential mechanism as shown as dashed line, dominates the dissipative conductivity. However at a larger value of a, the piezoelectric mechanism is the dominant contribution to $\sigma xx$. The relevant phonon momentum is related to the quantum well width and to the magnetic length $q^{-1} \sim a \sim \lambda$. The characteristics well width at which the cross over from the deformation potential to the piezo electric mechanism happens is given by $a \sim E_o k/eh$. The actual crossover happens at a smaller value of a, owing to a larger overlap integral of the electron with the phonons via the piezo electric interaction.

## CONCLUSION

An enhancement of the electron scattering in a two subband system occurs at zero magnetic field, when the second quantization sub band starts being filled with electrons. This effect is interns of a Lifeshitz topological transition of the Fermi surface. One phonon and two phonon mechanisms of


CC-0. In Public Domain. Gurukul Kangri Collection, Haridwar

Digitized by Arya Samaj Foundation Chennai and eGangotri



electron conductivity were calculated and compared and found to be good agreement with previously measured value, The effects of multiphonon scattering are important at high temperatures. It was also found that the broadening of each of the two considered Landau levels is larger than the characteristics phonon energy $T_\lambda$.

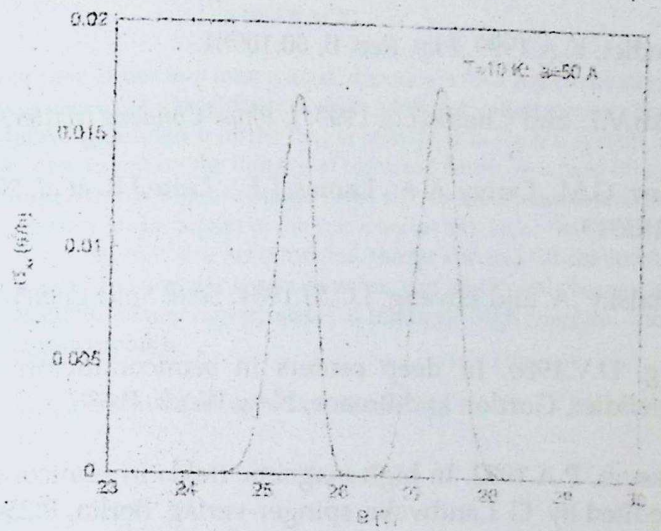


**Graph - 1 :** The dissipative conductivity as a function of magnetic field in the vicinity of the crossing of Landau levels.

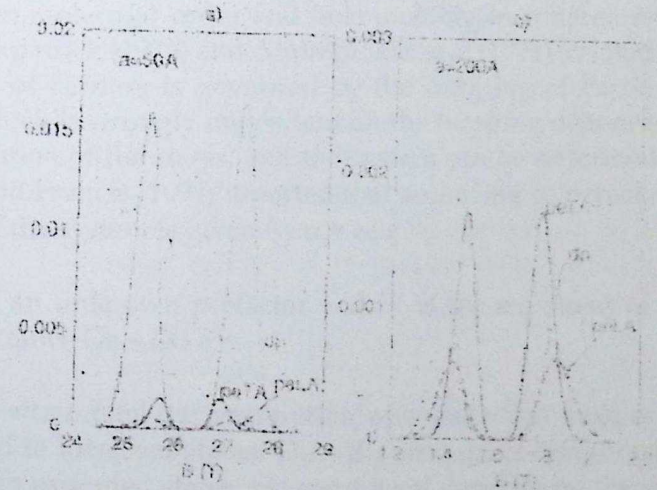


**Graph -2 :** A Comparison of contributions to $\sigma_{xx}$ from different mechanisms of electron-phonon interaction at two values of the quantum well width *a*.


CC-0. In Public Domain. Gurukul Kangri Collection, Haridwar

Digitized by Arya Samaj Foundation Chennai and eGangotri



## REFERENCES


1. Ablyazov,N.N., Kuchiev,M. and Raikh,M.E. 1991. *Phys. Rev.* B, 44 : 8802.

2. Apalkov,V.M. and Portnoi, M.E.2002. *Phys, Rev.* B, 65: 125310.

3. Benedict, K.A.1999. *Phy. Rev.* B, 60:10984.

4. Fal'ko,V.I. and Challis,L.J. 1993. *J. Phys. Condens Matter*, 5: 3945.

5. Gusev, G.M., Quivy,A.A., Lamas,T.E., Leite,J.R. *et al*, 2003, *Pys. Rev.* B, 67: 155313.

6. Kastalsky ,A. and Hwang, J.C.M.1984. *Solid State Commun*, 51 : 317.

7. Lang, D.V.1986, In deep centers in semiconductors edited by S.T. Pantelidies, Gordon and Breach, New Work, P.486.

8. Maksym, P.A.1992. In high magnetic fields in semiconductors Physics III, edited by G. Landwehr, spinger-verlag, Berlin, P.254.

9. Tuberfield,A.J., Haynes,S.R. *et al*, 1990. *Phys. Rev. B, Lett.* 65: 637.

10. Ulrich ,K. and Esquinazi, P.2004. *J. Low Temp. Phys.* 137: 217.



CC-0. In Public Domain. Gurukul Kangri Collection, Haridwar

ISSN-0970-6569
Bulletin of Pure and Applied Sciences. Vol.28D(No.1)2009.P.47-51
Digitized by Arya Samaj Foundation Chennai and eGangotri

# THE INFLUENCE OF TEMPERATURE AND THE FILLING OF STATES ON THE CONDUCTIVITY OF A VARIABLE RANGE HOPPING SYSTEM WITH AN EXPONENTIAL DISTRIBUTION OF LOCALIZED STATE ENERGIES.

**Ashok Kumar Singh, Janardan Choudhari*, Ashok Kumar***, Dilip Kumar Verma, and Manoj Ranjan**
HNK Inter College, Ara, Bihar, India,

**ABSTRACT**

A carrier may either hop over a small distance with a high activation energy or hop over a long distance with a low activation energy. The temperature dependence of the carrier transport in such a system is strongly dependent on the density of localized states. In a field effect transistor, an applied gate voltage gives rise to the accumulation of charge carriers in the region of the semiconducting layer that is close to the insulator. As these accumulated charge carriers fill the lower lying states of the organic semiconductor, any additional charges in the accumulation layer occupy states at relatively high energies. This causes higher mobility.

**Key words :** Carrier, hop, Activation energy, Gates, Mobility.

## INTRODUCTION

Brown and Jarrett (1997), Horowitz and Hajlaoui (1995) showed that the field effect mobility of holes in organic transistors depends on the temperature and applied gate bias. Gundlach *et al* (1997) reported that mobility is high in thin film transistors of evaporated pentacene. Garnier *et al* (1996) showed the connection between molecular order and hole mobility in conjugated oligomers and polymers. Kirkpatrick (1973) and Ambegaokar *et al* (1971) studied that at low bias the transport of carriers is governed by the hopping of carriers between localized states, which is strongly dependent on the hopping distances as well as the energy distribution of the states, and the system can be described as register network. Taylor and Francis (1994) reported that according to percolation theory the conductivity of the system is given by $\sigma = \sigma_0 e^{-Sc}$ .

Where $\sigma_0$ is an unknown prefactor and Sc is the exponent of the critical percolation conductance $Ge = Go\ e^{-Sc}$.

In the Horowitz model the assumption was made that most of the charge carriers are trapped in localized states. Then the amount of temporarily released charge carriers to an extended states transport level depends on the energy level of the localized states, temperature and the gate voltage. When the extended

*R.B.S. College, Chandi, Dhenuki, Bihar, **R.S.S. College, Chochha, ***Ganga Devi Mahila College, Patna, Bihar, India, ****Science College, Patna, Bihar.
CC-0. In Public Domain. Gurukul Kangri Collection, Haridwar

Digitized by Arya Samaj Foundation Chennai and eGangotri


state transport occur in highly ordered vaccum - evaporated molecular films, then we do not expect it to play a role in amorphous organic films. Where the charge carriers are strongly localized. We have studied the influence of temperature and the influence of filling of states on the conductivity. Using percolation theory we obtained an analytic expression for the conductivity and this was used to obtain the field effect mobility of carriers when the material is applied in a transistor.

## RESULTS AND DISCUSSION

In a transistor the charge density is not uniform, but it decreases with the distance x from the semi conductor insulator interface. The equation for carrier occupation is δ given by

$$\delta \approx \exp(\epsilon_F / K_B T_0)\, T\,(1-T/T_0)\, T\,(1+T/T_0)$$

where $\epsilon_F$ is the Fermi energy or chemical potential. $K_B$ is the Boltzmann constant, T is the temperature of charge carrier density, $T_0$ is parameter that indicates width of the exponential distribution. We have used the assumption that most carriers occupy the sites with energies occupy the sites with energies. $\epsilon << 0$ i.e. $-\epsilon_F >> K_B T_o$. This condition is full filled when δ and T are low.

Conductance $G_{jj} = G_0 e^{-S_{jj}}$ between site i and j site are –

$$S_{ij} = 2\alpha R_{jj} \frac{|\epsilon_i - \epsilon_F| + |\epsilon_j - \epsilon_F + |\epsilon_i - \epsilon_j|}{2K_B T}$$

Where the first term on right hand side describes the tunneling process which depends on the overlap of the electronic wave function of the sites i and j. In a lower order approximation this tunneling process may be characterized by the distance $R_{ij}$ between the sites an effective over lap parameter α. The second term takes into account the activation energy for a hop upwards in energy and the occupational probabilities of the sites i and j. The occupation δ(x) depends on the distance x through the gate induced potential V(x)

$$\delta(x) = \delta_0 \exp.(eV(x)/K_B T_0)$$

Where $\delta_0$ is the carrier occupation far from the semi conductor insulator capacitance per unit area $C_i$ is $F(0) = C_i V_G / \epsilon_S$


CC-0. In Public Domain. Gurukul Kangri Collection, Haridwar

Digitized by Arya Samaj Foundation Chennai and eGangotri

# THE INFLUENCE OF TEMPERATURE AND THE FILLING OF STATES ON THE CONDUCTIVITY OF A VARIABLE RANGE HOPPING SYSTEM WITH AN EXPONENTIAL DISTRIBUTION OF LOCALIZED STATE ENERGIES.

The source drain current of the transistor in the linear regime is

$$I = WV_D / \underset{0}{\overset{t}{L}} \int dx\, \sigma [\delta(x), T].$$

Where $V_D$ is the drain voltage, L, W and t are the length, width and thickness of the channel. The field effect mobility is

$$\mu_{FE} = L / C_i W V_D \; \partial I / \partial V_D$$

A graph is plotted between drain current voltage versus gate voltage $V_G$ characteristics have been measured of both a pentacene and a polythienylene Vinylene organic thin film transistor at a range of temperatures. The precursors of both organic semiconductors are spin coated from solution of on a substrate consisting of a heavily n-doped silicon gate electrode. The temperature dependence of field effective mobility is shown in graph (1). The dependence of activation energy on gate voltage is shown in graph (2). The obtained results were compared with previously observed and calculated values and are found is good agreement.

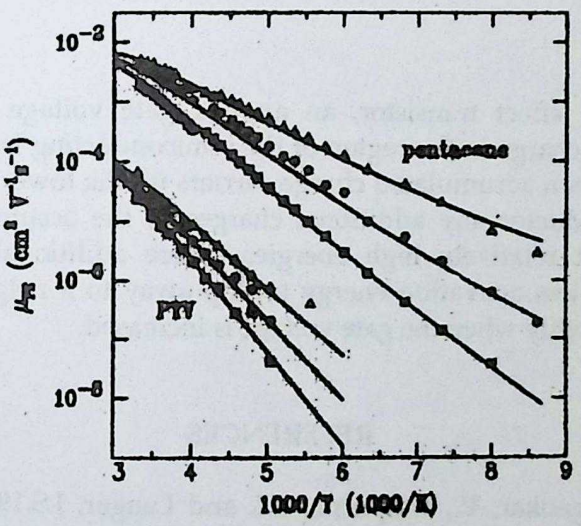


**Graph 1** : Field-effect mobility $\mu_{FE}$ in a pentacene and a polythienylene vinylene (PTV) thin-film transistor as a function of the temperature.



CC-0. In Public Domain. Gurukul Kangri Collection, Haridwar

Digitized by Arya Samaj Foundation Chennai and eGangotri


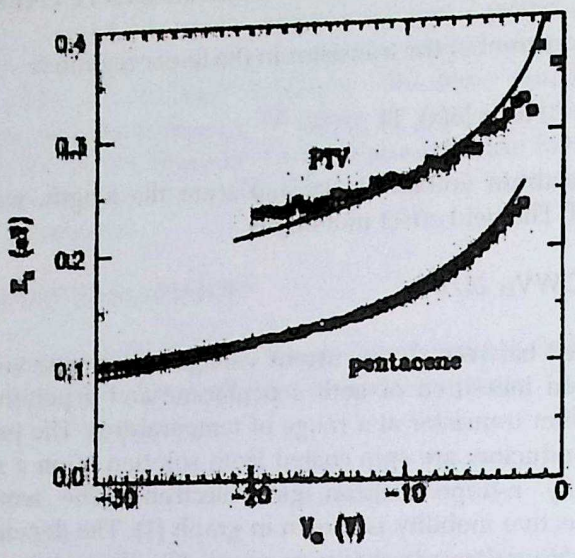


Graph 2 :Activation energy Ea for the field-effect mobility in a pentacene and a polythienylene vinylene (PTV) thin-film transistor as a function of the gate voltage $V_G$.

## CONCLUSION

In a field effect transistor, an applied gate voltage gives rise to the accumulation of charge in the region of the semiconducting layer that is close to the insulator. When accumulated charge carriers fill the lower lying states of the organic semiconductor any additional charges in the accumulation layer will occupy states at relatively high energies. These additional charges will on average require less activation energy to hop away to a neighboring site. This gives higher mobility when the gate voltage is increased.

## REFERENCES

1. Ambegaokar, V., Halpersin, B.I. and Langer, J.S.1971. *Phy. Rev.* B, 4: 2612.

2. Brown, A.R. and Jarrett, C.P. 1997. *Synth. Met.* 88: 37.

3. Garnier, F., Fichou , D. and Yassar, A. 1996. *Synth. Met.* 81: 163.


CC-0. In Public Domain. Gurukul Kangri Collection, Haridwar

Digitized by Arya Samaj Foundation Chennai and eGangotri



4. Gundlach, D.J. 1997. *IEEE Electron Device Lett.* 18: 87.

5. Horowitz, G. and Hajlaoui, R. 1995. *J. Phy.* III, 5: 355.

6. Kirkpattick, S. 1973. *Rev. Mod. Phys* 45: 574.

7. Taylor and Francis. 1994. Application of Percolation Theory.


CC-0.In Public Domain. Gurukul Kangri Collection, Haridwar

Digitized by Arya Samaj Foundation Chennai and eGangotri

CC-0. In Public Domain. Gurukul Kangri Collection, Haridwar

ISSN-0970-6569Digitized by Arya Samaj Foundation Chennai and eGangotri
*Bulletin of Pure and Applied Sciences.Vol.28D(No.1)2009:P.53 - 58*

# MOLECULAR INTERACTION IN TERNARY LIQUID MIXTURES - AN ULTRASONIC STUDY

**S. Thangapandian, V. Arumugam* and A.N. Kannappan**
Department of Physics, Annamalai University, Annamalainagar – 608 002, India

**ABSTRACT**

The experimental data for ultrasonic velocity, density and viscosity was recorded for the ternary systems of 1-propanol and acetophenone with chlorobenzene, bromobenzene and nitrobenzene at 303, 308 and 313K. From the experimental data, the adiabatic compressibility, free length, free volume and internal pressure for the mixtures were calculated. The formation of H-bond of type X—H–O (X= Cl, Br and $NO_2$) and the attractive interaction present in halogen mixtures were discussed.

**Key words :** Hydrogen bond, 1-propanol, Chlorobenzene, Bromobenzene, Nitrobenzene, Molecular Interaction.

## INTRODUCTION

The knowledge of physico-chemical properties of ternary liquid mixtures contributes to an understanding of the behaviour of different liquids and their functional groups. The physico-chemical properties of liquids and their mixtures have been studied by several workers (Kannappan *et al* 1991, Siva Prasad *et al* 1995, Hemalatha *et al* 2005 and Bhadja *et al* 2002) using the experimental data of ultrasonic velocity, density and viscosity. The strength of interaction depend on the nature of liquids, whether they are Polar or Non-polar.

Das *et al* 1994 have reported that the effect of interaction between like and unlike molecules of mixtures, having alcohol and Nitrobenzene as one component. Several investigations (Venkatesu *et al* 2004, Suijit Singh Bhatti *et al* 1983, Isht Vibhu *et al* 2004, Srinivasulu *et al* 1995 and Subramanyam Naidu *et al* 2002) were carried out using alcohol as one of the component in the molecular interaction studies. Since, acoustic parameters provides a better insight into molecular environments in liquid mixtures. It seemed important to study the molecular interaction in ternary liquid mixtures of 1-propanol and acetophenone with chlorbenzene, bromobenzene and nitrobenzene at 303,308 and 313K.

## EXPERIMENTAL METHODS

The ultrasonic velocities in liquid mixtures have been measured using an

*Corresponding author

CC-0. In Public Domain. Gurukul Kangri Collection, Haridwar

Digitized by Arya Samaj Foundation Chennai and eGangotri


ultrasonic interferometer (Model F81) supplied by Mittal Enterprises, New Delhi working at 3 MHz frequency with an accuracy of ± 0.1 $ms^{-1}$. The temperatures were controlled by circulating water around the liquid cell from a thermostatically controlled water bath (accuracy ± 0.1°C). The temperature of the cell was measured using a thermocouple (at the crystal) and was found to be accurate to ± 0.25°C. All the chemicals used were Analar grade of S.D. Fine chemical (purity>99%).

The density and viscosity were measured using a pycknometer and an Ostwald's viscometer respectively with an accuracy of 3 parts in $10^5$ for density and 0.001 $Nsm^{-2}$ for viscosity at 303, 308 and 313K.

Using the measured data, the acoustical parameters such as adiabatic compressibility ($\beta$), free length ($L_f$), free volume ($V_f$) and internal pressure ($\pi_i$) have been calculated using the following standard expressions (1-4):

$$\text{Adiabatic compressibility } \beta = (U^2\rho)^{-1} \quad (1)$$

$$\text{Intermolecular free length } L_f = K_T \beta^{1/2} \quad (2)$$

$$\text{Free Volume } V_f = \left[\frac{M_{eff} U}{\eta K}\right]^{3/2} \quad (3)$$

$$\text{Internal Pressure } \pi_i = bRT\left[\frac{K\eta}{U}\right]^{1/2}\left[\frac{\rho^{2/3}}{M_{eff}^{7/6}}\right] \quad (4)$$

where, $K_T$ is the temperature-dependent constant having a value $201.1209 \times 10^{-8}$ in M.K.S. system, $M_{eff}$ is the effective molecular weight, b is the cubic packing factor which is assumed to be 2 for all liquids and solutions, K is a constant equal to $4.28 \times 10^9$ in M.K.S. system, independent of temperature for all liquids; R is the gas constant; x is the mole fraction. The liquid mixtures of various concentrations in mole fraction were prepared by taking AR grade chemicals. In all systems, the mole fraction of the second component, i.e., acetophenone ($x_2$=0.3) was kept constant, while the mole fractions of the remaining two ie., 1-propanol and substituted benzenes ($x_1$ and $x_3$) were varied from 0.1 to 0.7 so as to have the mixture of different compositions.

## RESULTS AND DISCUSSION

The experimental values of density, viscosity and ultrasonic velocity for all the systems at 303, 308 and 313K are presented in table 1. The calculated acoustic parameters like adiabatic compressibility ($\beta$), free length ($L_f$), free volume ($V_f$), and internal pressure ($\pi_i$) are listed in table 2 for all the three systems.


CC-0. In Public Domain. Gurukul Kangri Collection, Haridwar

Digitized by Arya Samaj Foundation Chennai and eGangotri

# MOLECULAR INTERACTION IN TERNARY LIQUID MIXTURES - AN ULTRASONIC STUDY

**Table 1: Density (ρ), viscosity (η) and velocity (U) values of System I, II and III**

| Mole fraction | | ρ kgm$^{-3}$ | | | η x 10$^{3}$ Nsm$^{-2}$ | | | U ms$^{-1}$ | | |
|---|---|---|---|---|---|---|---|---|---|---|
| | | TEMPERATURE (K) | | | | | | | | |
| $X_1$ | $X_3$ | 303 | 308 | 313 | 303 | 308 | 313 | 303 | 308 | 313 |
| System – I: 1-Propanol + Acetophenone + Chlorobenzene | | | | | | | | | | |
| 0.7000 | 0.0000 | 914.6 | 911.0 | 907.1 | 1.8105 | 1.5611 | 1.4530 | 1294.7 | 1293.9 | 1284.1 |
| 0.5999 | 0.1000 | 921.8 | 919.1 | 910.3 | 1.6930 | 1.4849 | 1.3360 | 1297.5 | 1296.0 | 1293.0 |
| 0.5000 | 0.1999 | 949.2 | 948.7 | 946.2 | 1.5270 | 1.3220 | 1.2753 | 1323.3 | 1321.7 | 1317.5 |
| 0.4000 | 0.2999 | 976.4 | 972.1 | 968.6 | 1.4047 | 1.2440 | 1.1961 | 1334.1 | 1331.2 | 1329.4 |
| 0.2999 | 0.4000 | 998.5 | 997.1 | 993.8 | 1.3889 | 1.2109 | 1.1563 | 1354.3 | 1353.0 | 1347.4 |
| 0.1999 | 0.5000 | 1023.4 | 1022.2 | 1014.4 | 1.1654 | 1.1583 | 1.0789 | 1377.2 | 1375.7 | 1371.5 |
| 0.0999 | 0.6000 | 1043.2 | 1039.7 | 1032.1 | 1.1107 | 1.0911 | 0.9347 | 1389.1 | 1386.1 | 1384.8 |
| 0.0000 | 0.6999 | 1067.7 | 1064.3 | 1055.3 | 1.0826 | 1.0637 | 0.8959 | 1413.1 | 1407.1 | 1401.3 |
| System – II: 1-Propanol + Acetophenone+ Bromobenzene | | | | | | | | | | |
| 0.6000 | 0.0999 | 963.1 | 957.9 | 952.0 | 1.5132 | 1.4772 | 1.3786 | 1215.1 | 1206.1 | 1191.6 |
| 0.5000 | 0.1999 | 1032.6 | 1030.8 | 1026.7 | 1.4206 | 1.4049 | 1.3365 | 1220.1 | 1210.3 | 1199.0 |
| 0.3999 | 0.3000 | 1104.5 | 1102.1 | 1093.6 | 1.3761 | 1.3656 | 1.2921 | 1226.3 | 1216.5 | 1203.4 |
| 0.3000 | 0.4000 | 1161.0 | 1157.5 | 1155.5 | 1.3748 | 1.3448 | 1.2776 | 1234.2 | 1228.2 | 1210.2 |
| 0.2000 | 0.5000 | 1217.9 | 1216.1 | 1215.9 | 1.3584 | 1.2804 | 1.2465 | 1244.7 | 1238.7 | 1223.4 |
| 0.0999 | 0.6000 | 1274.6 | 1270.6 | 1268.8 | 1.3213 | 1.2344 | 1.2131 | 1256.6 | 1248.9 | 1233.8 |
| 0.0000 | 0.7000 | 1321.0 | 1319.1 | 1315.8 | 1.3122 | 1.1189 | 1.0210 | 1273.1 | 1267.8 | 1252.6 |
| System – III: 1-Propanol + Acetophenone + Nitrobenzene | | | | | | | | | | |
| 0.6000 | 0.0999 | 934.6 | 931.1 | 928.2 | 1.9339 | 1.9223 | 1.7787 | 1315.3 | 1308.9 | 1296.9 |
| 0.4999 | 0.1999 | 974.1 | 970.5 | 967.9 | 1.8235 | 1.8012 | 1.6376 | 1323.9 | 1318.4 | 1316.1 |
| 0.3999 | 0.3000 | 1012.3 | 1005.7 | 1001.1 | 1.8103 | 1.7368 | 1.5551 | 1341.6 | 1335.9 | 1329.6 |
| 0.2999 | 0.4000 | 1047.4 | 1039.2 | 1038.0 | 1.7769 | 1.6102 | 1.5368 | 1360.3 | 1351.3 | 1345.4 |
| 0.19999 | 0.5000 | 1071.4 | 1066.7 | 1042.3 | 1.7320 | 1.5318 | 1.4839 | 1381.7 | 1369.3 | 1358.1 |
| 0.0999 | 0.6000 | 1113.1 | 1096.7 | 1093.0 | 1.6866 | 1.5064 | 1.4721 | 1401.2 | 1389.2 | 1370.6 |
| 0.0000 | 0.6999 | 1133.4 | 1130.2 | 1118.0 | 1.5321 | 1.4861 | 1.3986 | 1420.1 | 1411.1 | 1395.3 |

**Table 2: Adiabatic compressibility (β), free length ($L_f$), free volume ($V_f$), and internal pressure ($\pi_i$) of System I, II and III**

| Mole fraction | | β x 10$^{10}$ Pa$^{-1}$ | | | $L_f$ x 10$^{11}$ m | | | $V_f$ x 10$^{7}$ m$^{3}$ mol$^{-1}$ | | | $\pi_i$ x10$^{4}$ Pa | | |
|---|---|---|---|---|---|---|---|---|---|---|---|---|---|
| | | TEMPERATURE (K) | | | | | | | | | | | |
| $X_1$ | $X_3$ | 303 | 308 | 313 | 303 | 308 | 313 | 303 | 308 | 313 | 303 | 308 | 313 |
| System – I: 1-Propanol + Acetophenone + Chlorobenzene | | | | | | | | | | | | | |
| 0.7000 | 0.0000 | 6.5227 | 6.5566 | 6.6857 | 5.0959 | 5.1091 | 5.1591 | 0.4715 | 0.5883 | 0.6477 | 720.99 | 678.96 | 666.29 |
| 0.5999 | 0.1000 | 6.4439 | 6.4778 | 6.5708 | 5.0650 | 5.0783 | 5.1146 | 0.5766 | 0.7007 | 0.8183 | 649.01 | 617.00 | 591.62 |
| 0.5000 | 0.1999 | 6.0162 | 6.0340 | 6.0885 | 4.8940 | 4.9013 | 4.9234 | 0.7597 | 0.9414 | 0.9889 | 579.63 | 548.36 | 547.24 |
| 0.4000 | 0.2999 | 5.7543 | 5.8050 | 5.8417 | 4.7863 | 4.8073 | 4.8225 | 0.9502 | 1.1364 | 1.2029 | 527.58 | 503.74 | 501.10 |
| 0.2999 | 0.4000 | 5.4603 | 5.4785 | 5.5425 | 4.6625 | 4.6702 | 4.6974 | 1.0726 | 1.3157 | 1.4013 | 495.97 | 470.52 | 467.19 |
| 0.1999 | 0.5000 | 5.1518 | 5.1691 | 5.2408 | 4.5288 | 4.5364 | 4.5678 | 1.5462 | 1.5579 | 1.7251 | 431.22 | 436.90 | 426.97 |
| 0.0999 | 0.6000 | 4.9678 | 5.0061 | 5.0524 | 4.4472 | 4.4643 | 4.4849 | 1.8120 | 1.8550 | 2.3363 | 400.94 | 403.48 | 377.83 |
| 0.0000 | 0.6999 | 4.6903 | 4.7455 | 4.8257 | 4.3212 | 4.3466 | 4.3831 | 2.0722 | 2.1142 | 2.7183 | 377.44 | 380.30 | 353.41 |
| System – II: 1-Propanol + Acetophenone+ Bromobenzene | | | | | | | | | | | | | |
| 0.6000 | 0.0999 | 7.0324 | 7.1765 | 7.3977 | 5.2912 | 5.3452 | 5.4269 | 0.6684 | 0.6853 | 0.7465 | 614.52 | 617.25 | 607.14 |
| 0.5000 | 0.1999 | 6.5054 | 6.6227 | 6.7751 | 5.0891 | 5.1348 | 5.1935 | 0.8651 | 0.8691 | 0.9236 | 550.86 | 558.45 | 554.65 |
| 0.3999 | 0.3000 | 6.0206 | 6.1313 | 6.3142 | 4.8958 | 4.9406 | 5.0138 | 1.0542 | 1.0537 | 1.1264 | 506.34 | 514.04 | 508.26 |
| 0.3000 | 0.4000 | 5.6545 | 5.7271 | 5.9090 | 4.7446 | 4.7750 | 4.8502 | 1.2138 | 1.2456 | 1.3156 | 471.41 | 474.13 | 472.57 |
| 0.2000 | 0.5000 | 5.2997 | 5.3591 | 5.4949 | 4.5934 | 4.6191 | 4.6772 | 1.4106 | 1.5303 | 1.5637 | 438.97 | 433.83 | 437.66 |
| 0.0999 | 0.6000 | 4.9685 | 5.0458 | 5.1774 | 4.4475 | 4.4820 | 4.5401 | 1.6660 | 1.8281 | 1.8425 | 407.54 | 400.80 | 405.85 |
| 0.0000 | 0.7000 | 4.6705 | 4.7165 | 4.8437 | 4.3121 | 4.3333 | 4.3913 | 1.9031 | 2.4010 | 2.7062 | 381.37 | 358.37 | 349.41 |
| System – III: 1-Propanol + Acetophenone + Nitrobenzene | | | | | | | | | | | | | |
| 0.6000 | 0.0999 | 6.1847 | 6.2688 | 6.4053 | 4.9621 | 4.9957 | 5.0498 | 0.4912 | 0.4920 | 0.5452 | 685.24 | 694.41 | 680.53 |
| 0.4999 | 0.1999 | 5.8571 | 5.9280 | 5.9647 | 4.8289 | 4.8580 | 4.8730 | 0.6034 | 0.6108 | 0.7028 | 626.90 | 633.09 | 612.89 |
| 0.3999 | 0.3000 | 5.4883 | 5.5716 | 5.6504 | 4.6744 | 4.7097 | 4.7429 | 0.6884 | 0.7279 | 0.8531 | 588.53 | 584.67 | 561.83 |
| 0.2999 | 0.4000 | 5.1596 | 5.2698 | 5.3223 | 4.5322 | 4.5804 | 4.6031 | 0.7943 | 0.9117 | 0.9714 | 550.43 | 531.60 | 528.52 |
| 0.1999 | 0.5000 | 4.8890 | 4.9998 | 5.2016 | 4.4118 | 4.4615 | 4.5507 | 0.9235 | 1.0954 | 1.1349 | 510.84 | 489.11 | 483.71 |
| 0.0999 | 0.6000 | 4.5757 | 4.7247 | 4.8703 | 4.2681 | 4.3371 | 4.4033 | 1.0672 | 1.2481 | 1.2662 | 481.10 | 459.59 | 463.78 |
| 0.0000 | 0.6999 | 4.3750 | 4.4435 | 4.5943 | 4.1734 | 4.2060 | 4.2768 | 1.3615 | 1.4117 | 1.5203 | 433.41 | 434.46 | 427.63 |


CC-0. In Public Domain. Gurukul Kangri Collection, Haridwar

Digitized by Arya Samaj Foundation Chennai and eGangotri



From the table (1) and (2) it is observed that the ultrasonic velocity and density increases with increase in mole fraction of substituted benzenes in all systems, whereas the viscosity values is in the reverse trend.

From the fig.1 and 2 it is observed that β and $L_f$ value decreases with increase in concentration. Since, the molecule become more compact and less compressible as the new entities are formed, such continues in adiabatic compressibility with solute concentration has been qualitatively ascribed to the effect of hydrogen bonding (Nikam *et al* 2001). By increasing the temperature it is observed that the free length increases, this may be due to the thermal expansion of liquids (Singh *et al* 1994).

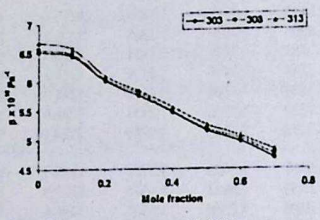


**Fig.1. Adiabatic compressibility Vs mole fraction of Chlorobenzene**

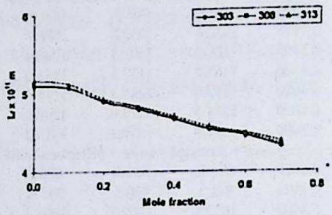


**Fig.2. Free length Vs mole fraction of Chlorobenzene**

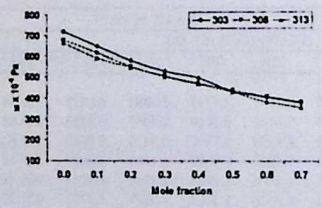


**Fig.3. Internal pressure Vs mole fraction of Chlorobenzene**

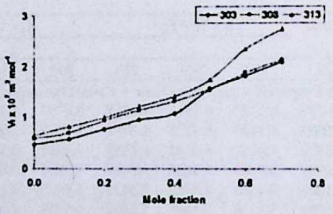


**Fig.4. Free volume Vs mole fraction of Chlorobenzene**

From fig.3, it is observed that the internal pressure $\pi_i$, decreases with increase in concentration. This decreases of $\pi_i$ can be attributed to the predominant effect of dispersion forces over other molecular interaction among the constituents. Here the $\pi_i$ value is maximum at the lower concentration indicates the strong intermolecular association (Das *et al* 1994).

It is noticed that the free volume $V_f$ (fig.4), increases with increase in concentration for all the systems. It is found that $V_f$ of a solute molecule at a particular temperature and pressure depends only on the internal pressure of the liquid in which it is immersed. Hence weakening of the molecular association, leads to the larger free volume (Hirschfelder *et al* 1959). The same trend of


CC-0. In Public Domain. Gurukul Kangri Collection, Haridwar

Digitized by Arya Samaj Foundation Chennai and eGangotri



acoustic parameters is obtained in the case of bromobenzene and nitrobenzene also.

## CONCLUSION

The hydrogen bond between 1-proponal and Acetophenone is become weaker due to the dissociation of 1-proponal by the addition of substituted benzenes. The observed values suggest that 1-proponal and acetophene interaction is weaker than the interaction in between acetophenone and substituted benzene. Here weak interaction between the unlike molecule is observed. The formation of H-bond of type X---H–O (X = Cl, Br, $NO_2$) between aromatic hydrocarbon and the alkanol, and changes in free volume, interstitial accommodation and confirmation changes in acetophenone and aromatic hydrocarbons in the aggregates of alkanol appear to occur in these three mixtures. Also attractive interactions are present in halogen mixtures and into substituted benzenes.

## REFERENCES

1. Bhadja, D.R. , Patel, Y.U. and Parasonia, P.H. 2002. *Ind, J. Pure & Appl. Phys.*, 24 47-45.
2. Bhatti, Suijit Singh and Singh, Devinder Pal . 1983. *Ind. J. Pure & Appl. Phy.*, 21 : 506-509.
3. Das, A.K. and Jha, B.L. 1994 . *J. of Molecular Liquids*, 59: 161-171.
4. Hemalatha, B., Vasantharani, P. and Kannappan, A.N. 2005. *J. Annamalai University, Part-B science*, 79, 87.
5. Hirschfelder, J.O., Curtis, C.F. and Bird, R.B.1959. Molecular theory of gases and liquids, John Wiley & Sons, N.Y., 29, 286. 1959.
6. Isht Vibhu, Amit Misra, Gupta, Manisha and Shukla , J.D. 2004. *Ind. J. Phys.*, 5: 1147-1155.
7. Kannappan, A.N. and Rajendran, V. 1991. *J. Pure & Appl. Ultrason.*, 13: 27-2.
8. Nikam, P.S., Jagdale, B.S., Sawant, A.D. and Mehdi Hasan, 2001. *Ind J. Pure & Appl. Phys.*, 39, 433-437.
9. Singh, D.P and. Prabhakar, K.P. 1994. *J. Pure & Appl Ultrason.*, 16, 41-45.
10. Siva Prasad, T. and Venkateswaer, P. 1995. *J. Pure & Appl. Ultrason.*, 17: 59-62.
11. Srinivasulu, V. and Naidu, P.R. 1995. *J. Pure & Appl. Ultrason.*, 17: 14-18.


CC-0. In Public Domain. Gurukul Kangri Collection, Haridwar

Digitized by Arya Samaj Foundation Chennai and eGangotri


12. Subramanyam Naidu, P. and Ravindra Prasad, K. 2002. *J. Pure & Appl. Ultrason.*, 24: 18-23.

13. Venkatesu, P., Chandra Sekar, G. and Prabhakara Rao M.V. 2004. *Phys and Chem. of liqs.*, 44, 287-291.


CC-0. In Public Domain. Gurukul Kangri Collection, Haridwar

Digitized by Arya Samaj Foundation Chennai and eGangotri

ISSN-0970-6569
Bulletin of Pure and Applied Sciences.Vol.28D(No.1)2009:P.59 - 65

# GROWTH STUDY OF NaCl,NaCl+NaBr AND NaBr CRYSTALS GROWN BY SOLUTION EVAPORATION METHOD AT AMBIENT TEMPERATURE

**Ketki A. Mistry, I.B.Patel and Priyanka Rustagi**
Department of Physics,Veer Narmad South Gujarat University,
SURAT-395007,India

**ABSTRACT**

Generally alkali halide crystals are ionic crystals which are highly soluble in water. From them sodium chloride and sodium bromide are most popular materials due to their optical properties. They have various scientific applications such as nano particles thin films NaCl is used. Powerful color centre laser is provided by it and it is the most common infrared transmission window for gas and liquid samples used with infrared and FTIR spectrophotometer.NaBr crystals are used to detect neutrino lines and in much more applications. Mainly they are easily available at affordable price and soluble in water. In the paper we have synthesized the crystals of NaCl ,NaCl+NaBr and NaBr grown by solution evaporation method at ambient temperature.•We have reported the changes in the size and transparency of NaCl , NaCl +NaBr and NaBr crystals by varying the evaporation area of the Petri dish and the height of the solution at ambient temperature and the results are reported in the paper.

Key words : Crystal growth, Solution growth, Alkali halide, Parameters.

## 1. INTERODUCTION

Among the alkali halide crystals, sodium chloride and sodium bromide are most famous materials due to their applications as an optical crystal. Optical quenching of the magneto plastic effect in NaCl crystal results that illuminating NaCl crystal by ultraviolet light (λ=350nm) suppress the magneto plastic effect (Golovin *et al.*,1997).NaCl is very useful in nanoparticale thin films. This thin films have a wide range of application and film deposition has been done successfully on a wide range of conducting and non conducting substrate fabrications such as NaCl (Mukherjee *et al.*,2006).Due to an effect of pulsed electromagnetic field in NaCl crystal under the mechanical loading by electron beam, it removes the discrepancy in determination of dislocation dynamic damping coefficient by two methods namely with an electron beam and By mechanical impact loading (Al'shits *et al.*,1999).Intrinsic vacancy mobility is not enhanced in NaCl crystals by microwave fields(Freeman *et al.*,1995).NaCl+NaBr

CC-0. In Public Domain. Gurukul Kangri Collection, Haridwar

Digitized by Arya Samaj Foundation Chennai and eGangotri


crystals were grown from solution of wide range of Br:Cl values and studied and the results indicated that NaBr surface forms domains and large areas of surface contain NaCl with no detectable NaBr (Christopher *et al.*,1997). NaBr crystals are used in insulator applications(Boghossian *et al.*,1979)One recent suggestion for bolometric experiments is to use NaBr crystals to detect neutrino lines.In order to grow crystals, the solution must be supersaturated; the concentration of the solution is more then the equilibrium concentration. Super saturation is the driving force, which governs the rate of crystal growth.

A typical solubility diagram is shown in the figure. the whole concentration-temperature field is separated by the saturated-solution line(solubility-curve)in to two regions; unsaturated and supersaturated solutions. The region of supersaturated solutions can be divided in to two sub-regions; metastable and labile zones. Nucleations will occure spontaneously in the labile zone. Metastable zone refers to the level of super saturation where spontaneous nucleation cannot occure and a seed crystal is essential to facilitate growth.

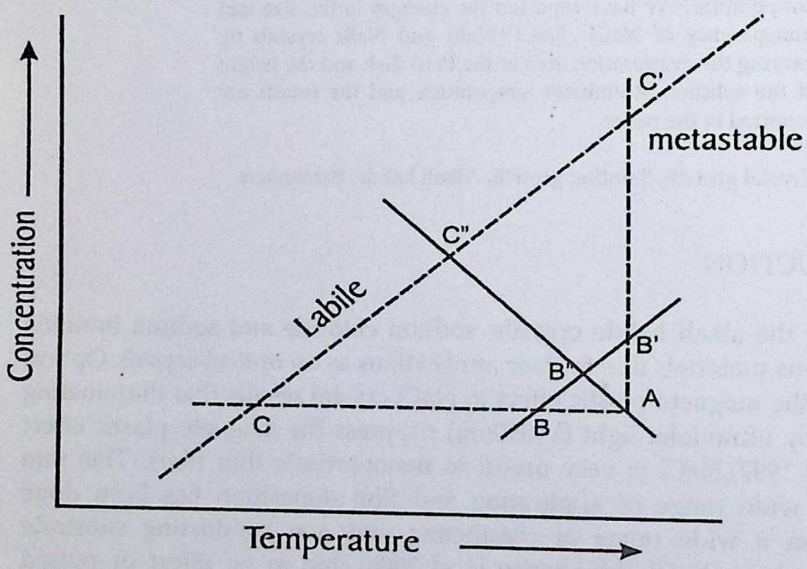


Fig - 1 solubility Diagram


CC-0. In Public Domain. Gurukul Kangri Collection, Haridwar

Digitized by Arya Samaj Foundation Chennai and eGangotri

# GROWTH STUDY OF NaCl,NaCl+NaBr AND NaBr CRYSTALS GROWN BY SOLUTION EVAPORATION METHOD AT AMBIENT TEMPERATURE

## 2. EXPERIMENTS

Growth of crystals from aqueous solution is one of the ancient methods of crystal growth. This method involves weeks, months and some times years. First of all to grow a seed crystal we have to make a saturated solution In order to grow a crystal, you need to make a solution which maximizes the chances for the solute particles to come together and form a nucleus, which will grow into our crystal. This means we want a concentrated solution with as much solute as we can dissolve (saturated solution).So we have made the saturated solution of NaCl and NaBr in Distilled water. Then we gave the heat and also stirred the solution. So we got the super-saturated solution and we have filtered it and filled them in two sets of Petri dishes of different diameters: 6 inch, 4inch, 3inch and 2inch .One set for NaCl and the another for NaBr. Through this we have change the evaporation area. Also we have filled these solutions in fore beakers of same dimensions (6 cm diameter and 9.5 cm height) at different heights. We covered these whole set by paper and kept it at clean and undisturbed place for couple of weeks. After some times we got the seed crystals of different size and the results are showen in Table 1 and Table 2.For NaCl+NaBr mixed crystal, we make a saturated solution of NaCl and NaBr in equal quanties then mixed them. Then add some amount of both NaCl and NaBr powder in that mixed solution and again gave heat and stirred it. The process continued until the NaCl+NaBr super saturated solution is made. Then filled that solution in bikers and Petri dishes as above of NaBr and NaCl and the results are shown in Table 1 and Table 2.

## 3. RESULTS

Table 1 shows the effect of evaporation area on the crystal growth and table 2 shows the effect of height of the solution on the crystal growth at ambient temperature. The photographs of these crystals are shown in the figure-2(a), figure-2(b), figure-2(c).

## 4. CONCLUSITION

- In NaCl solution as the evaporation area decreases the size of the crystal is also decreases and the crystals are opaque but in the case of beaker the crystal in small height solution is small in size and highly transparent but as the height increases the crystals become bigger but opaque.
- In NaBr as the evaporation area increases the crystals become bigger in size and more transparent while in beaker as the height increases the crystal becomes good shaped and transparent.



CC-0. In Public Domain. Gurukul Kangri Collection, Haridwar

Digitized by Arya Samaj Foundation Chennai and eGangotri


**Table 1 : Effect of diameter of Petri dish (at ambient temperature)**

| Solution | Time duration | 6 inch | 4 inch | 3 inch | 2 inch |
|---|---|---|---|---|---|
| NaCl | 4 days | Opaque medium size(cubic) (3x3x2 $mm^3$) crystal | Opaque medium size(cubic) (3x3x2 $mm^3$) crystal | Opaque small size(cubic) (2x2x1 $mm^3$) crystal | Opaque small size(cubic) (2x2x1 $mm^3$) Crystal |
| NaBr | 9 days | Medium size good shape (5x5x5 $mm^3$) transparent Crystal | Thin plate type transparent crystal | small size good shape (3x3x2 $mm^3$) transparent crystal | Thick layer, dendrite growth (transparent) |
| NaCl: NaBr Mixed | 19 days | Very big transparent (cubic) (14x15x5 $mm^3$) crystal | medium size transparent (cubic) (7x7x3 $mm^3$) crystal | Small size highly transparent (Cubic) (5x5x3 $mm^3$) crystal | Very small size (cubic) transparent (3x3x2 $mm^3$) crystal |


CC-0. In Public Domain. Gurukul Kangri Collection, Haridwar

Digitized by Arya Samaj Foundation Chennai and eGangotri

# GROWTH STUDY OF NaCl,NaCl+NaBr AND NaBr CRYSTALS GROWN BY SOLUTION EVAPORATION METHOD AT AMBIENT TEMPERATURE

**Table 2: Effect of height of the solution in beaker. (At ambient temperature).**

| solution | Time duration | 1.2 cm (30 ml) | 2 cm (50 ml) | 3.5 cm (100 ml) |
|---|---|---|---|---|
| NaCl | 18 days | Medium size ($5x4x2\ mm^3$) Transparent (Cubic) crystal | Medium size ($5x4x2\ mm^3$) Transparent (Cubic) crystal | Opaque crystal (Cubic) ($7x7x2\ mm^3$) |
| NaBr | 16 days | Thin plate type crystal | Thick layer dendrite growth | Medium size good shape ($5x5x5\ mm^3$) Transparent Crystal |
| NaCl: NaBr Mixed | 27 days | Very big size ($10x10x5\ mm^3$) (Cubic) crystal slightly opaque in middle | Small crystal ($5x5x3\ mm^3$) less transparent (Cubic) crystal | Very small size ($2x2x2\ mm^3$) Good transparent (cubic) crystal |


CC-0. In Public Domain. Gurukul Kangri Collection, Haridwar

Digitized by Arya Samaj Foundation Chennai and eGangotri



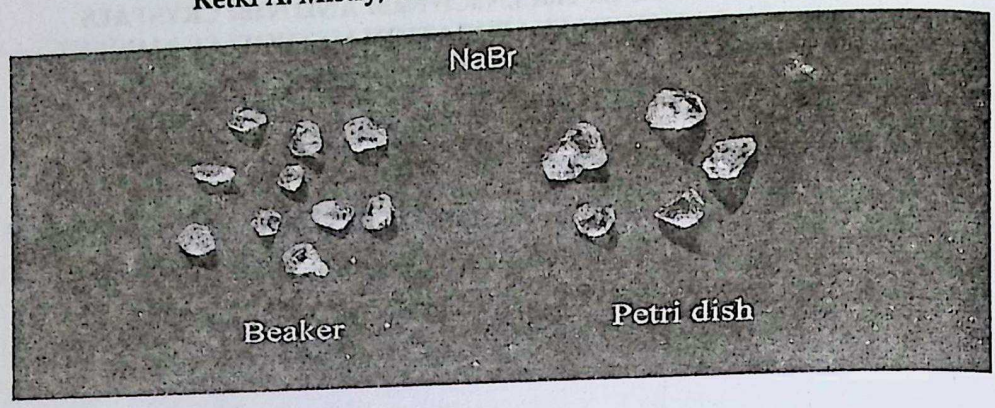


Figure-2(a)

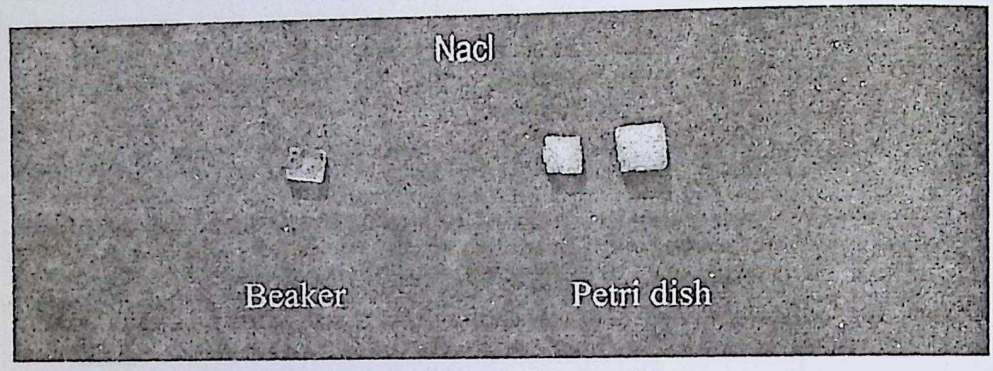


Figure-2(b)

Figure-2(c)


CC-0. In Public Domain. Gurukul Kangri Collection, Haridwar

Digitized by Arya Samaj Foundation Chennai and eGangotri



- In NaCl:NaBr ,as the evaporation area decreases the crystal become smaller and highly transparent but in case of beaker the height of the solution increases the crystal becomes smaller with good transparency.

- By means of time duration we can see that crystals take less time to be formed in patri dishes then beaker but crystals from beaker are batter then that of from patri dish.

## 5. ACKNOWLEDGEMENTS

The authors thank to Dr .I. B Patel for his guidance and his constant encouragement. Dr. K. C. Poria Head Department of Physics, Veer Narmad South Gujarat University, for providing laboratory facilities. & also DST – FIST PROGRAMS for giving Facilities.

## REFRENCES

1. Al'shits, V., Darinskaya, E., Legen'kov, M. and Morozov, V.1999.*Journal of Physics of the Solid State.*, Vol. 41(No.11): 1839-1841, 1999.

2. Boghossian, H. H. and Dubey,K.S.1979. *Journal of Themal Analysis and Calorimetry.*,Vol.15(No 2): 207-214 ,1979.

3. Christopher, D., Zangmeister, Jessica, Turner, A. and Jeanne, E. 1997.*Journal of Physics of Solid State* .,Vol.39(No.8), 1997.

4. Freeman, S.A., Booske,J.H. and Cooper,R.F.1995. *Phys. Rev. Lett.* 74: 2042 – 2045,1995.

5. Golovin, Yu.I., Morgunov,R.B. and Badylevich,M.B. 1997. *Journal of Physics of the solid state.*,Vol.39(No.8),1997.

6. Mukherjee, B. and Ravishankar,N. 2006.*Material Research Society.*, Vol. 901E ,2006.


CC-0. In Public Domain. Gurukul Kangri Collection, Haridwar

Digitized by Arya Samaj Foundation Chennai and eGangotri

CC-0. In Public Domain. Gurukul Kangri Collection, Haridwar

Digitized by Arya Samaj Foundation Chennai and eGangotri

*ISSN-0970-6569*
*Bulletin of Pure and Applied Sciences.Vol.28D(No.1)2009:P.67- 85*

# PRECESSION FORMULAS FOR GRAVITY PROBE-B AND ITS COMPLEMENTARY EXPERIMENTS OF LOCAL LIGHT SPEEDS

C. Y. Lo
Applied and Pure Research Institute, 7 Taggart Drive, Unit E, Nashua, NH 03060 USA

**ABSTRACT**

Calculation shows that different gauges lead to different formulas of the de Sitter precession. Therefore, gauge invariance for a given frame of reference is clearly invalid, and thus general relativity remains to be completed. In fact, the claim of diffeomorphic solutions being the same in physics, just as Einstein's "covariance principle," is due to an inadequate ability to distinguish the physics from mathematics. Moreover, since the Stanford experiment, Gravity Probe-B, measures only the accumulated effects of the de Sitter precession, it would be very difficult for gravity Probe-B to distinguish these three formulas because of the time averaging effect. Although the radial gauge has an arbitrary integral constant in the related formula, Gravity Probe-B is unable to show whether such a gauge or Whitehead's theory is invalid. However, as Zhou conjectured, an experiment on local light speeds would further support the Maxwell-Newton Approximation, in addition to tell whether Whitehead's theory is valid although his experiment is not sensitive to the globe's rotation. Concurrently, it is pointed out that the so-called physically measurable gauge invariant values are merely mathematical illusions.

**Key words:** Einstein's equivalence principle, Maxwell-Newton Approximation, Euclidean-like structure, de Sitter precession, Radial gauge, Whitehead's theory, Covariance principle, Lense-Thirring precession. 04.20.-q, 04.20.Cv

## 1. INTRODUCTION

Gravity Probe B (Everitt *et al.* 1996), which is armed with some of the most precise instruments ever built, has finally launched on April 17, 2004 after more than 44 years to build. The stated goal is to test general relativity. To be more precise, it tests the precessions due to gravity of the globe. However, related fundamental issues also need to be addressed. For instance, the issue of precession would lead to the question of what is the valid physical gauge because different gauges produce different precession formulas (see also section 4). In this paper, it will be shown that this issue of the physically realistic gauge remains unsolved by this experiment Gravity Probe-B although the related formulas are, in principle, distinguishable experimentally. [1)]

CC-0. In Public Domain. Gurukul Kangri Collection, Haridwar

Digitized by Arya Samaj Foundation Chennai and eGangotri


means that the physical gauge is unique for a given frame of reference (Lo 2002, 2003b). On the other hand, Einstein's "principle of covariance" (Einstein *et al.* 1952) says, "The general laws of nature are to be expressed by equations which hold good for all systems of co-ordinates, that is, are co-variant with respect to any substitutions whatever (generally co-variant)." The principle of general relativity demands covariance among different frames of reference. However, for different gauges of a given frame of reference, a question arises. Would the physical laws be the same as Einstein's equivalence principle demands?

Some theorists rejected Einstein's equivalence principle, but believed in the covariance principle; and claimed that covariance means that the laws of physics in different gauges need not be the same even if the frame of reference is the same.[2] However, they failed to provide different methods of measurement for different gauges. In contrast, based on that both the Schwarzschild solution and the harmonic solution produced the same first order deflection of light, Einstein (1954) claimed, "It should be noted that this result, also, of the theory is not influenced by our arbitrary choice of a system of coordinates." Of course, Einstein did not see that, for integrated effects such as the bending of light, the differences have been smoothed out (Lo 2004). He also did not see that his covariance principle is in conflict with his equivalence principle (Lo 2003b, 2004).

According to Einstein's claim, many believed that these two metrics produce the same formula for the precessions (Lo 2002). As shown in the book of Ohanian & Ruffini (1994), only one metric is used for the calculation. Moreover, based on the parameterized post-Newtonian approximation, Will[3] (2003) even claimed to have a covariant calculation of the formula for precessions.

However, the fact is Will (1976) made a misleading claim again (Lo 1997). First, since his post-Newtonian approximation is a generalization of the Maxwell-Newton Approximation, he has already made a gauge choice. Thus, the issue of gauge invariance was not addressed at all. Second, for different parameters, the parameterized post-Newtonian approximations used are not diffeomorphic to each other. Moreover, obviously Will was not aware of the inconsistency between the "covariance principle" and Einstein's requirement for weak gravity, as pointed out by the editors of the Royal Society (Bondi *et al.* 1959, Pring 2007).

Explicit calculation shows that these two metrics would produce two distinct formulas for a precession (Appendix A). Thus, the so-called "covariance principle" is illustrated as invalid since there is no way to provide distinct measurements with each gauge. To show unequivocally that there are unphysical metrics that can provide same valid physical predictions, the radial gauge (Lo 2004) that gives an arbitrary "event of horizon" is also considered. However, it is beyond the present accuracy of Gravity Probe-B, which provides only the time-average of data, to distinguish the physically correct one (or to reject an unphysical one) from the other metrics. Thus, an experiment on local light speeds would


CC-0. In Public Domain. Gurukul Kangri Collection, Haridwar

Digitized by Arya Samaj Foundation Chennai and eGangotri


be needed to verify (or to reject) validity of the Maxwell-Newton Approximation (MNA) further (Lo 2003b).

Although Eddington (1975) rejected the covariance principle and commented, "space is not a lot of points close together; it is a lot of distances interlocked." he still accepted both the Schwarzschild solution and the harmonic solution. About 60 years later, Zhou Pei-Yuan (1983) commented, "The concept that coordinates (of different gauges) don't matter in the interpretation of Einstein's theory ... necessarily leads to mathematical results which can hardly have a physical interpretation and are therefore a mystification of the theory." Zhou (1987) conjectured that the Schwarzschild solution would be invalid and his view is supported by pulsar-experiments because the Schwarzschild solution is incompatible with Einstein's radiation formula (Logunov *et al.* 1989).

In this paper, it will be shown the radial gauge would be clearly invalid because there is an arbitrary constant in the formula for the de Sitter Precession. However, it is often difficult to show that a gauge is excluded experimentally because the difference could be too small to be determined with measurements. As mentioned, distinct formulas need not mean that they are currently distinguishable by experiments. It is also pointed out that the experiment on local light speeds is complementary to Gravity Probe-B in testing general relativity. Such an experiment would help identifying the required physical gauge.

Currently, the "principle of covariance" and the related notion of gauge are included in all textbooks as if it were well established. Criticisms on the "covariance principle" were suppressed. Obviously, such a situation would not help the progress of general relativity.

## 2. INVALIDITY OF THE "PRINCIPLE OF COVARAINCE"

General relativity is established on two principles (Einstein 1954), namely: 1) Einstein's equivalence principle, which requires that a free falling point-like particle in a gravitational field is along a geodesic and results in a co-moving local Minkowski space; and 2) the principle of general relativity, that is "The law of physics must be of such a nature that they apply to systems of reference in any kind of motion." However, these two principles were practically inapplicable because, as pointed out by Whitehead (1922) and Fock (1964) space-time coordinates are ambiguous [4] in Einstein's theory.

Currently, these two principles are replaced with Pauli's (1958) version of the equivalence principle, [5] which requires only a mathematical existence of local Minkowski spaces, and unrestricted covariance, which Einstein called as the "principle of covariance" (Einstein *et al.* 1952), "The general laws of nature are to be expressed by equations which hold good for all systems of co-ordinates, that


CC-0. In Public Domain. Gurukul Kangri Collection, Haridwar

Digitized by Arya Samaj Foundation Chennai and eGangotri


is, are co-variant with respect to any substitutions whatever (generally co-variant)." Unfortunately, this "principle" results in acceptance of unphysical solutions in Einstein's theory (Kramer 1980). This should be expected since the "principle of covariance" is only an interim assumption due to Einstein's certain uncertainty of the space-time coordinates (Lo 2002).

Einstein's "covariance principle" allows different metrics for the same frame of reference, and thus is in conflict with Einstein's equivalence principle (Lo 2003b), which implies the space contractions are unique for a given frame of reference. For a spherical mass distribution, there is a "radial" gauge whose solution without radius contraction as follows (Lo 2004):

$$ds^2 = H(R)\, c^2dt^2 - dR^2 - G(R)^2\, R^2\, (d\theta^2 + \sin^2\theta d\varphi^2)\,, \qquad (1)$$

where H(R) and G(R) are functions of R, which is $[X^2 + Y^2 + Z^2]^{1/2}$. This metric is diffeomorphic to the isotropic solution,

$$ds^2 = [(1- M\kappa/2r)^2/(1 + M\kappa/2r)^2]c^2dt^2 - (1 + M\kappa/2r)^4\, (dx^2+dy^2+dz^2) \qquad (2)$$

where $\kappa = G/c^2$ ($G = 6.67\times10^{-8}$ erg cm/gm$^2$), M is the total mass of a spherical mass distribution with the center at the origin of the frame of reference K (x, y, z), and $r = [x^2 + y^2 + z^2]^{1/2}$. The related diffeomorphism is

$$R(r) = r - M\kappa \ln(M\kappa/2r) - (M\kappa)^2/4r + C_0, \qquad r > M\kappa/2 \qquad (3)$$

and

$$H(R) = (1 - M\kappa/2r)^2/(1 + M\kappa/2r)^2, \qquad RG(R) = (1 + M\kappa/2r)^2\, r, \qquad (4)$$

where $C_0$ (= R[Mκ/2]) is a non-negative constant. Thus, an "event of horizon" for Radial metric (1) corresponds to the arbitrary constant $C_0$. However, these two metrics (1) and (2) share the same frame of reference and lead to the same first-order deflection angle of a light ray (Lo 2004), i.e., $C_0$ does not show up in the formula. It will be shown that this arbitrary constant $C_0$ will appear in the first-order formula for de Sitter Precession.

A problem is that a satisfaction of Einstein's equivalence principle is assumed but not proven (Einstein *et al.* 1952, Einstein 1954). Since the coordinates are ambiguous his equivalence principle was mistakenly regarded (Norton 1989) the same as Pauli's. [6] However, it is has been clarified that the binary pulsars experiments must be explained in terms of the Maxwell-Newton Approximation (Lo 1995, 2000). Currently, the formula for de Sitter Precession is calculated in terms of the MNA (Ohanian & Ruffini 1994), and many believed incorrectly that the resulting formula is independent of the gauges. In fact, Einstein's covariance principle has been proven to be clearly invalid (Lo 2005a, 2008a).

## 3. THE SPACE-TIME METRICS FOR THE STANFORD EXPERIMENT

In general relativity, there are more than one metric solution for a frame of reference. For instance, for the gravity of a massive source of spherical static dis-


CC-0. In Public Domain. Gurukul Kangri Collection, Haridwar

Digitized by Arya Samaj Foundation Chennai and eGangotri


tribution, the well-known metric solutions are the Schwarzschild solution, the isotropic solution and the harmonic solution (Weinberg 1972; Will 1993; Misner *et al.* 1973). The latter two have the same first order. It will be shown that the Maxwell-Newton Approximation and the Schwarzschild solution would give distinct formulas for the precession of a spin under gravity.

The equation for the Maxwell-Newton Approximation (Lo 2000) for a massive source $T(m)_{\mu\nu}$ is,

$$\frac{1}{2}\partial^C\partial_C\bar{\gamma}_{\mu\nu} = 8\kappa T(m)_{\mu\nu}, \quad \text{where} \quad \bar{\gamma}_{\mu\nu} = \gamma_{\mu\nu} - \frac{1}{2}\eta_{\mu\nu}(\eta^{cd}\gamma_{cd}) \quad (5)$$

and $\gamma_{\mu\nu} = g_{\mu\nu} - \eta_{\mu\nu}$ is the deviation from the flat metric $\eta_{\mu\nu}$, and $\kappa = G/c^2$ ($G = 6.67 \times 10^{-11}$ $m^3kg^{-1}s^{-2}$) is the coupling constant. Note that the Maxwell-Newton Approximation, which is obtained directly (Lo 1999) from Einstein's equivalence principle, is different from the linear field equation obtained through linearization. In the Maxwell-Newton Approximation, the source term must be an energy-stress tensor of massive matter (Lo 1995).

For a spherical mass distribution with a steady uniform rotation in the z-direction, the solution of (5) is the following (Ohanian & Ruffini 1994):

$$ds^2 = (1-2M\kappa/r)dt^2 - (1+2M\kappa/r)(dx^2 + dy^2 + dz^2) + 4\kappa(A_z/r^3)(xdy - ydx)dt, \quad (6)$$

where M is the total mass, $A_z$ is the spin angular momentum coincides with the z-axis. For a rotating mass, the Schwarzschild solution is extended to the Kerr metric (Wald 1984). For the first order approximation, the first order of Kerr metric is reduced to

$$ds^2 = (1-2M\kappa/r)dt^2 - (1+2M\kappa/r)\,dr^2 - r^2\,(d\theta^2+\sin^2\theta d\varphi^2) + 4\,\kappa\,(A_z/r^3)(xdy-ydx)dt. \quad (7)$$

Note that the last terms, which correspond to the rotation in metrics (6) and (7), are identical. It thus follows that the Lense-Thirring precession (Ohanian & Ruffini 1994) in the first order from these two metrics are essentially the same.

## 4. DISTINCT FORMULAS FOR THE DE SITTER PRECESSION

However, two different metrics, actually produce different formulas for the *de Sitter* precession. In general relativity, the equation for the parallel transport of the spin $S^\mu$ involves the Christoffel symbols is,

$$\frac{dS^\mu}{d\tau} = -\Gamma^\mu_{\alpha\beta}S^\alpha\frac{dx^\beta}{d\tau}, \quad \text{where} \quad \Gamma^\mu{}_{\alpha\beta} = \frac{1}{2}g^{\mu\nu}\left(\partial_\alpha g_{\nu\beta} + \partial_\beta g_{\nu\alpha} - \partial_\nu g_{\alpha\beta}\right). \quad (8)$$

Then, one can calculate how the spin of a gyroscope change direction while the gyroscope moves along some free fall trajectory (Ohanian & Ruffini 1994).

From the Maxwell-Newton Approximation, one obtains the *de Sitter* precession formula as follows:


CC-0. In Public Domain. Gurukul Kangri Collection, Haridwar

Digitized by Arya Samaj Foundation Chennai and eGangotri


$$\frac{d\vec{S}}{d\tau} = -2(\vec{v}\bullet\vec{S})\vec{\nabla}\Phi + \vec{v}(\vec{S}\bullet\vec{\nabla}\Phi) + \vec{S}(\vec{v}\bullet\vec{\nabla}\Phi) = \vec{v}\times(\vec{S}\times\vec{\nabla}\Phi) + \vec{S}\times(\vec{v}\times\vec{\nabla}\Phi), \quad (9)$$

where $\Phi = -\kappa M/r$, the "Newtonian potential", v is the velocity of the gyroscope, and S is the spin. However, from the Schwarzschild solution, the *de Sitter* precession would have a different formula (see Appendix A) as follows:

$$\frac{d\vec{S}}{d\tau} = -3(\vec{v}\bullet\vec{S})\vec{\nabla}\Phi + 3\hat{r}(\vec{S}\bullet\hat{r})(\vec{v}\bullet\vec{\nabla}\Phi), \quad (10)$$

where $\hat{r}$ is the unit vector in the r-direction. Moreover, from solution (1), the *de Sitter* precession formula (see Appendix A) as follows

$$\frac{d\vec{S}}{d\tau} = A(R)[\vec{v}\times(\vec{S}\times\nabla\Phi) + \vec{S}\times(\vec{v}\times\nabla\Phi)] + 3[A(R)-1]\nabla\Phi(\vec{S}\bullet\vec{v}) - B(R)\nabla\Phi(\hat{R}\bullet\vec{v})(\hat{R}\bullet\vec{S}) \quad (11)$$

where $A(R) = (2 - \alpha + \ln\frac{\kappa M}{2R})$, $\alpha = \frac{C_0}{\kappa M}$, $\Phi = -\frac{-\kappa M}{R}$, and $\hat{R}$ is the unit vector in the R-direction. At the surface of earth, we have $\kappa M/R \sim 6.95\text{X}10^{-10}$.

For a circular orbit situation, we have $(\vec{v}\bullet\vec{\nabla}\Phi) = 0$, and thus

$$\frac{d\vec{S}}{d\tau} = -2(\vec{v}\bullet\vec{S})\vec{\nabla}\Phi + \vec{v}(\vec{S}\bullet\vec{\nabla}\Phi), \quad (9')$$

$$\frac{d\vec{S}}{d\tau} = -3(\vec{v}\bullet\vec{S})\vec{\nabla}\Phi, \quad (10')$$

$$\frac{d\vec{S}}{d\tau} = A(R)\vec{v}(\vec{S}\bullet\nabla\Phi) + [A(R)-3]\nabla\Phi(\vec{S}\bullet\vec{v}), \quad \text{where } A(R) = (2 - \alpha + ln\frac{\kappa M}{2R}), \quad (11')$$

that is, formulas (9) - (11) are reduced to (9′) - (11′) respectively. Nevertheless, they are very different. For instance, if S is perpendicular to v, the right hand-side of formula (10′) is zero, but the right hand-side of formula (9′) is $\mathbf{v}(\mathbf{S}\bullet\nabla\Phi)$, a possibly non-zero quantity. Moreover, for the Radial gauge there is an arbitrary constant in formula (11′), in addition to the logarithmic terms.

In textbooks, such as the one by Ohanian & Ruffini (1994) formula (9) is derived. However, formula (10) was not derived since they believed that formula (9) is independent of the choice of a gauge. For the same incorrect belief, some (Weinberg 1972; Will 1993) derived formula (9) with the post-Newtonian Approximation, which has an implicit choice of gauges.

However, since the effect of precession is very small, we can measure only the accumulated effects. Then, these two formulas are probably difficult to be distinguished in practice since the time average of $\mathbf{v}(\mathbf{S}\bullet\nabla\Phi)$ and $-(\mathbf{v}\bullet\mathbf{S})\Phi$ over a period of circular time would be the same. To see this problem, let us take


CC-0. In Public Domain. Gurukul Kangri Collection, Haridwar

Digitized by Arya Samaj Foundation Chennai and eGangotri


$$\vec{v} = (-\hat{y}\sin\omega t + \hat{z}\cos\omega t)v \qquad \text{and} \qquad \vec{\nabla}\Phi = \frac{\kappa M}{r^2}(\hat{y}\cos\omega t + \hat{z}\sin\omega t). \tag{12}$$

Then

$$(\vec{v}\bullet\vec{S})\vec{\nabla}\Phi + \vec{v}(\vec{S}\bullet\vec{\nabla}\Phi)$$
$$= \frac{\kappa M}{r^2}\left[\hat{y}(-S^y\sin 2\omega t + S^z\cos 2\omega t) + \hat{z}(S^y\cos 2\omega t + S^z\sin 2\omega t)\right], \tag{13}$$

of which the average over a period of circular time would practically be zero since the spin $S^\mu$ changes very little over a period. To have a reliable analysis, a computer simulation is recommended.

Moreover, the task of distinguishing the Schwarzschild solution from an isotropic solution one can be accomplished by measuring simply the local light speeds (Zhou 1987, Lo 2003b). For the same reason, the unphysical metric solution (1) of the radial gauge would be rejected. Thus, the experiment Gravity Probe-B seems not be able to distinguish the Schwarzschild metric from the metric obtained from the Maxwell-Newton Approximation. However, for the radial metric (1), we have approximately $A(R) \sim -(19.2 + \alpha)$ ($\alpha$ is an arbitrary positive constant) at the surface of the earth. Thus, it is possible that formula (11) could be excluded directly by the Gravity Probe-B experiment (Everitt *et al.* 1996).

## 5. DISCUSSIONS AND CONCLUSIONS

The metric (6) from the Maxwell-Newton Approximation and the first order of the Kerr metric (7) are different in the first order, but they share the same frame of reference. For the problem of light bending, Einstein has shown that metrics of distinct first orders can give the same light deflection angle since for accumulating effects, the gauge differences are smoothed out (Lo 2004). Thus, Einstein claimed that his theory is gauge invariant.

This problem of gauge non-invariance was overlooked because many also unaware of that Einstein's "covariance principle" is in conflict with Einstein's equivalence principle. Recently, this has been illustrated (Lo 2005b) and supported by the formula of Landau & Lifshitz.

One might argued that diffeomorphic solutions are equivalent mathematically, but nobody was able to provide the related distinct measurements for different gauges for the case of having the same frame of reference. Furthermore, Einstein's "covariance principle" has been proven invalid (Lo 2005a) (see also Appendix B). Thus, as Logunov & Mestvirishvili (1989) pointed out, Einstein's theory actually does not have definite predictions.


CC-0. In Public Domain. Gurukul Kangri Collection, Haridwar

Digitized by Arya Samaj Foundation Chennai and eGangotri


However, it has been shown that the Maxwell-Newton Approximation is valid (Lo 2000). It thus follows that the Stanford experiment Gravity Probe-B would further confirm the Maxwell-Newton Approximation (Lo 2000).

The problem of ambiguity in coordinates was due to Einstein's theoretical errors on measurement (Lo 2005b) that failed to identify that the space contractions are actually measured in a local space at free fall. Einstein's way out was that the coordinates have no meaning other than labeling the position as in mathematics. However, Einstein and his followers actually did not practice what Einstein preached. [7)]

It has been overlooked that Einstein's theory of measurement would lead to light speeds that are in conflict with the observed bending of light (Lo 2003a, 2006a). However, the theoretical framework of general relativity actually implies that a physical space has a frame of reference that necessarily has the Euclidean-like structure (Lo 2003b). Then, it is clear that Will's (Bodenner & Will 2003; Gerard & Piereaux 1999) approach of specifying "genuinely measurable" quantities provides only an invalid claim of mathematical illusion (Lo 2008a).

*The Euclidean-like structure has made clear the physical meaning of the space coordinates*, and at most only one metric gives a realistic space contraction (Lo 2003b). To this end, one can measure local light speeds (Einstein *et al.* 1952; Einstein 1954), to decide experimentally a realistic metric. Since the rotation of the globe is very small, one can neglect the terms related to rotation (Lo 2003b). For instance, for the Schwarzschild solution, the local vertical and horizontal light speeds would be, respectively,

$$\frac{dr}{dt}=1-\frac{2M\kappa}{r}, \qquad \text{and} \qquad \frac{rd\theta}{dt}\approx 1-\frac{M\kappa}{r}. \tag{14}$$

On the other hand, metric (7) from the Maxwell-Newton Approximation would give a light speed for all directions to be,

$$1-\frac{2M\kappa}{r}. \tag{15}$$

For the Radial solution (1), since $\alpha > 0$ and $-\ln(M\kappa/2R) - 2 > 0$, the local vertical and horizontal light speeds above the earth surface would be, respectively,

$$\frac{dR}{dt}=1-\frac{M\kappa}{R}, \quad \text{and} \quad \frac{Rd\theta}{dt}\approx 1+[\alpha-\ln(M\kappa/2R)-2](M\kappa/R)>1. \tag{16}$$

Note that the light horizontal speeds are different from these three metrics. [8)] The invalidity of (16) is obvious. Moreover, since measuring the light horizontal speeds of different heights is allowed by modern technology (Lo 2003b, Li *et al.* 1990), the measured results would show that the Schwarzschild solution is invalid as Zhou (1983) conjectured. And the Maxwell-Newton Approximation would be further confirmed (Lo 1995, 2000).


CC-0. In Public Domain. Gurukul Kangri Collection, Haridwar

Digitized by Arya Samaj Foundation Chennai and eGangotri

## PRECESSION FORMULAS FOR GRAVITY PROBE-B AND ITS COMPLEMENTARY EXPERIMENTS OF LOCAL LIGHT SPEEDS

However, owing to misunderstanding of Einstein's equivalence principle, theorists such as Ohanian & Ruffini (1994) claimed that the measured coordinate light speed is inevitably c. This is incorrect since the derivation of light bending is based on such speeds (Einstein *et al.* 1952; Einstein 1954). In fact, the Michelson & Morley (1887) experiments showed that light speeds in the two perpendicular arms are different although it is far smaller than expected from ether theory. [9)]

Nevertheless, as mentioned (Lo 2003b), the local light speed experiment may not be accurate enough to measure the gravitational effects due to rotation. However, the Gravity Probe-B can measure the Lense-Thirring precession, a gravitational effect due to rotation (Ohanian & Ruffini 1994). Thus, these two experiments are complimentary tests for general relativity.

In addition, the metric in Whitehead's theory is diffeomorphic to the Schwarzschild solution, and they have the same Euclidean-like structure. The metric of Whitehead's theory (Coleman 2005) has another form as follows:

$$ds^2 = (1-2M\kappa/r)\, c^2dt^2-(1+2M\kappa/r)\, dr^2- r^2\, (d\theta^2+\sin^2\theta d\varphi^2) + 4(M\kappa/r)cdtdr, \quad (17)$$

which will be transformed to the Schwarzschild solution by the diffeomorphism,

$$cdt\rightarrow cdt - (2M\kappa/r)\, (1 - 2M\kappa/r)^{-1}dr, \quad (18a)$$

or

$$ct \rightarrow ct - 2M\kappa \ln(r - 2M\kappa) + C_1, \quad \text{where } C_1 \text{ is a constant.} \quad (18b)$$

Moreover, from earlier calculations, it is clear that metric (17) would give the same time-average de Sitter Precession, to which the cross-term has no contribution. Thus, Gravity Probe-B would not be able to tell whether general relativity or Whitehead's theory is valid. However, the experiment on local light speeds would tell whether Whitehead's theory is valid.

## ACKNOWLEDGMENTS

The author gratefully acknowledges stimulating discussions with Prof. Au Chi, Prof. S. -J. Chang, Prof. A. J. Coleman, Prof. Alan H. Guth, Prof. P. Morrison, and Professor C. Wong. Special Thanks are to D. Rabounski for valuable comments and useful suggestions. This work is supported in part by Innotec Design, Inc., USA.

## APPENDIX A: DISTINCT FORMULAS FOR THE DE SITTER PRECESSION

Since the space metric elements in the isotropic metric and the Schwarzschild metric are different in the first order, the precession formulas would be different for these two metrics.


CC-0. In Public Domain. Gurukul Kangri Collection, Haridwar

Digitized by Arya Samaj Foundation Chennai and eGangotri



However, many still believe that general relativity is gauge invariant. It will be shown through explicit calculations that this is simply not true. The equation for the parallel transport of the spin $S^\mu$ involves the Christoffel symbols,

$$\frac{dS^\mu}{d\tau} = -\Gamma^\mu_{\alpha\beta} S^\alpha \frac{dx^\beta}{d\tau}, \tag{8}$$

where

$$\Gamma_{\mu,\alpha\beta} = \frac{1}{2}\left(\frac{\partial g_{\mu\alpha}}{\partial x^\beta} + \frac{\partial g_{\mu\beta}}{\partial x^\alpha} - \frac{\partial g_{\alpha\beta}}{\partial x^\mu}\right) = g_{\mu\nu}\Gamma^\nu_{\alpha\beta}.$$

Then, one can calculate the change of spin direction of a gyroscope while it moves along some free fall trajectory (Ohanian & Ruffini 1994).

Since both metrics are static and the time-axis is orthogonal to a space axis, the non-zero $\Gamma_{\kappa,\alpha\beta}$ are:

$$\Gamma_{x,xx} = \frac{1}{2}\left(\frac{\partial g_{xx}}{\partial x}\right), \quad \Gamma_{x,yy} = \frac{1}{2}\left(2\frac{\partial g_{xy}}{\partial y} - \frac{\partial g_{yy}}{\partial x}\right) \quad \Gamma_{x,zz} = \frac{1}{2}\left(2\frac{\partial g_{xz}}{\partial z} - \frac{\partial g_{zz}}{\partial x}\right),$$

$$\Gamma_{x,xy} = \frac{1}{2}\left(\frac{\partial g_{xx}}{\partial y}\right), \quad \Gamma_{x,xz} = \frac{1}{2}\left(\frac{\partial g_{xx}}{\partial z}\right), \quad \Gamma_{x,yz} = \frac{1}{2}\left(\frac{\partial g_{xy}}{\partial z} + \frac{\partial g_{xz}}{\partial y} - \frac{\partial g_{yz}}{\partial x}\right),$$

$$\Gamma_{x,tt} = -\frac{1}{2}\left(\frac{\partial g_{tt}}{\partial x}\right), \quad \Gamma_{x,xy} = \Gamma_{x,yx}, \quad \Gamma_{x,xz} = \Gamma_{x,zx}, \quad \Gamma_{x,yt} = -\Gamma_{y,xt} = \frac{1}{2}\left(\frac{\partial g_{xt}}{\partial y} - \frac{\partial g_{yt}}{\partial x}\right),$$

$$\Gamma_{x,zt} = -\Gamma_{z,xt} = \frac{1}{2}\frac{\partial g_{xt}}{\partial z}, \text{ and } \Gamma_{y,zt} = -\Gamma_{z,yt} = \frac{1}{2}\frac{\partial g_{yt}}{\partial z}. \tag{A1}$$

For the isotropic solution, for the first order, we have an orthogonal metric with

$$\gamma_{tt} = \gamma_{xx} = \gamma_{yy} = \gamma_{zz} = -2\frac{\kappa M}{r} = 2\Phi, \quad \gamma_{xt} = -2\kappa A_z \frac{y}{r^3} \text{ and } \gamma_{yt} = 2\kappa A_z \frac{x}{r^3} \tag{A2}$$

Thus

$$\Gamma_{x,tt} = -\Gamma_{x,xx} = \Gamma_{x,yy} = \Gamma_{x,zz} = -\frac{1}{2}\frac{\partial \gamma_{tt}}{\partial x}, \text{ and } \Gamma_{x,xy} = \frac{1}{2}\frac{\partial \gamma_{tt}}{\partial y}. \quad \Gamma_{x,zt} = 3\kappa A_z \frac{yz}{r^5},$$

$$\text{and } \Gamma_{x,yt} = -\Gamma_{y,xt} = \kappa A_z\left(\frac{1}{r^3} - 3\frac{z^2}{r^5}\right). \tag{A3}$$

Since in the rest frame $S'^t = 0$ and $dx'^\mu/d\tau = (1, 0, 0, 0)$, we have $g'_{\mu\nu} S'^\mu dx'^\nu/d\tau = 0$. It follows that

$$S^t = -\frac{1}{g_{tt}\dfrac{dt}{d\tau}} \sum_{i,j=1}^{3}\left(S^i g_{ij} \frac{dx^j}{d\tau}\right) \approx \vec{S} \bullet \frac{\vec{v}}{c}. \tag{A4}$$

Finally, from the Maxwell-Newton Approximation, one obtains the precession formula as follows:

$$\frac{d\vec{S}}{d\tau} = -2(\vec{v} \bullet \vec{S})\vec{\nabla}\Phi + \vec{v}(\vec{S} \bullet \vec{\nabla}\Phi) + \vec{S}(\vec{v} \bullet \vec{\nabla}\Phi) + P_{LT} = \vec{v} \times (\vec{S} \times \vec{\nabla}\Phi) + \vec{S} \times (\vec{v} \times \vec{\nabla}\Phi) + P_{LT},$$


CC-0. In Public Domain. Gurukul Kangri Collection, Haridwar

Digitized by Arya Samaj Foundation Chennai and eGangotri



where $P_{LT} = \frac{K}{r^3}\left[\vec{S}\times\vec{A}+(\vec{v}\times\vec{A})(\vec{S}\bullet\vec{v})-3(\hat{r}\bullet\vec{A})\{\vec{S}\times\hat{r}+(\vec{v}\times\hat{r})(\vec{S}\bullet\vec{v})\}\right]$ (9)

is the term for the Lense-Thirring precession, and $\hat{r}$ is the unit vector, $\vec{A} = (0, 0, A_z)$ as defined in (8), $\Phi = -\kappa M/r$, the "Newtonian potential", v is the velocity of the gyroscope, c = 1, and S is the spin. For the time average, we have only

$$P_{LT} \sim \frac{K}{r^3}\left[-\frac{1}{2}\vec{S}\times\vec{A}+\{(\vec{v}\times\vec{A})-3(\hat{r}\bullet\vec{A})(\vec{v}\times\hat{r})\}(\vec{S}\bullet\vec{v})\right] \sim -\frac{K}{2r^3}\vec{S}\times\vec{A}.$$

Thus, the effects of *Lense-Thirring* precession can be distinguished from the effects of *de Sitter* precession.

However, from the Schwarzschild solution, the metric elements of space are:

$$\gamma_{tt} = -2\frac{\kappa M}{r} = 2\Phi, \quad \gamma_{xx} = -2\kappa M\frac{x^2}{r^3} = 2\Phi\frac{x^2}{r^2}, \quad \text{and} \quad \gamma_{xy} = -2\kappa M\frac{xy}{r^3} = 2\Phi\frac{xy}{r^2}. \quad \text{(A5)}$$

Then, we obtain,

$$\frac{1}{2}\frac{\partial g_{xx}}{\partial x} = -\nabla_x\Phi\left(2-3\frac{x^2}{r^2}\right), \qquad \frac{1}{2}\frac{\partial g_{xx}}{\partial y} = 3\nabla_y\Phi\left(\frac{x^2}{r^2}\right) \qquad \frac{1}{2}\frac{\partial g_{xy}}{\partial y} = -\nabla_x\Phi\left(1-3\frac{y^2}{r^2}\right),$$

and

$$\frac{1}{2}\frac{\partial g_{xy}}{\partial z} = 3\nabla_z\Phi\left(\frac{xy}{r^2}\right) = 3\kappa M\frac{xyz}{r^5}. \quad \text{(A6)}$$

Thus, from the Schwarzschild solution, the *de Sitter* precession would have a different formula as follows:

$$\frac{d\vec{S}}{d\tau} = -3(\vec{v}\bullet\vec{S})\vec{\nabla}\Phi+3\hat{r}(\vec{S}\bullet\hat{r})(\vec{v}\bullet\vec{\nabla}\Phi), \quad (10)$$

where $\hat{r}$ is the unit vector in the r-direction.

Moreover, from solution (3), the metric elements of space are:

$$\gamma_{tt} = -2\frac{\kappa M}{R} = 2\Phi, \quad \gamma_{xx} = -[G^2(R)-1](1-\frac{X^2}{R^2}) \qquad \text{and} \quad \gamma_{xy} = [G^2(R)-1]\frac{XY}{R^2}, \quad \text{(A7)}$$

where $[G^2(R)-1] \approx \frac{2\kappa M}{R}(1-\alpha+\ln\frac{\kappa M}{2R})$. Then, to the first order, we obtain,

$$\frac{1}{2}\frac{\partial g_{tt}}{\partial x} \approx \nabla_x\Phi, \qquad \frac{1}{2}\frac{\partial g_{xx}}{\partial x} \approx B(R)\nabla_x\Phi\left(1-\frac{X^2}{R^2}\right), \qquad \frac{1}{2}\frac{\partial g_{xx}}{\partial y} \approx \nabla_y\Phi\left(A(R)-B(R)\frac{X^2}{R^2}\right)$$

$$\frac{1}{2}\frac{\partial g_{xy}}{\partial x} \approx \nabla_y\Phi\left([A(R)-1]-B(R)\frac{X^2}{R^2}\right), \quad \text{and} \quad \frac{1}{2}\frac{\partial g_{xy}}{\partial z} \approx -B(R)\nabla_z\Phi\frac{XY}{R^2}. \quad \text{(A8)}$$

where

$$A(R) = (2-\alpha+\ln\frac{\kappa M}{2R}), \qquad B(R) = 3A(R)-2, \qquad \text{and} \qquad \alpha = \frac{C_0}{\kappa M}.$$


CC-0. In Public Domain. Gurukul Kangri Collection, Haridwar

Digitized by Arya Samaj Foundation Chennai and eGangotri


At near the surface of earth, we have $\kappa M/R \sim 6.95 \times 10^{-10}$. Thus, the logarithmic term should not be neglected.

From this unphysical solution (1), the *de Sitter* precession would have a different formula as follows:

$$\frac{d\vec{S}}{d\tau} = A(R)[\vec{v}\times(\vec{S}\times\nabla\Phi)+\vec{S}\times(\vec{v}\times\nabla\Phi)]+3[A(R)-1]\nabla\Phi(\vec{S}\bullet\vec{v})-B(R)\nabla\Phi(\hat{R}\bullet\vec{v})(\hat{R}\bullet\vec{S})$$

$$= A(R)[\vec{S}(\vec{v}\bullet\nabla\Phi)+\vec{v}(\vec{S}\bullet\nabla\Phi)+(\vec{v}\bullet\vec{S})\nabla\Phi]-3\nabla\Phi(\vec{S}\bullet\vec{v})-B(R)\hat{R}(\vec{v}\bullet\nabla\Phi)(\hat{R}\bullet\vec{S}) \quad (11)$$

where $\hat{R}$ is the unit vector in the R-direction. The terms for the Lense-Thirring precession would be similar as those in (9).

It follows that the time-average of formula (10′) and (11′) would be essentially the same as that for (9′),

$$\left\langle\frac{d\vec{S}}{d\tau}\right\rangle = \frac{3}{2}\frac{\kappa M}{r^3}(\vec{r}\times\vec{v})\times\vec{S}\,. \quad (A9)$$

Thus, for the *de Sitter* precession, on the average, S precesses about the axis of the obit with an angular velocity (Ohanian & Ruffini 1994)

$$\Omega_G = \frac{3}{2}\frac{\kappa M}{r^3}(\vec{r}\times\vec{v}) = -\frac{3}{2}(\nabla\Phi\times\vec{v})\,. \quad (A10)$$

Note that the differences between formulas (9′), (10′) and (11′) are averaged out. The total precession would be

$$\left\langle\frac{d\vec{S}}{d\tau}\right\rangle = \Omega_T\times\vec{S}\,, \qquad \text{where } \Omega_T = -\frac{3}{2}(\nabla\Phi\times\vec{v})+\frac{K\vec{A}}{2r^3}\,. \quad (A11)$$

The additional term comes from the *Lense-Thirring* precession.

Nevertheless, since A(R) includes an arbitrary constant $\alpha$, the formula for the *de Sitter* Precession is clearly not gauge invariant. Moreover, since $\alpha$ could be rather large, the effect of the averaged out term would be experimentally distinguishable. It should be noted also that although solution (1), the Schwarzschild solution, and the Maxwell-Newton Approximation give the same time-average precession, it remains to show (A9) and (A11) as predictions of Einstein's theory.

In general relativity, the problem of precession actually goes much deeper than determining the correct gauge in the calculation of a "test particle" theory. In fact, although the Maxwell-Newton Approximation may have dynamic solutions for a two-body problem, the Einstein equation of 1915 does not has a dynamic solution (Lo 1995, 2000) as Gullstrand (1921, 1922) suspected.

## APPENDIX B: GAUGE, COORDINATES, AND MEASUREMENT

In Einstein's "principle of covariance", what has been missing is the relation between coordinates and measurements. A difference between physics and


CC-0. In Public Domain. Gurukul Kangri Collection, Haridwar

Digitized by Arya Samaj Foundation Chennai and eGangotri



mathematics is that a coordinate system in physics is related to measurement and its method, whereas a coordinate system in mathematics need not be related to those. It is this oversight on his theory of measurement that Einstein failed to produce a self-consistent general relativity (Lo 2005a, 2005b).

The crucial point of the covariance principle is the validity of any Gaussian coordinate system as a space-time coordinate system in physics. For this, Einstein's supporting arguments (Einstein *et al.* 1952) are as follows:

> "That this requirement of general covariance, which takes away from space and time the last remnant of physical objectivity, is a natural one, will be seen from the following reflexion. All our space-time verifications invariably amount to a determination of space-time coincidences. If, for example, events consisted merely in the motion of material points, then ultimately nothing would be observable but the meetings of two or more of these points. Moreover, the results of our measurings are nothing but verifications of such meetings of the material points of our measuring instruments with other material points, coincidences between the hands of a clock and points on the clock dial, and observed point-events happening at the same place at the same time. The introduction of a system of reference serves no other purpose than to facilitate the description of the totality of such coincidences."

Note that the meaning of measurements is crucially omitted. Moreover, in order to predict events, one must be able to relate events of different locations in a definite manner (Lo 2005a). *This means a valid method of measurement is necessary.*

The outcome of a real experiment cannot depend on a choice of physical coordinates because their physical meaning is based on measurements. However, in general relativity the physical meaning of the coordinates would implicitly depend on the gauge, which may not be physically realizable (Lo 2008a).

For example, some theorists argued,"... deflection of light bending is described by solving equations of motion in some background curved spacetime. The result must be independent of any coordinates since the light curve is a geometric object. The physical observation should be also possible to measure the angles which are independent of coordinates. Coordinates are just representations of geometric objects. I think that any physical argument can be expressed in a very clear way especially through mathematics." However, this argument actually involves some implicit assumptions that could be overlooked.

Physical coordinates are representations of geometric objects since such coordinates are based on real measurements. However, mathematical coordinates need not be based on measurements and the coordinates for a gauge is based on assumed measurements, which may or may not be realizable. Thus, the


CC-0. In Public Domain. Gurukul Kangri Collection, Haridwar

Digitized by Arya Samaj Foundation Chennai and eGangotri



coordinates for a gauge need not be representing geometric objects, In other words, the above arguments may not be valid for the mathematical coordinates (for a gauge) because the related measurements may not be realizable.

A crucial criterion is that physics involves actual measurement, whereas mathematics involved only assumed measurements or no measurements at all. Consider two diffeomorphic solutions that have the same frame of reference K such as the isotropic solution and Schwarzschild solution respectively as follows:

$$ds^2 = [(1 - M\kappa/2\rho)^2/(1 + M\kappa/2\rho)^2]c^2dt^2 - (1 + M\kappa/2\rho)^4 (dx'^2 + dy'^2 + dz'^2), \quad \text{(B1a)}$$

where

$$x' = \rho\sin\theta\cos\varphi, \quad y' = \rho\sin\theta\sin\varphi, \quad z' = \rho\cos\theta, \text{ and } \rho > M\kappa/2. \quad \text{(B1b)}$$

and

$$ds^2 = (1 - 2M\kappa/r)c^2dt^2 - (1 - 2M\kappa/r)^{-1}dr^2 - r^2d\theta^2 - r^2\sin^2\theta d\varphi^2, \quad \text{(B2a)}$$

where

$$x = r\sin\theta\cos\varphi, \quad y = r\sin\theta\sin\varphi, \quad z = r\cos\theta, \text{ and } r > 2\kappa M \quad \text{(B2b)}$$

where $\kappa = G/c^2$ ($G = 6.67\times10^{-8}$ erg cm/gm$^2$), M is the total mass of a spherical mass distribution.

These two systems are reduced to the Minkowski space when M = 0. Radicals r and ρ are related by

$$r = \rho (1 + M\kappa/2\rho)^2, \quad \text{for} \quad r > 2\kappa M. \quad \text{(B3)}$$

These two metrics are equivalent in terms of mathematics. *However, from (B3) it is clear that only one of the gauges (and its coordinates) can be physically realizable*, i.e., with a physical coordinate system that is based on measurements. Then the assumed physical meaning of other coordinate systems is not physically realizable because space contractions are unique.

A major problem is, however, that we still do not have a sure way to choose a physical coordinate system (Lo 2008a). Thus, we still do not have a sure way that any physical argument can always be expressed in a very clear way especially through mathematics, although we should have,

According to Einstein (1954; Einstein et al. 1952) , the Einstein-Minkowski condition implies (Lo 2007d) that at each point of a physical space, there is a resting local Minkowski space (dT, dR, $dX_\theta$, $dX_\varphi$) at free fall. Here dT is the local time, dR is at the direction from the origin outward, $dX_\theta$ is in the θ-direction, and $dX_\varphi$ is in the φ-direction. Then, we consider the space contractions and the time dilation in terms of the local Minkowski space (dT, dR, $dX_\theta$, $dX_\varphi$).

If the isotropic metric satisfies Einstein's equivalence principle, one would have

$$dR=(1+M\kappa/2\rho)^2d\rho, \quad dX_\theta=(1+M\kappa/2\rho)^2d\theta, \quad dX_\varphi=(1+M\kappa/2\rho)^2\sin\theta d\varphi \quad \text{(B4a)}$$



CC-0. In Public Domain. Gurukul Kangri Collection, Haridwar

Digitized by Arya Samaj Foundation Chennai and eGangotri



and

$$dT = [(1 - M\kappa/2\rho)/(1 + M\kappa/2\rho)]dt. \qquad \text{(B4b)}$$

If the Schwarzschild metric satisfies Einstein's equivalence principle, one would have

$$dR = (1 - 2M\kappa/r)^{-1/2}dr, \qquad dX_\theta = rd\theta, \qquad dX_\varphi = r\sin\theta d\varphi \qquad \text{(B5a)}$$

and

$$dT = (1 - 2M\kappa/r)^{1/2}dt \qquad \text{(B5b)}$$

Here, (B4) and (B5) are formally equivalent in mathematics. However, the issue of measurement has not been considered.

In terms of measurements, these two metrics are very different. According to (B5a), there is no space contraction in the θ-direction and the φ-direction, but according to (B4a), there are space contractions. Experimentally, we do not know the gauge until measurements tell us what the gauge is. Since the Euclidean-like structure is determined by measurements, in the real world there is only one Euclidean-like structure. In the final analysis, physics is based on measurements.

To justifythe "covariance principle", it was also argued (Le Bas 2007),

> "If one makes the mistake of attributing incorrect physical properties to one's coordinates -- for example, assuming that because two objects in different coordinate systems are both labeled r, they must measure the same distance, or assuming that any coordinate labeled *r* must measure proper radial distance -- then one can mistakenly conclude that computations in different coordinate systems disagree. But as long as one identifies genuinely measurable quantities, their values cannot depend on coordinates."

It turns out that such a notion of "genuinely measurable" quantities is a mathematical illusion only (Lo 2008a). [10] In fact, such a notion of gauge invariant quantity has the same problem as that in Einstein's "covariance principle" -- the issue of measurement is ignored. In terms of calculations, the outcome is independent of the coordinates only if the meaning of the coordinates does not change.

Some theorists claimed that Logunov has proved Einstein's covariance principle. However, the approach of Logunov (1990) actually also failed because his derivation is based on the space contraction formula of Landau & Lifshitz (1962). Although their formula seems to be derivable unconditionally, its physical validity depends on whether Einstein's equivalence principle is satisfied (Lo 2003a, 2008b). Thus, an implicit assumption is that the gauge is physically valid. Therefore, his coordinate systems are restricted only to the physical gauge. Thus, *such an invalid claim is due to inadequate understanding of Einstein's equivalence principle that the physical validity of their formula depends* (Lo 2003a).

Digitized by Arya Samaj Foundation Chennai and eGangotri



Einstein (1982) once remarked, "If you want to find out anything from the theoretical physicists about the methods they use, I advise you stick closely to one principle: don't listen to their words, fix your attention on their deeds." *Einstein and his followers actually use* the physical meaning of coordinates is implicitly. Moreover, all physical predictions must be understood in terms of the physical meaning of coordinates (Lo 2003a, 2005b, 2006b).

ENDNOTES

1) Theoretically, for the first order approximation, the harmonic gauge is valid for this problem of precession (Lo 1999, 2000). However, there are more than one metric having the same first order approximation.

2) Carlo Cercignani, Vice Director *Il Nuovo Cimento B* reported that the editorial interpretation of the covariance principle is that for different gauges (such as the Schwarzschild metric and the isotropic metric) with the same frame of reference, the precession formula should be different but equally valid. (March 23, 2007). Moreover, some journals believed in Einstein's covariance principle (Lo 2005a, 2008a) because they failed to distinguish the difference between mathematics and physics.

3) C. M. Will is Chair of NASA's Science Advisory Committee for Gravity Probe B, and is the President of the International Society on General Relativity and Gravitation (2004-2007).

4) Whitehead (1922, p. 83) objected, for instance, "By identifying the potential mass impetus of a kinematics element with a spatio-temporal measurement Einstein, in my opinion, leaves the whole antecedent theory of measurement in confusion, when it is confronted with the actual conditions of our perceptual knowledge. The potential impetus shares in the contingency of appearances. It therefore follows that measurement on his theory lacks systematic uniformity and requires a knowledge of the actual contingent physical field before it is possible."

5) Pauli's (1958) version is as follows: "For every infinitely small world region (i.e. a world region which is so small that the space- and time-variation of gravity can be neglected in it) there always exists a coordinate system $K_0(X_1, X_2, X_3, X_4)$ in which gravitation has no influence either in the motion of particles or any physical process." However, Einstein (Einstein et al. 1952, p. 144] remarked, "For it is clear that, e.g., the gravitational field generated by a material point in its environment certainly cannot be 'transformed away' by any choice of the system of coordinates, i.e. it cannot be transformed to the case of constant $g_{\mu\nu}$." Thus, clearly Pauli has made errors in functional analysis.


CC-0. In Public Domain. Gurukul Kangri Collection, Haridwar

Digitized by Arya Samaj Foundation Chennai and eGangotri


6) Pauli's (1958) version was commonly but mistakenly regarded as Einstein's equivalence principle. For instance, Misner, Thorne, & Wheeler (1973) falsely claimed that Einstein's equivalence principle is as follows:

"In any and every local Lorentz frame, anywhere and anytime in the universe, all the (Nongravitational) laws of physics must take on their familiar special-relativistic form. Equivalently, there is no way, by experiments confined to infinitestimally small regions of spacetime, to distinguish one local Lorentz frame in one region of spacetime frame any other local Lorentz frame in the same or any other region."

However, this version also missed the Einstein-Minkowski condition.

7) The principle of causality (Lo 1995) assumes that the causes of phenomena are identifiable. This principle is commonly used in symmetry consideration in electrodynamics. In general relativity, Einstein and other theorists have used this principle implicitly on symmetry considerations (Einstein *et al.* 1952; Einstein 1954; Ohanian & Ruffini 1994; Eddington 1975; Pauli 1958; Weinberg 1972; Will 1993; Misner *et al.* 1973; Wald 1984). Thus, the physical meaning of space coordinates has been used not only subsequently, but also right at the beginning (Einstein *et al.* 1952). Some other consequences are that parameters unrelated to any physical cause in a solution is not allowed and that a dynamic solution must be related to a dynamic source.

8) Nevertheless, the light speeds (14) - (16) all give the same deflection angle of first order approximation. On the other hand, one could define light speed ($ds^2 = 0$) as $dl/dt$, where $dl^2 = g_{ij}\,dx^i\,dx^j$ (i, j, = 1, 2, 3) since $dl$ is the local distance according to Einstein's theory (Einstein et al. 1952, Einstein 1954). Then, all the above metrics give the same but only half of the observed deflection angle (Lo 2003a, 2006a).

9) Michelson & Morley (1887) stated that the effect (of change speed) was emphatically not "null" within the accuracy of the experiment, but was far smaller than expected from the addition of speeds (Miller 1933).

10) For instance, it is impossible to have a precession formula presented with gauge invariant "genuinely measurable" quantities. This further illustrates that such quantities are created only by mathematical illusions.

## REFERENCES

1. Le, Bas Louise, Publishing Editor, the Royal Society, A Board Member's Comments (July 24, 2007).
2. Bodenner, J. and Will, C. M., 2003. *Am. J. Phys.* 71 (8): 770 (August 2003).


CC-0. In Public Domain. Gurukul Kangri Collection, Haridwar

Digitized by Arya Samaj Foundation Chennai and eGangotri



3. Bondi, H., Pirani, F. A. E., and Robinson, I. 1959. *Proc. R. Soc. London* A **251**: 519-533.
4. Coleman, A. J. 2005. "J. L. Synge on Whitehead's Principle of Relativity," arXiv: physics/0505027 ,Vol. 1, 4 May 2005.
5. Eddington A. S., 1975. ***The Mathematical Theory of Relativity*** (Chelsea, New York).
6. Einstein, A.1954. ***The Meaning of Relativity*** (Princeton Univ. Press, Princeton), p. 63, p. 87 & p. 93.
7. Einstein, A. 1982. 'On the Method of Theoretical physics (1934)' in ***Ideas and Opinions*** (Dover, New York).
8. Einstein, A., Lorentz, H. A., Minkowski, H., and Weyl H., 1952. ***The Principle of Relativity*** (Dover, New York), p.162.
9. Everitt, C. W. F. *et al.* 1996. In Proc. Seventh Marcel Grossmann Meeting on Gen. Relativ., Stanford, July 1994, ed. R. Jantzen & M. Keiser, Ser. ed. R. Ruffini, 1533 (World Sci., Singapore).
10. Fock, V. A. 1964. ***The Theory of Space Time and Gravitation*** (Pergamon Press, New York).
11. Gérard, J. M. and Piereaux, S., 1999. "The Observable Light Deflection Angle," arXiv:gr-qc/9907034 ,Vol.1 , 8 Jul 1999.
12. Gullstrand, A., 1921. *Ark. Mat. Astr. Fys.* **16**, No. 8.
13. Gullstrand, A., 1922. *Ark. Mat. Astr. Fys.* **17**, No. 3.
14. Kramer, D., Stephani, H., Herlt, E., and MacCallum, M., 1980. ***Exact Solutions of Einstein's Field Equations***, ed. E. Schmutzer (Cambridge Univ. Press, Cambridge).
15. Landau, L. D. and Lifshitz, E. M. 1962. ***Classical Theory of Fields*** (Addison-Wesley, Reading Mass.).
16. Li Yonggui, Zhao Zhiqiang, Zhou Xiaofan, and Zhou Peiyuan 1990, "Measurement of the Relative Difference of Light Velocity in the Horizontal and Vertical Directions on the Earth's Surface", Proceeding of the Fourth Asia Pacific Physics Conference, Seoul, Korea, August 13-17, 1990, 2, 1155-1159.
17. Lo, C. Y., 1995, *Astrophys. J.*, **455**: 421-428.
18. Lo, C. Y., 1997. *Astrophys. J.* **477**: 700-704.
19. Lo, C. Y., 1999. *Phys. Essays*, **12** (3) : 508-526.
20. Lo, C. Y., 2000. *Phys. Essays*, **13** (4) : 527-539.
21. Lo, C. Y., 2002. *Phys. Essays*, **15** (3) : 303.
22. Lo, C. Y., 2003a. *Phys. Essays* **16** (1): 84-100.
23. Lo, C. Y., 2003b. *Chinese J. of Phys.*, **41** (4): 332.
24. Lo, C. Y., 2004. *Chinese Physics*, **13** (2): 159-167.
25. Lo, C. Y., 2005a. *Phys. Essays*, **18** (1) : 112-124.
26. Lo, C. Y., 2005b. *Phys. Essays*, **18** (4) : 539.
27. Lo, C. Y., 2006a. *Progress in Phys.*, Vol. 1 : 10-13.
28. Lo, C. Y., 2006b. *Astrophys. Space Sci.*, **306**: 205-215.
29. Lo, C. Y., 2007. *Bulletin of Pure and Applied Sciences*, **26D** (2): 73-88.


CC-0. In Public Domain. Gurukul Kangri Collection, Haridwar

Digitized by Arya Samaj Foundation Chennai and eGangotri


30. Lo, C. Y., 2008a. *Bulletin of Pure and Applied Sciences*, **27D** (1):1-15.
31. Lo, C. Y., 2008b."Einstein's Requirement for Weak Gravity versus Einstein's Covariance Principle", **Conference on Physical Interpretation of Relativity Theory**, Imperial College, London, September 12 – 15, 2008b.
32. Logunov, A. A., 1990. ***Lectures in Relativity and Gravitation: A Modern Look***, translated by Alexander Repyev (Nauka, Moscow, & Pergamon, New York, 1990), Section 1.22.
33. Logunov, A. and Mestvirishvili, M., 1989. ***The Relativistic Theory of Gravitation*** (Mir Publishers, Moscow), p. 106 & 165.
34. Michelson ,A. A. and Morley, E. W., 1887. *Am. J. Sci.* 34 : 333-345.
35. Miller, D. C., 1933. *Reviews of Modern Physics* 5: 203-241.
36. Misner, C. W., Thorne, K. S., and Wheeler, J. A., 1973. ***Gravitation*** (Freeman, San Francisco).
37. Norton, J., 1989. "What was Einstein's Principle of Equivalence?" in Einstein's Studies Vol. 1: ***Einstein and the History of General Relativity***, eds. D. Howard & J. Stachel (Birkhäuser, 1989); http://www.alberteinstein.info.
38. Ohanian, H. C. and Ruffini, R., 1994. ***Gravitation and Spacetime*** (Norton, New York), p. 198.
39. Pauli, W., 1958. ***Theory of Relativity*** (Pergamon, London).
40. Fiona Pring, 2007. The Royal Society, on Board Member's Comments, "... to require that the components of the metric be bounded. This is a coordinate-dependent condition, and is physically meaningless." (Jan. 8, 2007).
41. Wald , R. M., 1984. ***General Relativity*** (The Univ. of Chicago Press, Chicago).
42. Weinberg, S., 1972. ***Gravitation and Cosmology*** (John Wiley, New York).
43. Whitehead, A. N., 1922. ***The Principle of Relativity*** (Cambridge Univ. Press, Cambridge).
44. Will, C. M., 1976. *Astrophys. J.* 204: 224-234.
45. Will, C. M., 1993. ***Theory and Experiment in Gravitational Physics*** (Cambridge University Press).
46. Will, C. M., 2003. *Phys. Rev.* D, 67: 062003-1.
47. Zhou, Pei-Yuan, 1987. "Further Experiments to Test Einstein's Theory of Gravitation", International Symposium on Experimental Gravitational Physics (Guangzhou, 3-8 August 1987, ed. Peter F. Michelson (World Scientific, Singapore).
48. Zhou, (Chou) Peiyuan, 1983. "On Coordinates and Coordinate Transformation in Einstein's Theory of Gravitation" in ***Proc. of the Third Marcel Grossmann Meetings on Gen. Relativ.***, ed. Hu Ning, Science Press & North Holland, 1-20.


CC-0. In Public Domain. Gurukul Kangri Collection, Haridwar

Digitized by Arya Samaj Foundation Chennai and eGangotri

CC-0. In Public Domain. Gurukul Kangri Collection, Haridwar

Digitized by Arya Samaj Foundation Chennai and eGangotri

2009

# Bulletin of Pure and Applied Sciences

387-RPS-D.D.A.Flat, Mansarover Park, Post Box No.9043, Shahdara, Delhi-110032 (India)
(ajaykumarsharma1955@yahoo.com,ajay_shrm@yahoo.com,editorbulletin@yahoo.co.in
,subscriptionbulletin@yahoo.com)Phone : (011) 22138726

**Ref. No. : Bull/Subs/2009/** **Dated :**

**Dear Sir/Madam,**

We are herewith submitting the annual subscription bills in duplicate for **"January to December" 2009** as under and request you, kindly arrange an early payment by **Bank Demand Draft** drawn in favour of ***BPAS RESEARCHO*** payable at ***DELHI***, send to us alongwith a copy of the bill & oblige.

| S.No. | Name of the Journal & its annual subscription rates | Volume | Quantity | Amount |
|---|---|---|---|---|
| 1. | **Bulletin of Pure and Applied Science Sec.A-Zoology ISSN-0970-0765** *(Rs. 1000 US $ 60 U.K. £ 30)* | **28A** | | |
| 2. | **Bulletin of Pure and Applied Sciences Sec. B – Botany ISSN-0970-4612** *(Rs. 1000 US $ 60 U.K. £ 30)* | **28B** | | |
| 3. | **Bulletin of Pure and Applied Sciences Sec. C – Chemistry ISSN-0970-4620** *(Rs. 1000 US $ 60 U.K. £ 30)* | **28C** | | |
| 4. | **Bulletin of Pure and Applied Sciences Sec. D – Physics ISSN-0970-6569** *(Rs. 1000 US $ 60 U.K. £ 30)* | **28D** | | |
| 5. | **Bulletin of Pure and Applied Sciences Sec. E – Math & Stat. ISSN-0970-6577** *(Rs. 1000 US $ 60 U.K. £ 30)* | **28E** | | |
| 6. | **Bulletin of Pure and Applied Sciences Sec. F – Geology ISSN-0970-4639** *(Rs. 1000 US $ 60 U.K. £ 30)* | **28F** | | |
| 7. | **Bio-Science Research Bulletin (Micro-biology & Bio-tech.)ISSN-0970-0889** *(Rs. 1000 US $ 60 U.K. £ 30)* | **25** | | |
| 8. | **Library Progress (International) (For Library,Information & Computer Sc.) ISSN-0970-1052** *(Rs. 1000. US $ 60 U.K. £ 30)* | **29** | | |
| | **Total** | | | |

Central Library
Gurukul Kangri University
Haridwar-249404

**Authorised Sign.**

CC-0. In Public Domain. Gurukul Kangri Collection, Haridwar

Digitized by Arya Samaj Foundation Chennai and eGangotri

Dr. A.K.Sharma
**Editor-in-chief**
Bulletin of Pure & Applied Sciences(India)
387-RPS- DDA Flat, M.S.Park, Post Box-9043
Shahdara,Delhi-110032, India

**SUBJECT:-** Annual Subscription request for January-December 2009

Dear Sir

With reference to your valuable Research Journals, we invite your kind attention on the following ticked (√ ) Journals,

(A) Please arrange bill in duplicate /triplicate towards the annual subscription for the following ticked (√ ) Research Journals for **January – December 2009 ( complete volume).**

| S.No. | Name of the Journal | Volume | No. of Copies | Annual Subscription |
|---|---|---|---|---|
| 1. | **Bulletin of Pure and Applied Sciences** *Section-A-Zoology ISSN-9070-0765* | 28 A | 1 | Rs.1000 /US$60/UK£30 |
| 2. | **Bulletin of Pure and Applied Sciences** *Section-A-Botany ISSN-9070-4612* | 28 B | 1 | Rs.1000 /US$60/UK£30 |
| 3. | **Bulletin of Pure and Applied Sciences** *Section-C-Chemistry ISSN-9070-4620* | 28 C | 1 | Rs.1000 /US$60/UK£30 |
| 4. | **Bulletin of Pure and Applied Sciences** *Section-D-Physics ISSN-9070-6569* | 28 D | 1 | Rs.1000 /US$60/UK£30 |
| 5. | **Bulletin of Pure and Applied Sciences** *Section-E-Math. & Stat. ISSN-9070-6577* | 28 E | 1 | Rs.1000 /US$60/UK£30 |
| 6. | **Bulletin of Pure and Applied Sciences** *Section-F-Geology ISSN-9070-4639* | 28 F | 1 | Rs.1000 /US$60/UK£30 |
| 7. | **Bio-Science Research Bulletin** *( Microbiology & Bio-technology) ISSN-0970-0889* | 25 | 1 | Rs.1000 /US$60/UK£30 |
| 8. | **Library Progress(International)** *(Library,Information & Computer Applications) ISSN-0970-1052* | 29 | 1 | Rs.1000 /US$60/UK£30 |

(B)We are herewith enclosing a Bank Demand Draft of (name of the Bank).....
No.....dated.....for an amount of Rs.....drawn infavour of **" *BPAS RESEARCHO* "** payable at **"DELHI"** towards the annual subscription of the above ticked (√ ) Journals. Please send the Journals at the following address, when published :

.....
.....
.....
Postal Pin code.....Telephone.....Mobile.....

(Limited back volumes are available at the same rates) **(Seal & Sign. of the Head of Institute)**

CC-0. In Public Domain. Gurukul Kangri Collection, Haridwar

Digitized by Arya Samaj Foundation Chennai and eGangotri

*ISSN-0970-6569*
*Bulletin of Pure and Applied Sciences. Vol.28D(No.2)2009:P-87-103*

# DETECTION OF THE GRAVITATIONAL WAVE WITH THE LIGO AND EINSTEIN'S THEORETICAL ERRORS ON MEASUREMENTS

C. Y. Lo
Applied and Pure Research Institute, 7 Taggart Drive, Unit E, Nashua, NH 03060 USA

**ABSTRACT**

The design of the LIGO was according to the calculations of Thorne's equation which is based on Einstein's theory of measurement. However, there is no valid justification for his theory of measurement. Experimentally the observed bending of light is also against Einstein's theory of measurement, but supports the Euclidean-like structure of a frame for measuring the distance. Nevertheless, analysis shows that the wave-induced phase delay of Thorne, is valid although it is due to the changed light speed but not changing the length of arms. Thorne assumed that gravity would not induce any change of the light speed, in addition to that the LIGO were built on a free falling frame. These differences are distinguishable since the change of light speed is unrelated to the movement of end masses. Thus, an additional benefit of the LIGO is its potential ability to test Einstein's theory of measurements and thus would confirm Einstein's equivalence principle further. Moreover, there are other experiments such as measuring local light speeds would also verify the validity of Einstein's equivalence principle.

**Key words:** Einstein's Principle of Equivalence, Euclidean-like Structure, Einstein-Minkowski Condition, LIGO, Light Speeds, Gravitational Wave Detection, Einstein's Theory of Measurement, Covariance Principle. 04.20.-q, 04.20.Cv

"Science sets itself apart from other paths to truth by recognizing that even its greatest practitioners sometimes err." -- S. Weinberg Physics Today, November 2005.

## 1. INTRODUCTION

Since the behavior of binary pulsars has been interpreted successfully as due to gravitational radiation (Lo 1995, 2000), the physical existence of gravitational waves is generally accepted. Moreover, theoretically the Maxwell Newton Approximation, [1)] which generates gravitational waves, has been established independent of the Einstein equation (Lo 1999). However, a direct observation of the gravitational waves has not been successful because a gravitational wave would be very weak in nature (Weinberg 1972).

To obtain the required sensitivity of detection, two gigantic laser interferometer gravitational wave observatories (LIGO) have been built, and currently they represent the hope of detecting the gravitational waves directly. These ap-

CC-0. In Public Domain. Gurukul Kangri Collection, Haridwar

Digitized by Arya Samaj Foundation Chennai and eGangotri


paratus, with high sensitivity, is designed according to Thorne's equation, (see eq. [16]) which is based on Einstein's theory of measurement (Einstein *et al.* 1923).

Thorne's equation shows that the wave-induced displacement of a test mass from a fixed object is proportional to the distance between the test mass and the object. Another major assumption of Thorne's theory is that the earth is a system at free fall. However, Thorne's criticism of Einstein's equivalence principle (see section 4) shows that he did not understand this principle. Moreover, it is known (Lo 2005a) that Einstein's equivalence principle is in conflict with his covariance principle which is necessary for Einstein's theory of measurement.

On the other hand, in the calculation of the bending of light, the Euclidean-like structure (Lo 2002, 2003b) is not changed by gravity.[2] According to the geodesic equation, gravitational waves would induce a displacement of a particle, but this has nothing to do with the distance between the particle and a fixed object. As will be shown, Einstein's theory on measurement, which is independent of the theoretical framework of general relativity, is actually not consistent with Einstein's equivalence principle (see Sections 2 & 3). Would this mean that the sensitivity of the interferometer is independent of the length of the arms?

In this paper, first it will make clear that Einstein's theory of measurement is an additional assumption that actually has no physical justification. Then, it will be shown that, according to Einstein equivalence principle, the phase delays are due to changes of the light speeds, although they are the same as those produced by Thorne's theory for the LIGO. This is another case that a wrong theory had produced the right amount of prediction (Lo 2004). Nevertheless, it is still possible to test which theory is valid experimentally with the LIGO since the light speed is independent of whether the test mass is movable or not.

## 2. EINSTEIN'S THEORETICAL ERRORS AND MEASUREMENTS

Einstein's theory on measurement adapts the distance in Riemannian geometry, which is defined in terms of the metric. However, Einstein's theory of measurement is actually not based on his equivalence principle (Lo 2005b). Whitehead (1962, p. 83), criticized this as invalid in physics, and pointed out,

> "By identifying the potential mass impetus of a kinematic element with a spatio-temporal measurement Einstein, in my opinion, leaves the whole antecedent theory of measurement in confusion, when it is confronted with the actual conditions of our perceptual knowledge. The potential impetus shares in the contingency of appearances. It therefore follows that measurement on his theory lacks systematic uniformity and requires a knowledge of the actual contingent physical field before it is possible."

Since Einstein's notion of distance depends on the metric, which in turn depends on the motion of matter, using such a theory to describe motion can only lead to confusion. The basic error is confusing the notions of distance and invariance.


CC-0. In Public Domain. Gurukul Kangri Collection, Haridwar

Digitized by Arya Samaj Foundation Chennai and eGangotri

# DETECTION OF THE GRAVITATIONAL WAVE WITH THE LIGO AND EINSTEIN'S THEORETICAL ERRORS ON MEASUREMENTS

In the initial development of Riemannian geometry, the metric was identified formally with the notion of distance in analogy as the case of the Euclidean space (Misner *et al.* 1973). Such geometry is often illustrated with the surface of a sphere, a subspace embedded in a flat space (Dirac 1975). Then, the distance is determined by the flat space and can be measured with a static method, i.e., attachment. For a general case, however, the issue of measurement was not addressed, before Einstein's theory of measurement.

In general relativity, the invariant line element in a space $S(x, y, z, t)$ is

$$ds^2 = g_{\mu\nu} dx^\mu dx^\nu , \qquad (1)$$

where $g_{\mu\nu}$ is a space-time metric in a Riemannian space (Weinberg 1972). However, to relate (1) to a distance in $S$ requires identifying the means of physical measurement for a distance. Since $g_{\mu\nu}$ is not a constant metric, one cannot hope to derive from (1) a simple distance formula as in Euclidean geometry where the spatial distance $d(P_1, P_2)$ of points $P_1$ and $P_2$ is still

$$d(P_1, P_2) = [(x_1 - x_2)^2 + (y_1 - y_2)^2 + (z_1 - z_2)^2]^{1/2}. \qquad (2)$$

However, it is found (Lo 2002, 2003b) that the Euclidean-like structure [2] with distance formula (2) must exist independent of the metric (1). For example, consider the Schwarzschild solution (Weinberg 1972) of Riemannian space $(x, y, z, t)$,

$$ds^2 = (1 - 2M\kappa/\rho)\, c^2dt^2 - (1 - 2M\kappa/\rho)^{-1}d\rho^2 - \rho^2 d\theta^2 - \rho^2 \sin^2\theta d\varphi^2, \qquad (3)$$

where

$$x = \rho \sin\theta \cos\varphi, \quad y = \rho \sin\theta \sin\varphi, \quad \text{and} \quad z = \rho \cos\theta. \qquad (4)$$

Here $\kappa$ is a coupling constant, and $M$ is the total mass. Equation (4) clarifies that the frame has a spherical coordinate system, and therefore has a Euclidean-like structure that satisfies the Pythagorean Theorem. Also, the light speed is defined (Einstein *et al.* 1923) in terms of $dx/dt$, $dy/dt$, and $dz/dt$ (see also Section 3).

Einstein (Einstein *et al.* 1923) called the Euclidean-like structure as "in the sense of Euclidean geometry". However, he did not understand that the Euclidean-like structure is independent of the metric, and, in fact, they are complementary to each other in physics. Nevertheless, such a structure is only a necessary but not a sufficient condition (Lo 2004). For example, both the space with the Schwarzschild metric (3) and the space with the isotropic metric (Weinberg 1972) have the same frame with a Euclidean-like structure. However, the Schwarzschild solution does not satisfy Einstein's equivalence principle because it is incompatible with the Maxwell-Newton Approximation (Lo 1995).

To understand the Euclidean-like structure, it would be useful to clarify what "measure" means to Einstein. In his theory, the measuring instruments are resting but in a free fall state. From Einstein's equivalence principle, [3] time dila-


CC-0. In Public Domain. Gurukul Kangri Collection, Haridwar

Digitized by Arya Samaj Foundation Chennai and eGangotri


tion and space contractions are obtained. Then, he (Einstein *et al.* 1923) claimed, "In the general theory of relativity, space and time cannot be defined in such a way that differences of the spatial coordinates can be directly measured by the unit measuring-rod, or differences in the time coordinates by a standard clock". However, for an extended object, such an operation of measurement may not be executable. Thus, such a notion of measurement is not well defined.

Nevertheless, if the measuring instruments are attached to the frame of reference, since the measuring instruments and the coordinates being measured are under the same influence of gravity, a Euclidean-like structure emerges as if gravity did not exist. This operational defined Euclidean-like structure is necessarily a complimentary to the metric of a physical space (Lo 2002, 2003b). In other words, *the physical meaning of space-time coordinates has already been provided in the theoretical framework of general relativity.* Thus, the criticisms of Whitehead (1962) and Fock (1964) are actually not valid for general relativity.

To clarify this, let us consider the theory of Landau and Lifshitz (1975). Accordingly, the local distance *dl* is determined by

$$dl^2 = -\left[ g_{\alpha\beta} - \frac{g_{0\alpha} g_{0\beta}}{g_{00}} \right] dx^\alpha dx^\beta, \quad \alpha, \beta = 1,2,3, \tag{5}$$

for

$$ds^2 = g_{00}(dx^0)^2 + 2g_{0\alpha} dx^0 dx^\alpha + g_{\alpha\beta} dx^\alpha dx^\beta$$

if the metric satisfies Pauli's version of the equivalence principle, that is, the metric has a proper signature. Thus (Lo 2003a),

$$ds^2 = g_{00}(dx')^2 + g'_{\alpha\beta} dx^\alpha dx^\beta = g_{00}\left[ dx^0 + \frac{g_{0\alpha} dx^\alpha}{g_{00}} \right] + \left[ g_{\alpha\beta} - \frac{g_{0\alpha} g_{0\beta}}{g_{00}} \right] dx^\alpha dx^\beta \tag{6a}$$

where

$$dx'^0 = dx^0 + \frac{g_{0\alpha} dx^\alpha}{g_{00}}, \quad g'_{\alpha\beta} = g_{\alpha\beta} - \frac{g_{0\alpha} g_{0\beta}}{g_{00}} \tag{6b}$$

are the new local time coordinate and metric elements.

Formula (5) for space contraction *dl* is valid (Lo 2003a) if Einstein's equivalence principle is satisfied. The local distance formula (5) makes no difference if $g_{\alpha 0} = 0$. However, this formula is crucial otherwise. For example, the metric for Einstein's rotating disk in the coordinate system $K^*(x', y', z', t)$ is,

$$ds^2 = (c^2 - \Omega^2 r^2)\, dt^2 - 2\Omega r^2\, d\phi' dt - dr^2 - r^2\, d\phi'^2 - dz'^2, \tag{7a}$$

where

$$z = z', \quad x' = r\cos\phi', \text{and} \quad y' = r\sin\phi'. \tag{7b}$$


CC-0. In Public Domain. Gurukul Kangri Collection, Haridwar

Digitized by Arya Samaj Foundation Chennai and eGangotri



Here $K(x, y, z, t)$ is a Galilean (inertial) system of reference and the system $K'(x', y', z')$ in a uniform rotation $\Omega$ relatively to $K$. We have $\phi = \phi' + \Omega t$, and (7b) manifests the Euclidean-like structure. Then, one would have the space contraction

$$(1 - \Omega^2 r^2/c^2)^{-1/2}\, r d\phi', \tag{8}$$

in the $\phi'$-direction, according to (6) (see also [10a]).

However, the "standard" arguments of Ohanian and Ruffini (1994) is as follows:

> "... and the spacetime interval becomes $ds^2 = g_{\mu\nu} dx^\mu dx^\nu$. This expression determines the spacestime distances. For example, a coordinate displacement $dx^1$ along the x-axis has a length $\sqrt{(-g_{11})}\, dx^1$, that is, the measured distance differs from $dx^1$ by a factor $\sqrt{(-g_{11})}$. Likewise, a coordinate time ($t$ time) displacement $dx^0$ has a duration $\sqrt{g_{00}}\, dx^0$ when measured by the proper time of a clock at rest."

Thus, one would have concluded that there is no space contraction from metric (7). Moreover, some theorists would not accept the formula of Landau and Lifshitz (1975) because $dx'^0$ in (6b) may not be integrable. Although they mentioned this characteristic, many considered their derivation problematic. Now, one must address the issue whether the validity of (5) depends on (6b) is integrable.

On the other hand, the arguments of Landau & Lifshitz are not faultless because the local frame is not always physically realizable [4] (Lo 2003a). Moreover, Einstein (1954) only assumed validity of his equivalence principle and the *Einstein-Minkowski condition* [5] that the local space of a particle under gravity must be locally Minkowskian. However, for the case of a uniformly rotating disk, one may show explicitly from special relativity that the validity of formula (5) is independent of whether (6b) is integrable and $dx'^0$ would be just a local time.

Consider a particle $P$ resting at $(r', \phi', z')$ of $K^*(r', \phi', z', t)$, the space of the rotating disk. The local space L* of $P$ is $(dr', dX, dz', dT)$ which has a Minkowski metric. In $K$, $P$ has a position $(r, \phi, z)$ and its local space $(dr, rd\phi, dz, dt)$ has the Minkowski metric in $K$. These two local spaces have a relative velocity $r\Omega$ in the $\phi$-direction in $K$. Since $r' = r$, and $z' = z$, we have $dr' = dr$, and $dz' = dz$.

Then, the two local spaces are related by the transformation as follows:

$$dX = (1 - (r\Omega/c)^2)^{-1/2} (rd\phi - r\Omega dt), \tag{9a}$$

and

$$dT = (1 - (r\Omega/c)^2)^{-1/2} (dt - (r\Omega/c^2)\, rd\phi). \tag{9b}$$

From $\phi = \phi' + \Omega t$, one obtains

$$dX = (1 - (r\Omega/c)^2)^{-1/2}\, rd\phi', \tag{10a}$$


CC-0. Panini Kanya Maha Vidyalaya Collection. Gurukul Kangri Collection, Haridwar

Digitized by Arya Samaj Foundation Chennai and eGangotri


and

$$dT = (1 - (r\Omega/c)^2)^{1/2} \{dt - (1 - (r\Omega/c)^2)^{-1} (r\Omega/c^2)\, r d\phi'\} \qquad (10b)$$

Clearly, the validity of formula (5) is independent of whether (6b) is integrable. Eq. (6b) is not integrable because $dt'$ is related to different inertial systems at different r and t (Lo 2005b). Thus, such an objection to the formula of Landau & Lifshitz (1975) would show an inadequate understanding of special relativity.

However, eq. (10a) shows that, *the local distance in the $\phi'$-direction is measured from a local space at a free fall.* If the circumference of a circle in $K'$ is measured, each must be in a different free fall state at each point. Thus, the local distance of Landau & Lifshitz is not a distance in $K'$ as they claimed (Lo 2005b). Thus, formula (5) can be consistent with the Euclidean-like structure (7b).

Since the space contraction is measured in a free fall local space, this is a dynamic measurement. The measuring instrument is in a free fall state under the influence of gravity, while the Euclidean-like structure determines the static distance between two points in a frame of reference. There is no physical reason to considered $dl$ as the local distance. One should not confuse eq. (10a) with

$$dX = [1 - (r\Omega/c)^2]^{-1/2} [r d\phi], \qquad (11a)$$

which is the initial result of Einstein (Einstein 1954, Einstein *et al.* 1923). However, since $rd\phi$ and $rd\phi'$ are different, (11a) has nothing to do with space contraction in the rotating disk K*. Thus Einstein justification for measurement actually is invalid. Einstein calimed also that the circumference of a circle in K* with radius $r$ is

$$\oint ds = (1 - \Omega^2 r^2/c^2)^{-1/2} r \int_0^{2\pi} d\phi = 2\pi r(1 - \Omega^2 r^2/c^2)^{-1/2} > 2\pi r, \qquad (11b)$$

in disagreement with (7b). (11b) is invalid since dX is in L*. *Einstein's error is that he has mistaken (10a) the dynamic measurement as a static measurement* (Lo 2005b).

Einstein incorrectly believed that a space-time metric could be regarded as defining a locally measured distance as in the case of an embedded subspace (Dirac 1975). The problem is that the mathematically defined local distance cannot be physically measured in the same way as the case in a Gaussian space.

## 3. THEORIES OF MEASUREMENT AND THE LIGHT BENDING

In addition to theoretically invalidity, it will be shown that there are experimental evidences against Einstein's theory on measurement. Here we would consider Einstein's derivation the observed bending of light rays (Einstein 1954) based on the Maxwell-Newton Approximation, [1)] which has been firmly established with Einstein's equivalence principle (Lo 1999).

Currently, the meaning of Einstein's equivalence principle was commonly


CC-0. In Public Domain. Gurukul Kangri Collection, Haridwar

Digitized by Arya Samaj Foundation Chennai and eGangotri



mistaken (Lo 2002, Ray 2005, Schiff 1960) to be the same as the 1911 preliminary application of equivalence with Newtonian gravity. This is fundamentally incorrect since the gravitation potential is a scalar in Newtonian theory, but is a second rank tensor in general relativity.

Based on the Maxwell-Newton Approximation, the metric generated from the static massive energy-stress tensor $T(m)_{\mu\nu}$,

$$T(m)_{tt} = \sigma \quad \text{and} \quad T(m)_{\mu\nu} = 0 \quad \text{otherwise,} \tag{11a}$$

where $\sigma$ is the mass density, Einstein obtained the static spacetime metric,

$$ds^2 = c^2 (1 - \frac{K}{4\pi}\int dV_0 \frac{\sigma}{R})dt^2 - (1 + \frac{K}{4\pi}\int dV_0 \frac{\sigma}{R})(dx^2 + dy^2 + dz^2), \tag{11b}$$

If Einstein's equivalence principle is valid (and so is the Einstein-Minkowski condition), for an observer $P$ at point $(x, y, z, t)$ with an arbitrary velocity $v$, under only the influence of gravity, there is a co-moving local Minkowski coordinate system $(X, Y, Z, T)$,

$$ds^2 = c^2dT^2 - dX^2 - dY^2 - dZ^2. \tag{12}$$

For a spherical mass distribution $\sigma$, consider a resting observer P one has [4)]

$$c^2dT^2 = c^2 (1 - \frac{K}{4\pi r}\int dV_0\sigma)dt^2, \quad \text{where} \quad r = (x^2 + y^2 + z^2)^{1/2}; \tag{13a}$$

and

$$(dX^2 + dY^2 + dZ^2) = (1 + \frac{K}{4\pi r}\int dV_0\sigma)(dx^2 + dy^2 + dz^2). \tag{13b}$$

It follows from eq. (13a), the red shift for a frequency, which would have been $\nu_0$ in a Minkowski space

$$\nu = \nu_0 (g_{tt})^{1/2} = \nu_0 (1 - \frac{K}{4\pi r}\int dV_0\sigma) \tag{14a}$$

and

$$L = \frac{d\lambda}{dt} = c(1 - \frac{K}{4\pi r}\int dV_0\sigma), \quad \text{where} \quad d\lambda^2 = (dx^2 + dy^2 + dz^2), \tag{14b}$$

is the local light speed. Thus, Einstein's equivalence Principle is essential.

If we imagine the sun, of mass $M$, concentrated at the origin of our system of coordinates, then a ray of light, traveling parallel to the $x_3$-axis, in the $x_1$-$x_3$ plane, at a distance $\Delta$ from the origin, is deflected, in all by an amount

$$\alpha = \int_{-\infty}^{+\infty} \frac{1}{L}\frac{\partial L}{\partial x_1} dx_3 = \frac{KM}{2\pi\Delta} \tag{14c}$$

where $M = \int \sigma dV_0$ (Einstein *et al.* 1923, Einstein 1954]. Note also that $\Delta$ is measured,


CC-0. In Public Domain. Gurukul Kangri Collection, Haridwar

Digitized by Arya Samaj Foundation Chennai and eGangotri



as "in the sense of Euclidean geometry (Einstein *et al.* 1923)." *Here, the defection is against a straight line in the Euclidean-like structure of a curved space.*

In fact, *all Einstein's predictions are in terms of the Euclidean-like structure.* The secular rotation of the elliptic orbit of the planet in the same sense as the revolution of the planet, amounting in radius per revolution to $24\pi^3a^2/(1 - e^2)c^2T^2$. In addition to $\Delta$, $e$ the numerical eccentricity and $a$ the semi-major axis of the planetary orbit in centimeters are defined in terms of the Euclidean-like structure, and $T$ the period of revolution in seconds is defined in terms of the time of a "quasi-Minkowskian space" (Weinberg 1972). Einstein stated that the light speed is measured "in the sense of Euclidean geometry (Einstein *et al.* 1923)." This confirms that the distance in a physical space is decided by the Euclidean-like structure, but not by the "local distance" of the metric.

If the effective arm length of the interferometer in the LIGO were decided by the metric, the light speeds would be different. Then, according to the local distance of a metric, Liu (1987) had defined a coordinate light speed as follows:

$$\frac{dl}{dt} = \varpi_{cor}(n^i) = \frac{c\sqrt{g_{00}}}{\gamma_i n^i + 1} \qquad \text{where} \qquad \gamma_i = -\frac{g_{0i}}{\sqrt{g_{00}}}, \qquad (15)$$

and $n^i$ is the directional vector. For an orthogonal metric, one has simply $\omega_{cor} = c(g_{00})^{1/2}$, which is the invalid 1911 formula of Einstein for the light bending. Thus, it is clear that the observed light bending supports that the distance is decided by the Euclidean-like structure instead of the metric (Lo 2006).

A problem related to the speeds of light is the notion of expanding universe. In such a notion, the expansion comes from the change of the metric of the universe, but the Euclidean-like structure is assumed to have no change. Then, the observed redshifts are attributed to the receding velocity of galaxies defined in terms of the local distance *dl* similar to (15) (Weinberg 1972; Ohanian & Ruffini 1994; Liu 1987). However, if the speeds of light must be defined in terms of the Euclidean-like structure, what is the justification to define the receding velocity differently? Moreover, if the local distance can be measured only from a local space at free fall, does it make sense to define the receding velocity based on such a local distance? The explanation of such redshifts in terms of the Robertson-Walker metric need not depend on this dubious receding velocity (Lo 2006). Thus, validity of such a theory of measurement is an important issue that should be further examined by experiments. For this, the LIGO would play a role.

## 4. THORNE'S SENSITIVITY OF THE LASER INTERFEROMETER

In current theory, to achieve maximum sensitivity of the LIGO, it is desirable to adjust the interferometer in such a way that in the absence of a gravitational wave, the light beams emerging from the two arms are out of phrase, $\phi = \pi$, and they interfere destructively. When a gravitational wave, then changes the


CC-0. In Public Domain. Gurukul Kangri Collection, Haridwar

Digitized by Arya Samaj Foundation Chennai and eGangotri



length of one arm relative to the other by an amount x, the phrase between emerging light beams changes by an additional amount $\Delta\phi = 4\pi nx/\lambda$, where n is the number of back-and-forth reflections along such arm and $\lambda$ is the wave length of the light. This $\Delta\phi$ was obtained with Einstein's theory of measurements.

In the past, all these interferometers have arm lengths of a few meters or a few tens of meters, and claimed to attain sensitivities of order $\kappa A \cong 10^{-19}$ (the minimum gravitational-wave amplitude, where $\kappa = (16\pi G/c^4)^{1/2} = 2.04 \times 10^{-24} s/(g\ cm)^{1/2}$) for gravitational waves of a frequency of about *1 kHz*. However, none of these meters has succeeded in detecting any gravitational waves.

To obtain the required sensitivity of detection for gravitational waves, two gigantic laser interferometer gravitational wave observatories (LIGO) have been built. The confidence on these new apparatus is based on the perceived high sensitivity, owing to Einstein's theory of measurement (Einstein *et al.* 1923). The related Thorne's equation of motion (Misner *et al.* 1973; eq. [35.14]) is as follows:

$$m\frac{d^2\delta x^j}{dt^2} = \frac{1}{2}m\frac{\partial^2 h_{jk}^{TT}}{\partial t^2}x^k \qquad (16)$$

where $\delta x^k$ is the displacement of the test particle with mass m from a fixed object, $x^k$ is the Euclidean-like distance of the test particle from the fixed object, and $h_{jk}^{TT}$ is the first order of the dimensionless 'gravitational wave field' that induces the displacement. Then the integration of eq. (16) gives,

$$\delta x^j = \frac{1}{2}h_{jk}^{TT}x^k \qquad (17)$$

The superscript $^{TT}$ is to remind us that the field is 'transverse and traceless'. Then, the induced phase delay in the interferometer could be calculated (Thorne 1987).

Since the sources of the gravitational waves [6] are very far away, the waves look very nearly planar as they pass through the observer's proper reference frame. If we orient the *x, y, z* spatial axes, so the propagation in the z direction, then the transversality of the waves and traceless mean that the non-zero components of the wave field are: $h_{xx}^{TT} = -h_{yy}^{TT}$, $h_{yx}^{TT} = h_{xy}^{TT}$.

Thus, there are two polarizations, called respectively the '+' and '×' polarization. For a '+' polarization, we have

$$\delta x(t) = \frac{1}{2}Lh_+(t) \qquad \text{for mass on } x \text{ axis,} \qquad (18)$$

$$\delta y(t) = -\frac{1}{2}Lh_+(t) \qquad \text{for mass on } y \text{ axis.}$$


CC-0. In Public Domain. Gurukul Kangri Collection, Haridwar

Digitized by Arya Samaj Foundation Chennai and eGangotri


where the arm length of the interferometer is $L$. Then, for a light ray with wavelength $\lambda$, the total phase delay is

$$\Delta\phi_T = 8\pi B\frac{\delta x}{\lambda} = 4\pi B\frac{L}{\lambda}h_+ \ , \tag{19}$$

where $B$ is the number of bounce back and forth in the arms. Thus, the LIGO could have sensitivity of the order of $\kappa A \cong 10^{-22}$ since the arm lengths are long. In Einstein's theory of measurement, $\delta x(t) = (1/2)Lh_+(t)$ could be interpreted simply as due to the difference of length (between the test particle and the fixed object) induced by the gravitational wave.

Moreover, it has been assumed (Misner *et al.* 1973; eq. [13.73]) that the frame of reference is at free fall, although the LIGO is built on earth. The radius of earth is $6.3 \times 10^3$ km, but the expected gravitational wave length is only about 15 km. Thus, the earth cannot be regarded as a test particle.

Please note that Misner *et al.* (1973) have mistaken Pauli's (1958) version [3] as Einstein's equivalence principle. In Pauli's version, the "covariance principle" must be used. It thus follows that coordinates have to be arbitrary. Also, the 1911 preliminary application of equivalence between acceleration and Newtonian gravity was mistaken as Einstein's equivalence principle (Schiff 1960).

Moreover, Thorne (Thorne 1994) incorrectly [7] criticized Einstein's equivalence principle (Lo 2003a) as follows:

> *"In deducing his principle of equivalence, Einstein ignored tidal gravitation forces; he pretended they do not exist. Einstein justified ignoring tidal forces by imagining that you (and your reference frame) are very small."*

However, Einstein has already explained these problems in his letter of 12 July 1953 to Rehtz (Norton 1989) as follows:

> *"The equivalence principle does not assert that every gravitational field (e.g., the one associated with the Earth) can be produced by acceleration of the coordinate system. It only asserts that the qualities of physical space, as they present themselves from an accelerated coordinate system, represent a special case of the gravitational field."*

Here Einstein has made clear that this principle applies to a physical space where physical requirements are sufficiently satisfied.

## 5. ENSTEIN'S EQUIVALENCE PRINCIPLE AND SENSITIVITY OF THE LASER INTERFROMETER

A space contraction is a dynamic measurement since the measuring instrument is in a free fall state. Independently, the Euclidean-like structure determines the static distance between two points in a frame of reference, and this distance is used in the bending of light. In Einstein's theory of measurement, he has mistaken this dynamic local measurement as a static measurement.


CC-0. In Public Domain. Gurukul Kangri Collection, Haridwar

Digitized by Arya Samaj Foundation Chennai and eGangotri



However, while there is no change in the Euclidean-like structure, the velocity of light would change (Lo 2002, 2003b). Moreover, because of time dilation, the frequency f of the light could change too. Thus, we have

$$f_w = f_0\sqrt{g'_{tt}} \text{ and } \qquad C_w = c\sqrt{\frac{g'_{tt}}{-g'_{xx}}} = f_w\lambda_w. \tag{20}$$

where $f_0$ is the light frequency when gravity is absence, $f_w$ is the light frequency, $C_w$ is the light speed in the $x$-direction and $\lambda_w$ is the light wavelength when gravitational wave is present. When the gravitational wave is not present, we have

$$f = f_0\sqrt{g_{tt}} \qquad \text{and} \qquad C_g = c\sqrt{\frac{g_{tt}}{-g_{xx}}} = f\lambda. \tag{21}$$

where $f$ is the frequency, $C_g$ is the light speed, and $\lambda$ is the wavelength.

Then the phase changes and the phase delay within the arm length $L$ as

$$\Delta\phi = \phi_w - \phi = 2\pi L\left(\frac{1}{\lambda_w} - \frac{1}{\lambda}\right) = 2\pi\frac{L}{\lambda}\left(\frac{f_w C_g}{fC_w} - 1\right) = 2\pi\frac{L}{\lambda}\left(\sqrt{\frac{g'_{xx}}{g_{xx}}} - 1\right). \tag{22}$$

To the first order approximation, [6] we have

$$g'_{xx} \cong g_{xx} + h_{xx}, \quad \text{and thus} \quad \sqrt{\frac{g'_{xx}}{g_{xx}}} \approx 1 + \frac{1}{2}h_{xx} \tag{23}$$

Thus,

$$\Delta\phi = \phi_w - \phi = \pi\frac{L}{\lambda}h_{xx}. \tag{24}$$

It thus follows that the total phase delay is again the same as in (19). However, in (24) the phase shift $\Delta\phi$ is due to a change of the light speed.

On the other hand, in (19) phase delay is due to the displacements in (18), which are due to that the end mass oscillates longitudinally (Thorne 1987; p. 417). It was assumed that the light speed does not change. This is another case that a wrong theory could produce correct results (Lo 2004). The change of light speed and the assumed change of length happen to have exactly the same effect for the phase delay. A crucial difference is that we have shown that the phase delay is independent of whether the end mass is movable or not. Thus, to test the theories, one could simply try also the case of fixed end masses. [8]

## 6. DISCUSSIONS AND CONCLUSIONS

The theory of Thorne has three major problems. First, his equation of motion is based on Einstein's theory of measurement that has been proven as not


CC-0. In Public Domain. Gurukul Kangri Collection, Haridwar

Digitized by Arya Samaj Foundation Chennai and eGangotri


self-consistent (Lo 2005b) and in disagreement with the assumption used in calculating the observed bending of light (Lo 2003a, 2006). The second problem is that Thorne was not aware that the Einstein equation of 1915 has no wave solution (Gullstrand 1921, 1922; Lo 2006a).[6] Although Misner *et al.* (1973) claimed that plane wave solutions exist, their derivation is invalid (Lo 2000, 1997b). The third problem is his implicit assumption that the light speed does not change, but instead a gravitational wave would induce change in the length of the arms.

The second problem has been solved by a modified Einstein equation, and it has the Maxwell-Newton Approximation as the first order equation (Lo 1995). However, *the belief that as a gravitational wave passes by, objects (or space) would change their length is incorrect because gravity does not change the Euclidean-like structure.* This means that although the mirror will be moved by a gravitational wave, such a movement is independent of the arm length.

The radius of earth is $6.3 \times 10^3$ *km*, but the expected gravitational wave length is only about *15 km* (Misner *et al.*, 1973). *Thus, the earth can not be considered as a test particle as when only the gravity of the Sun is considered.* Therefore, Thorne's theory is inapplicable to the LIGO (Lo 2006a).

Nevertheless, it is interesting that the phrase delay obtained by Thorne (1987) is actually a result of light speed change. This is another example that a wrong theory[10] could produce correct results (Lo 2004). The change of light speed and the assumed change of length happen to have exactly the same effect for the phase delay. To show that Thorne's theory is incorrect experimentally, we can simply fix the end mass. However, since the observation of gravitational waves is a passive experiment, such a method of testing general relativity is not very practical unless an additional fixed end-mirror is put into the interferometer.

Although Einstein's theory on measurements is independent of the theoretical framework of general relativity (Lo 2003b), his theory on measurement is crucial to the current notion of an expanding universe (Lo 2006). Moreover, if such a minor modification were difficult, there are other experiments, such as the experiment on local light speeds (Lo 2003b, Zhou 1987), would further confirm that Einstein's equivalence principle is correct and the "covariance principle" invalid (Lo 2005a). It should be noted that the distance in a physical Riemannian space is determined by the Euclidean-like structure, whereas the metric determines only the space contractions (Lo 2003a, 2005b, 2006a, 2007c).[11]

Our purpose is to inform those who operate the LIGO that the so obtained phase delay is still valid. In addition, a modification with additional fixed end-mirrors would enable the LIGO to test Thorne's theory and thus Einstein's theory of measurement. More important, the LIGO would confirm Einstein's equivalence principle further, and would end the misinterpretation of Pauli.

Weinberg (2005) pointed out, "Our work in science is cumulative. We really do know more than our predecessors, and we can learn about the things that


CC-0. In Public Domain. Gurukul Kangri Collection, Haridwar

Digitized by Arya Samaj Foundation Chennai and eGangotri


were not understood in their times by looking at the mistakes they made." He also remarked, "Perhaps most important, by showing that we are aware of mistakes made by even the greatest scientists, we set a good example to those who follow other supposed paths to truth. We recognize that our most important scientific forerunners were not prophets whose writings must be studied as infallible guides—they were simply great men and women who prepared the ground for the better understandings we have now achieved." [12] For instance, Einstein's invalid justification for his theory of measurement has misled us to believe it as a natural extension of special relativity. However, it has been found that Einstein's covariance principle, which is an interim assumption to deal with the problems in Einstein's theory of measurement, is actually invalid (Lo 2005a, 2008).

Fundamental concepts are difficult to grasp. It is interesting to note that the originator of a physical theory often does not understand his theory in full. However, this need not necessarily mean that subsequent theorists would understand it better. For instance, Einstein (1982b) understands $E = mc^2$ correctly, but many subsequent theorists such as Will (1981) misinterpreted it as unconditionally valid. Consequently, the existence of the fifth force (the charge-mass interaction), which leads to the necessary unification of gravity and electromagnetism, was over looked (Lo & Wong 2006; Lo 2007a, 2007b). This is probably the main reason that attempts for such unify have not been successful.

## ACKNOWLEDGMENTS

The author gratefully acknowledges stimulating discussions with S. L Cao, Richard C. Y. Hui, David P. Chan, S. J. Chang, A. J. Coleman, Liu Liao, and Eric J. Weinberg. Special thanks are to D. Rabounski for useful suggestions. This work is supported in part by Innotec Design, Inc., U.S.A. and the Szecheon Co. Hong Kong.

## ENDNOTES

1) The Maxwell-Newton Approximation with sources of massive matter could be identified as a special case of the "linearized approximation" that has been found to be incompatible with Einstein equation for a dynamic situation.

2) Einstein's equivalence principle implies the existence of a Euclidean (Minkowskian) metric only locally (at a given point or along a geodesic). Independently, it has been found that in a physical space the frame of reference necessarily has a Euclidean-like structure (Lo 2002, 2003b).

3) Pauli's (1958) version of the principle of equivalence was commonly but mistakenly regarded as Einstein's equivalence principle, although Einstein


CC-0. In Public Domain. Gurukul Kangri Collection, Haridwar

Digitized by Arya Samaj Foundation Chennai and eGangotri


strongly objected to this version as a misinterpretation (Norton 1989). Moreover, Wald (1984) simply ignored Einstein's equivalence principle (Lo 2007c).

4) A frame of reference is physical realizable if its coordinates are part of the coordinate system of a physical space, or equivalently physical measurements can be performed in such a frame.

5) For the Einstein-Minkowski condition, Einstein (1954; Einstein et al. 1923) addressed only the diagonal metrics or metrics without a crossing space-time element. This creates a false impression that the Einstein-Minkowski condition is trivial. For instance, Synge (1971), an excellent mathematician, failed to investigate the physics of Einstein's equivalence principle.

6) Einstein equation has no wave solution since there is no term to accommodate the energy-stress tensor of a gravitational wave that must move with the wave (Lo 1997b). For this reason, Einstein equation must be modified. It has been proven that an additional term for the energy-stress of waves in Einstein equation would explain the observed behavior of binary pulsars (Lo 1995). However, the 1993 Nobel Committee failed to see that the Hulse & Taylor experiments actually support a modified Einstein equation (Lo 2000, 2009c).

7) Thorne is not alone in misunderstanding Einstein's principle (Lo 2007c).

8) This test can be performed with an additional fixed end-mirror.

9) The first order comes from the modified Einstein equation of 1995 (Lo 1995).

10) Wrong theories would also misinterpret experimental results. For instance, the formula $E = mc^2$ was misinterpreted, different from Einstein (1982b), as unconditional equivalence between mass and any type of energy (Lo & Wong 2006; Lo 1997a). Also, Will (1981) misinterpreted the Kreuzer Experiment (Lo 1997a), and the Eötvös Experiment (Lo 2007c).

11) However, as shown by the diffeomorphisms (Weinberg 1972), the meaning of coordinates would depend on the gauge. Nevertheless, the second order for the bending of light can be obtained from the impact parameter b, which is gauge independent mathematically. Physically, however, there is no method of measurement for b such that it is gauge independent. Thus, the so-called gauge invariant measurable quantity is only an illusion (Lo 2009a).

12) The charge-mass interaction has been discovered, and thus unification between gravitation and electromagnetism is proven to be necessary (Lo 2007a, 2007b). Moreover, current as well as unexplained old experiments (Buehler 2004; Liu 2007; Lo 2009b; Musha 1997; Musha & Kanamoto 1994; Tajmar *et al.* 2007) have confirmed the existence of this interaction.

## REFERENCES

1. Buehler, D. R. 2004. *J. of Space Mixing*, 2: 1-22. living@doylebuehler.com


CC-0. In Public Domain. Gurukul Kangri Collection, Haridwar

Digitized by Arya Samaj Foundation Chennai and eGangotri


2. Dirac, P. A. M. 1975. ***General Theory of Relativity*** (John Wiley, New York).

3. Einstein, A. 1954. ***The Meaning of Relativity*** (1921) (Princeton Univ. Press).

4. Einstein, A. 1982a. 'The Problem of Space, Ether, and the Field in Physics' (1934) in ***Ideas and Opinions*** (Dover).

5. Einstein, A. 1982b. 'E = $mc^2$' (1946) in ***Ideas and Opinions*** (Dover, New York).

6. Einstein, A., Lorentz, H. A., Minkowski, H., Weyl, H. 1923. ***The Principle of Relativity*** (Dover, New York).

7. Fock, V. A. 1964. ***The Theory of Space Time and Gravitation***, translated by N. Kemmer (Pergamon Press).

8. Gullstrand, A. 1921. *Ark. Mat. Astr. Fys.* 16, No. 8 (1921); ibid, 1922. 17, No. 3.

9. Landau, L. D., and Lifshitz, E. M. 1975. ***The Classical Theory of Fields*** (Pergamon Press, New York).

10. Liu, Liao 1987. ***General Relativity*** (High Edu. Press, Shanghai, China), p. 42.

11. Liu, W. Q. 2007. http://www.cqfyl.com.

12. Lo, C. Y. 1995. *Astrophys. J.* 455: 421; Editor Chandrasekhar suggests and approves the Appendix: The Gravitational Energy-Stress Tensor for the necessity of modifying Einstein equation.

13. Lo, C. Y. 1997a. *Astrophys. J.* 477: 700-704.

14. Lo, C. Y. 1997b. *Phys. Essays*, **10** (3) : 424.

15. Lo, C. Y. 1999. *Phys. Essays*, **12** (3), 508.

16. Lo, C. Y. 2000. *Phys. Essays*, **13** (4) : 527.

17. Lo, C. Y. 2002. *Phys. Essays*, **15** (3), 303.

18. Lo, C. Y. 2003a. *Phys. Essays*, **16** (1), 84-100.

19. Lo, C. Y. 2003b. *Chinese J. of Phys.*, Vol. **41**, No. 4 : 233.

20. Lo, C. Y. 2004. *Chin. Phys.*, Vol. **13** ,No. 2: 159.

21. Lo, C. Y. 2005a. *Phys. Essays*, **18** (1) : 112.

22. Lo, C. Y. 2005b. *Phys. Essays*, **18** (4) : 547-560.

23. Lo, C. Y. 2006a. *Astrophys. Space Sci.*, 306: 205-215.

24. Lo, C. Y. 2006b. *Progress in Physics*, Vol. 1: 10-13.

25. Lo, C. Y. 2006c. *Progress in Phys.* Vol. 4: 14-18.

26. Lo, C. Y. 2006d. *Bulletin of Pure and Applied Sciences*, Vol. 25D (1): 41-47.

27. Lo, C. Y. 2007a. *Bulletin of Pure and Applied Sciences*, Vol. 26D (1): 29-42.


CC-0. In Public Domain. Gurukul Kangri Collection, Haridwar

Digitized by Arya Samaj Foundation Chennai and eGangotri


28. Lo, C. Y. 2007b. Physical Interpretation of Relativity Theory: Proceedings of International Meeting. Moscow, 2 – 5 July 2007/ Edited by M.C. Duffy, V.O. Gladyshev, A.N. Morozov, P. Rowlands. – Moscow: BMSTU, 2007. p. 82.

29. Lo, C. Y. 2007c. *Bulletin of Pure and Applied Sciences*, **26D** (2): 117-132.

30. Lo, C. Y. 2007d. *Chin. Phys.* (Beijing), **16** (3): 635-639.

31. Lo, C. Y. 2008. *Bulletin of Pure and Applied Sciences*, **27D** (1): 1 - 12.

32. Lo, C. Y. 2009a. *Bulletin of Pure and Applied Sciences*, **28D** (1): 67-85.

33. Lo, C. Y. 2009b. The Mass-Charge Repulsive Force and Space-Probes Pioneer Anomaly, **Physical Interpretation of Relativity Theory: Proceedings of International Meeting, 6 – 9 July 2009,** Moscow: BMSTU.

34. Lo, C. Y. 2009c. *Phys. Essays*, **22** (4) : 512.

35. Lo, C. Y. & Wong, C. 2006. *Bulletin of Pure and Applied Sciences*, **25D** (2): 109.

36. Misner, C. W., Thorne, K. S., & Wheeler, J. A. 1973. *Gravitation* (Freeman, San Francisco).

37. Musha, T. & Kanamoto, T. 1994. Proc. of the 38th Space Sci. and Tech. Conf., *JSASS*, 1994, pp. 31-32 (J).

38. Musha, T. 1997. Proc. of the 37th Conf. on Aerospace Propulsion, JSASS, 1997, pp. 342-349 (J).

39. Norton, J. 1989. Einstein's Studies Vol. 1: ***Einstein and the History of General Relativity***, Eds. D. Howard & J. Stachel (Birkhäuser, Boston).

40. Ohanian, H. C. & Ruffini, R. 1994. ***Gravitation and Spacetime*** (Norton, New York).

41. Pauli, W. 1958. ***Theory of Relativity*** (Pergamon, London).

42. Ray, R. assistant editor of Phys. Rev. D, made the same mistake as Lo (2002) and Schiff (1960) did (Private communication, Jan. 10, 2005).

43. Schiff, L. I. 1960. *Am. J. Phys.* 28 (4): 340-343.

44. Synge, J. L. 1971. ***Relativity: The General Theory*** (North-Holland, Amsterdam).

45. Tajmar, M. & Clovis de Matos, 2007. http://news.softpedia.com/news/The-First-Test-That-Proves-General-Theory-of-Relativity-Wrong-20259.shtml

46. Thorne, K. S. 1987. Gravitational Radiation in *300 Years of Gravitation*, ed. S. W. Hawking & W. Israel (Cambridge Univ. Press, New York).

47. Thorne, K. S. 1994. ***Black Holes and Time Warps*** (Norton, New York).

48. Wald, R. M. 1984. ***General Relativity*** (The Univ. of Chicago Press, Chicago).

49. Weinberg, S. 1972. ***Gravitation and Cosmology***: (John Wiley Inc., New York).



CC-0. In Public Domain. Gurukul Kangri Collection, Haridwar

Digitized by Arya Samaj Foundation Chennai and eGangotri


50. Weinberg, S. 2005. 'Einstein's Mistakes', *Phys. Today*, 58 (11): 31.

51. Whitehead, A. N. 1962. ***The Principle of Relativity*** (Cambridge Univ. Press, Cambridge).

52. Will, C. M. 1981. ***Theory and experiment in gravitational physics*** (Cambridge Univ. press, Cambridge).

53. Zhou Pei-yuan, 1987. International Symposium on Experimental Gravitational Physics (Guangzhou, 3-8 Aug. 1987), ed. P. F. Michelson, 110-116 (World Sci., Singapore).


CC-0. In Public Domain. Gurukul Kangri Collection, Haridwar

Digitized by Arya Samaj Foundation Chennai and eGangotri

CC-0. In Public Domain. Gurukul Kangri Collection, Haridwar

Digitized by Arya Samaj Foundation Chennai and eGangotri

ISSN-0970-6569
*Bulletin of Pure and Applied Sciences.Vol.28D(No.2)2009:P.105-115*

# GROWTH AND CHARACTERIZATION OF TETRA (THIOUREA) POTASSIUM CHLORIDE (TTPC) A SEMIORGANIC NLO MATERIAL

**M. Iyanar, J. Thomas Joseph Prakash[1], C. Muthamizhchelvan[2], and S. Ponnusamy[2]**

Department of Physics, National College, Trichy-620 001; Tamilnadu

**ABSTRACT**

The growth and characterization of a nonlinear Tetra (thiourea) Potassium Chloride (TTPC) is reported. In the present study we have synthesized the Tetra (thiourea) Potassium Chloride (TTPC) by taking the appropriate ratio of thiourea and potassium chloride. The calculated amounts of the reactants were thoroughly dissolved in double distilled water and stirred well for about two hours using a magnetic stirrer. Then the mixture was evaporated to dryness, by heating below an optimum temperature of 60°C to prevent possible decomposition. The colorless crystalline sample of TTPC was obtained and dissolved thoroughly in double distilled water at 30°C to form a saturated solution. This was then filtered twice to remove suspended impurities and allowed to crystallize by slow evaporation at 30°C. The harvested single crystal has been subjected to XRD, FTIR, TG/DTA, UV-Vis., etc in order to know its suitability for device fabrication. From the X-ray diffraction analysis we understood that the grown single crystal belongs to tetragonal crystal system having the lattice dimensions a=20.4854Å, b=20.6430Å, c=8.5278Å and volume V=3578.7050A$^3$.

**Key words :** Synthesize, Characterization analyses, Nonlinear optical material, Single crystal, Crystallization

## 1. INTRODUCTION

Second Order Non linear optical (SONLO) materials have a significant impact on laser technology, optical communication, and optical storage technology and electro optic modulation. The search for new frequency conversion materials over the past decade has led to the discovery of many semi organic materials. These materials posses large non linearity, high resistance laser induced damage and low angular sensitivity ( Ushashree *et al* 1999, Rajsekaran *et al* 2001)]. The common wisdom has been that an optical material should have a large charge transfer and the optical transparency with less dislocation density ( Zhang 2001 ) . Organic materials show their properties prominently due to their fast and large nonlinear response over a broad frequency range, inherent synthetic flexibility, and large optical damage

Corresponding author:E-mail: inrnct@gmail.com
[1]Department of Physics, Thiru Kolanjiappar Government Arts College, Virudhachalam-606 001,
[2]Department of Physics, SRM University, Kancheepuram – 603203, Tamilnadu

CC-0. Panini Kanya Maha Vidyalaya Collection. Haridwar

Digitized by Arya Samaj Foundation Chennai and eGangotri



threshold. However, organic materials suffer from problems, such as volatility, low thermal stability, mechanical weakness, etc. Inorganic materials possess excellent mechanical and chemical properties but most of them show low nonlinear efficiency. The need for materials which combine large nonlinear optical characteristics with resistance to physical and chemical attack led to the investigation of semi-organics ( Newman *et al* 1990, Marcy *et al* 1992, Ramabadran *et al* 1992, Lin *et al* 1989 ) . Semi-organic materials have the potential for combining high optical nonlinearity and chemical flexibility of organics with the physical ruggedness of inorganic substances. The advantages of semi-organic materials are that they can be grown from aqueous solution and form large three-dimensional crystals. The crystals can be easily cut and polished with specific phase-matching loci, acceptance angle, and the effective nonlinear coefficient, for frequency doubling of 1064 nm. Ligands like thiourea and thiocyanate with S and N donors are capable of combining with metal to form stable complexes through coordinated bonds. These complexes show ligand to metal charge transfer (LMCT) by an electron movement from ligand to metal and metal to ligand (MLCT) in addition to $\pi$-$\pi^*$ conjugation. Metals with $d_{10}$ configuration like zinc, cadmium, mercury readily combine with thiourea resulting in stable compounds with high optical nonlinearity and good physiochemical behavior.

In the recent past different types of semi organic single crystals have been grown by researchers (Zhang 2001,Newman *et al* 1990, Marcy *et al* 1992 ). Recently the metal complexes of thiourea are being explored. Some of the examples of these complexes are Zinc Thiourea Chloride (ZTC), Bisthiourea Cadmium Chloride (BTCC) and Copper Thiourea Chloride (CTC). These crystals have better nonlinear optical properties than KDP.

In this paper, we have successfully grown the compound mentioned in the title by taking appropriate ratio of thiourea and potassium chloride. It is a potential semi organic nonlinear optical material having a molecular formula $C_4H_{16}Cl\,KN_8S_4$. It was grown by slow evaporation solution growth technique at room temperature. The grown single crystals have been analyzed by adopting different characterization.

## 2. EXPERIMENTAL PROCEDURE

### 2.1 Material Synthesis and growth of TTPC

The recrystallized material of TTPC was synthesized by taking thiourea (AR grade) and potassium chloride (AR grade) in the ratio of 4:1 using water as the solvent. The solution was stirred continuously for 24 hours and subsequently heated to get the homogeneous mixture. Then the saturated solution was allowed to cool to room temperature and kept in a vibration free area with a


CC-0. In Public Domain. Gurukul Kangri Collection, Haridwar

Digitized by Arya Samaj Foundation Chennai and eGangotri



tightly closed plastic cover for controlled evaporation. TTPC was synthesized according to the following reaction mechanism:

$$KCl + 4[CS(NH_2)_2] \rightarrow K[CS(NH_2)_2]_4Cl$$

## 2.2 Solubility

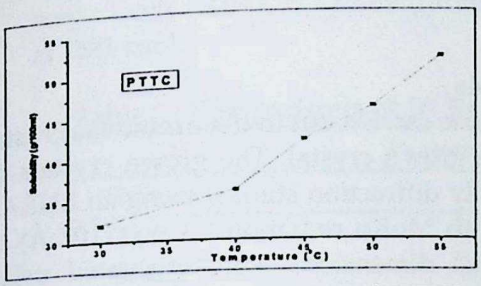


**Figure - 1 : Solubility curve of TTPC**

Solubility studies have been carried out using recrystallized salt of TTPC in water. The solubility was determined by 100 ml of solvent was taken in an airtight container and recrystallized salt was added. The experiment was carried out in a constant temperature bath with a cryostat facility. The bath was set to 35 °C and the solution was stirred continuously for five hours with motorized stirrer by ensuring homogeneous temperature and concentration throughout the volume of the solution. The solution was further stirred for five hours after attaining the saturation and the equilibrium concentration of the solute was analyzed gravimetrically. The experiment was carried out at different temperatures, and the solubility curve is drawn. The solubility of TTPC in water is shown in Figure 1.

## 2.3 Crystal Growth

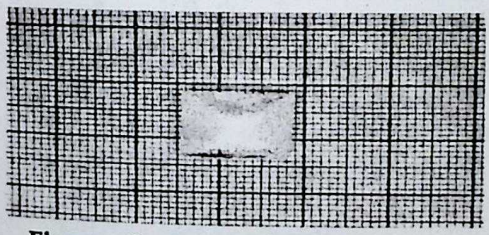

**Figure - 2 : As-grown crystal of TTPC**

The solvent evaporation technique was employed for the growth of TTPC crystal at room temperature. According to the solubility data the saturated solution of TTPC was obtained by dissolving the recrystallized material with continuous stirring of the solution using magnetic stirrer. The saturated solution


CC-0. In Public Domain. Gurukul Kangri Collection, Haridwar

Digitized by Arya Samaj Foundation Chennai and eGangotri



was further purified by filtering through the glass filter paper provided with fine pores of size 1 micrometer porosity. The filtered solution was tightly closed with thick filter paper so that the evaporation could be minimized. The solution was kept in an undisturbed condition. Good quality single crystals of tetra (thiourea) potassium chloride (TTPC) have been collected from the mother solution in a time span of 20 days with dimension 14 x 12 x 2 $mm^3$. The grown single crystal is shown in Figure. 2

## 3. RESULTS AND DISCUSSIONS

### 3.1 Single crystal X-ray diffraction analysis

The single X-ray diffraction study was carried out to determine the crystal system and the lattice dimensions of the grown crystal. The grown crystals of TTPC were subjected to single crystal X-ray diffraction studies using an ENRAF NONIUS CAD-4 X-ray Diffractometer with MoKo radiation ( $\lambda$ = 0.7107 Å) to obtain the unit cell dimensions. The cell dimensions were evaluated using standard software. From this measurement we found that the grown specimen belongs to tetragonal system with the lattice parameters a = 20.48 Å, b = 20.64 Å, c = 8.52 Å, and V= 3578.90 $A^3$. The results are given in Table 1.

**Table. 1: Single crystal XRD data of TTPC**

| | |
|---|---|
| Identification code | TTPC |
| Cell parameters | a = 20.48 Å |
| | b = 20.64 Å |
| | c = 8.52 Å |
| | $\alpha$ = 90° |
| | $\beta$ = 90° |
| | $\gamma$ = 90° |
| Volume | 3578.90 $Å^3$ |
| System | Tetragonal |
| Chemical formula | $C_4H_{16}Cl\,KN_8S_4$ |

### 3.2 Fourier Transform Infra-red (FTIR) analysis

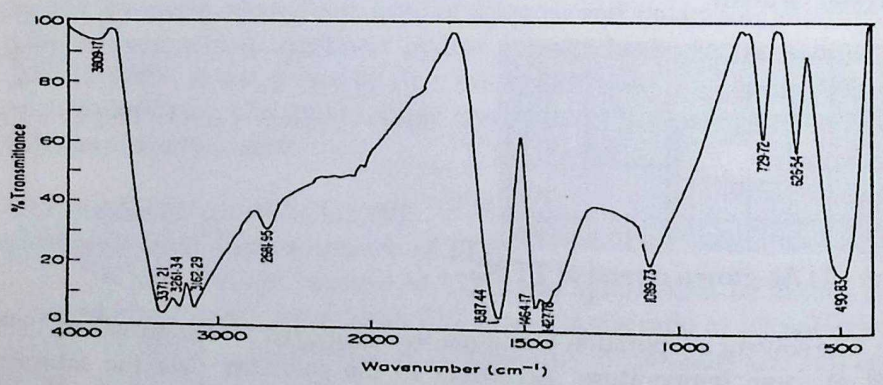


**Figure - 3 : FTIR spectrum of TTPC**


CC-0. In Public Domain. Gurukul Kangri Collection, Haridwar

Digitized by Arya Samaj Foundation Chennai and eGangotri



The FTIR spectrum of TTPC crystal was in the KBr pellet technique in the frequency region 400-4000 $cm^{-1}$ using PERKIN ELMER RX1 Fourier Transform Infrared spectrometer. The recorded FTIR spectrum of TTPC crystal is shown in Figure 3. The observed bands along with their vibration assignment are summarized and compared with thiourea in Table 2. The asymmetric and symmetric $NH_2$ stretching vibration bands were observed at 3261 and 3162 $cm^{-1}$, respectively. The CH symmetric stretching vibration was observed a sharp peak at 2681 $cm^{-1}$.

**Table.2 : Comparisons of IR Band Frequencies ($cm^{-1}$) Thiourea and TTPC**

| Wavenumber ($cm^{-1}$) | | |
|---|---|---|
| Thiourea | TTPC | assignment |
| 3280 | 3261 | $\gamma_{as}(NH_2)$ |
| 3167 | 3162 | $\gamma_{s}(NH_2)$ |
| - | 2681 | $\gamma_{s}(CH)$ |
| 1593 | 1587 | $\delta(NH_2)$ |
| 1472 | 1464 | $\gamma_{as}(CN)$ |
| 1417 | 1427 | $\gamma_{as}(CS)$ |
| 1089 | 1089 | $\gamma_{as}(CN)$ |
| 740 | 729 | $\gamma_{s}(CS)$ |
| 648 | 626 | $\gamma_{as}(NCS)$ |
| 469 | 490 | $\gamma_{s}(NCS)$ |

The $NH_2$ bending vibration appears at 1587 $cm^{-1}$. The CN asymmetric and symmetric stretching vibrations were observed at 1464 and 1089 $cm^{-1}$, respectively. The strong bands appearing at 1427 and 729 $cm^{-1}$ in the spectrum were assigned to CS asymmetric and symmetric stretching vibration. To confirm the metal coordination of thiourea either through S or N, the CN and CS stretching of complex TTPC were compared with free ligand (thiourea). It was established that the CN stretching vibration of thiourea (1089 and 1472 $cm^{-1}$) were shifted to a higher wavenumber of TTPC (1087 and 1464 $cm^{-1}$) and the CS stretching vibrations of thiourea (740 and 1417 $cm^{-1}$) were shifted to a lower wavenumber of TTPC (729 and 1427 $cm^{-1}$). This clearly indicates the coordination of sulfur with metal .

### 3.3 Thermal analysis

The thermo gravimetric analysis of TTPC crystal were carried out between 20 °C and 800 °C in the nitrogen atmosphere at a heating rate of 20 °C $min^{-1}$ using Perkin-Elmer thermal analyzer (STA 409 PC). The obtained spectrum is shown in Figure 4.


CC-0. In Public Domain. Gurukul Kangri Collection, Haridwar

Digitized by Arya Samaj Foundation Chennai and eGangotri



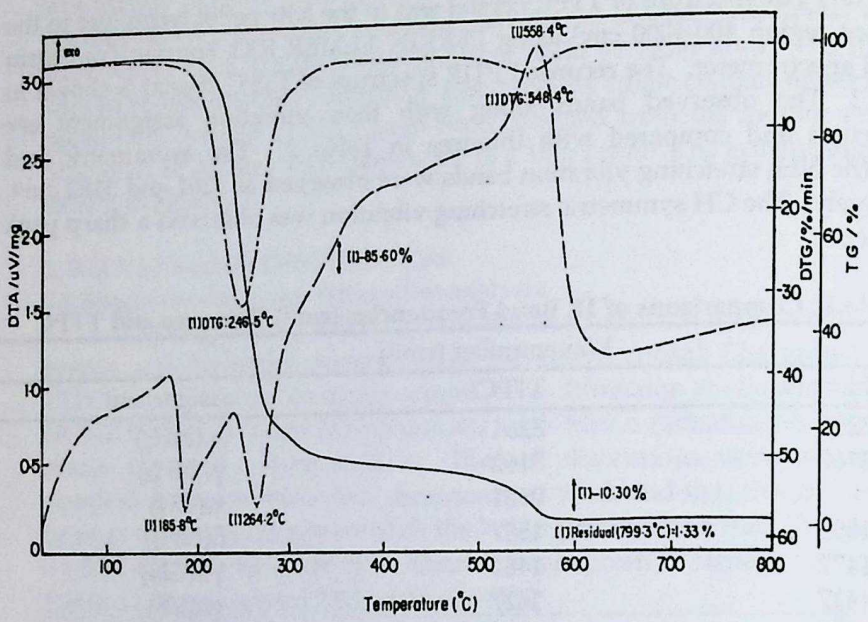


**Figure - 4 : TG/DTA spectra of TTPC**

From the TG/DTA spectrum, we observed that the weight loss below 245 °C was due to weakly entrapped lattice water and above it, due to the removal of strongly entrapped lattice water. This was followed by a major weight loss at 550 °C due to decomposition of the substance. The DTA analysis was also carried out in the same atmospheric condition. There was an endothermic transition between 180 and 260 °C which was good in agreement with the TGA trace. The sharp endothermic peak at around 186 °C was assigned to the melting point of the title compound. Sharpness of the endothermic peak observed in DTA showed good degree of crystallinity of the specimen ( Hameed *et al* 2000). Hence it might be useful for making the NLO devices below its melting point.

### 3.4 Differential scanning calorimetric analysis

Differential scanning calorimeter (DSC) study was performed using DSC200 PC in the temperature range 20-400 °C at a heating rate of 20 K/min in the nitrogen atmosphere and the spectrum is shown in Figure 5. 7.000 mg sample was used for the present analysis. From this measurement, we found that the crystal was stable up to its melting point 186.1°C.


CC-0. In Public Domain. Gurukul Kangri Collection, Haridwar

Digitized by Arya Samaj Foundation Chennai and eGangotri



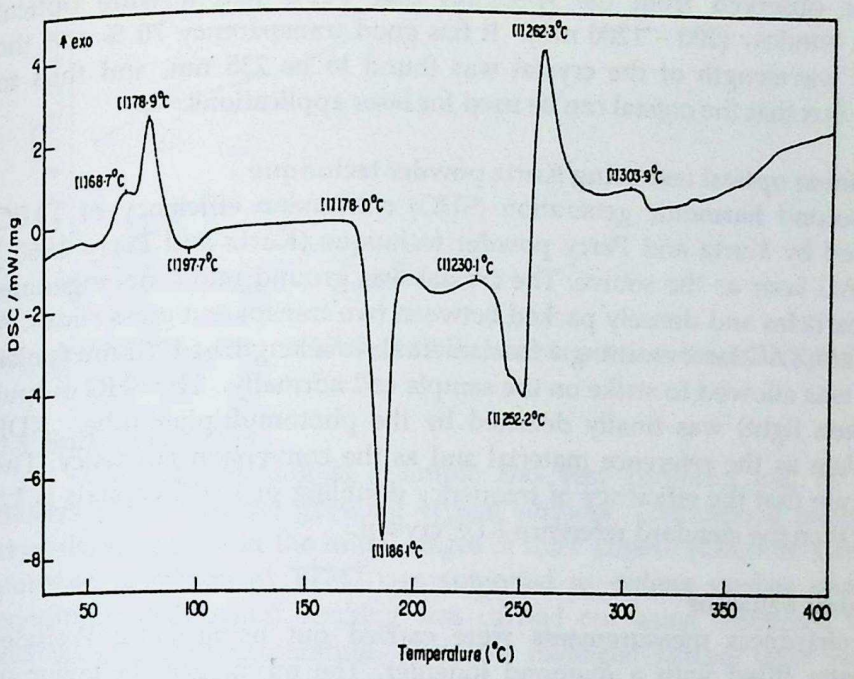


**Figure - 5 : DSC spectrum of TTPC**

### 3.5 Optical assessment

The transmission spectrum of TTPC crystal was recorded in the range 200–1200 nm using SHIMADZU UV-1061 UV-Visible spectrophotometer. The recorded spectrum is shown in the Figure 6.

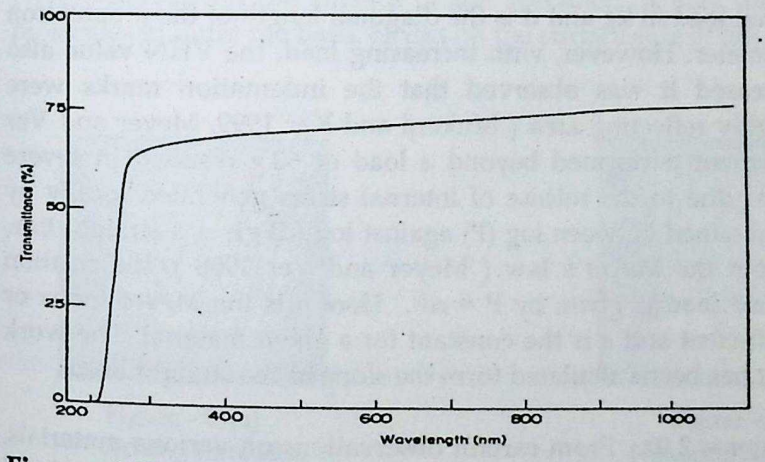


**Figure - 6 :Transmittance spectrum of TTPC**


CC-0. Mumukshu Bhawan Varanasi Collection. Haridwar

Digitized by Arya Samaj Foundation Chennai and eGangotri



It was observed from the spectrum that TTPC had a wide optical transmission window (200 – 1200 nm). It has good transparency 70 % and the lower cutoff wavelength of the crystal was found to be 235 nm, and thus to ascertain the fact that the crystal can be used for laser applications.

### 3.6 Nonlinear optical test using Kurtz powder technique

The second harmonic generation (SHG) conversion efficiency of TTPC was measured by Kurtz and Perry powder technique (Kurtz and Perry 1968 ) using Nd:YAG laser as the source. The crystal was ground into a homogenous powder of particles and densely packed between two transparent glass slides. A Q-switched Nd:YAG laser emitting a fundamental wavelength of 1064 nm (pulse width 8 ns) was allowed to strike on the sample cell normally. The SHG output 532 nm (green light) was finally detected by the photomultiplier tube. KDP crystal is taken as the reference material and as the conversion efficiency. The results indicate that the efficiency of frequency doubling in TTPC crystals is 1.5 times better than the standard reference KDP crystal.

### 3.7 Mechanical behavior

Microhardness measurements were carried out using Leitz Weitzler hardness tester fitted with a diamond indenter. The mechanical behavior of TTPC crystal was analyzed by using Vickers Microhardness test at room temperature. The crack free, smooth surface of TTPC crystal was chosen for this analysis. The crystal was mounted properly on the base of the microscope. Now the selected faces were indented gently by the loads varying from 10 to 60 g for a dwell period of 5 s. The plot of Vickers Microhardness Vs. load is shown in Figure 7. The hardness was calculated using the relation $H_v = \frac{(1.854 \times P)}{d^2}$ kg/mm$^2$. Where P is the applied load in kg and d is the diagonal length of the indentation impression in micrometer. However, with increasing load, the VHN value also simultaneously increased it was observed that the indentation marks were surrounded by a highly reflecting area ( Mukerji and Kar 1999, Meyer and Ver 1908 ). The measurement performed beyond a load of 60 g resulted in severe cracks. This might be due to the release of internal stress generated locally by indentation. A plot obtained between log (P) against log (d) gives a straight line, which is derived from the Meyer's law ( Meyer and Ver 1908 ), the relation connecting the applied load is given by $P = ad^n$. Here $n$ is the Meyer index or work hardening coefficient and $a$ is the constant for a given material. The work hardening coefficient has been calculated form the slope of the straight line.

The value of $n$ is 2.02. From careful observations on various materials, Onitsch (Onistch 1950) pointed out that an $n$ lies between 1 and 1.6 for hard materials and it is more than 1.6 for soft materials. This established that the TTPC crystals were soft substances.


CC-0. In Public Domain. Gurukul Kangri Collection, Haridwar

Digitized by Arya Samaj Foundation Chennai and eGangotri


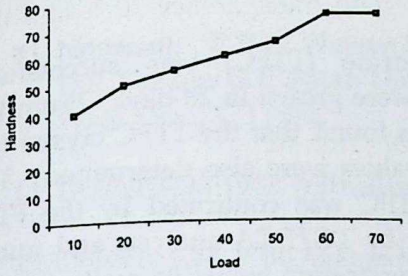


**Figure - 7 : Variation of Vicker's Microhardness number with applied load**

### 3.8 Surface analysis

Chemical etching is a simple and very powerful tool to analyze the defects present in the growing crystal surfaces. Dislocations easily appear in crystals, especially in the initial stages of their growth (Chernov 1989) . Cut and polished specimen of TTPC was subjected to etching studies under identical conditions (110-plane). Etching was carried out using deionized water as an etchant at room temperature. Once the damaged surface layer was removed during etching, a fresh surface appeared which in turn gave clear etch pits. The etched surfaces were dried by gently pressing them between two filter papers and then immediately examined and their microstructure was analyzed using an optical microscope in the reflection mode. The recorded images are given in Figures 8(a) and 8(b). From the fig. one can understand that the growth striations were observed. It might be due to variation of supersaturation during growth and it generated the growth striations in the crystal faces (Figure 8(a)). Etch pits were observed on the surface of the specimen. It may due to the insufficient molecules to build the basic blocks on the surface side of the specimen.

**Figure - 8: (a) (etching time 10 s)**

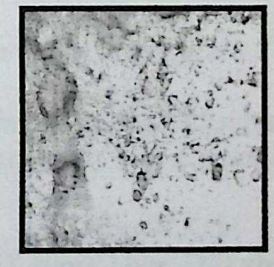

**Figure - 8 (b): ( etching time 20 s)**


CC-0. In Public Domain. Gurukul Kangri Collection, Haridwar

Digitized by Arya Samaj Foundation Chennai and eGangotri



## 4. CONCLUSION

The tetra (thiourea) potassium chloride (TTPC) was successfully synthesized and good quality single crystals were grown in 20 days. From the single crystal X-ray diffraction analysis, it was found that the TTPC crystal has tetragonal system. The unit cell parameter values were also determined. The presence of various functional groups of TTPC was confirmed by the FTIR analysis. The thermal behavior was assessed by TG/DTA analysis and found that the specimen might be useful for NLO application below its melting point 186 °C. Optical transmission range of TTPC was measured to be 200-1200 nm i.e. the grown crystal has a good optical transmission in the entire visible region. The Vicker's Microhardness was calculated in order to understand the mechanical stability of the grown crystals. Kurtz power nonlinear experiment confirmed that the TTPC crystal was a promising nonlinear optical material. The straight striations and kinks were observed on the crystal surface during etching.

## REFERENCES

1. Ambujam, K., Rajarajan,K., Selvakumar,S., Madhavan, J.,Gulam Mohamed and Sagayaraj, P.2007.*Opt. Mat.*, 29 : 657.

2. Chernov,A.A.1989. *Contemp. Phys.*,30 : 251.

3. Gokul Raj, S., Ramesh Kumar,G., Mohan, R., and Babu Varghese.2006. *J.Mol.Struct.*, 825:158.

4. Hameed, A.S.H., Ravi,G., Dhanasekaran,R. and Ramasamy,P. 2000. *J. Cryst. Growth.*, 212 :227.

5. Kurtz,S.K. and Perry, J.J.1968. *J. Appl. Phys.*, 39 : 3798.

6. Lin,J.T., Wang,W.S. and Arend, H.1989.*Proc. SPIE*, 1104 : 100.

7. Madhavan,J., Aruna,S., Prabha,K., Packium Julius,J., Ginson P. Joseph, Selvakumar ,S. and Sagayaraj,P.2006. *J. Cryst. Growth.*, 293 : 409.

8. Marcy, H.O.,Warren,L.F., Webb,M.S., Ebbers,C.A., Velsko, S.P., Kennedy,G.C. and Catella, G.C.1992.*Appl. Opt.*, 31 : 5051.

9. Meyer, E. and Ver,Z.1908. *Dtsch. Ing*,52 : 645.


CC-0. In Public Domain. Gurukul Kangri Collection, Haridwar

Digitized by Arya Samaj Foundation Chennai and eGangotri


10. Mukerji, S., and Kar,T.1999. *Cryst. Res. Technol.*, 34 : 1323.

11. Newman, P.R., Warren,L.F., Cunningham,P., Chang,T.Y., Cooper, D.E.,Burdge, G.L.,Polak-Dingels,P. and LoweMa, C.K.1990. *Mater. Res. Sot. Symp. Proc.*, 173 : 557.

12. Onistch,E.M.1947. *Mikroskopie*, 2 : 131.

13. Onistch, E.M. 1950.*Mikroskopie*, 95 : 12.

14. Rajsekaran,R., Rajendrian, R.V., Mohan Kumar,R., Jayavel, R., Dhanasekaran,R. and Ramasamy, P.2003. *Mat. Chem. Phys.*, 82 : 273.

15. Rajsekaran,R., Ushashree,P.M., Jayavel,R. and Ramasamy, P.2001. *J. Cryst. Growth.*, 229 : 563.

16. Ramabadran,U., Zelmon, D.E. and Kennedy,G.C.1992. *Appl. Phys. Lett.*, 60 : 2589.

17. Zhang, G.P.2001.*Phys. Rev. Lett.*, 86 : 10.


CC-0. In Public Domain. Gurukul Kangri Collection, Haridwar

Digitized by Arya Samaj Foundation Chennai and eGangotri

CC-0. In Public Domain. Gurukul Kangri Collection, Haridwar

Digitized by Arya Samaj Foundation Chennai and eGangotri

ISSN-0970-6569
Bulletin of Pure and Applied Sciences. Vol.28D(No.2)2009:P.117-120

# THE EFFECT OF BYCHKOV - RASHBA SPIN-ORBIT COUPLING IN THE OPTICAL TRANSITION SPECTRA AND ENERGY LEVELS OF PARABOLIC DOTS

**Anant Ranjan, Abhishek Kumar*, Janardan Chaudhary**, Asim Kumar*** and Madan jee**

University Department of Physics, B.R.A. Bihar University, Muzaffarpur, (BIHAR), India.

**ABSTRACT**

We studied the effect of Bychkov-Rashba spin-orbit coupling in the optical transition spectra and the energy levels of two parabolic dots placed vertically and interacting only through the Coulomb interaction. The zero field spin hot spots in our vertically coupled quantum dots manifests in the dipole transition energies. For coupled quantum dots with one dot containing two electrons while the other with a single electron, the spin-orbit effect strongly depends on the inter dot separation. In the quantum dots the electric field can arise from the inversion asymmetry of the potential restricting the motion of the electrons to a two dimensional plane. Another source for the electric field in the quantum dot is the potential confines the electron into the dot in the two dimensional plane.

**Key words :** Coupling, Quantum dot, Spin-orbit, Dipole transition.

## INTRODUCTION

Awschalom *et al* (2002) investigated the spin properties of semiconductor nanostructures in solid state devices. Nitta *et al* (1997) showed that spin-orbit coupling provides a means to influence the spin states through the orbital degrees of freedom. Stano and Fabian (2005) studied that in the quantum dots, spin hot spots are composed of two or more states and the degeneracy is lifted due to the spin orbit coupling. Bychkov and Rashba (1984) investigated that there is no contribution of the Bychkov-Rashba spin-orbit potential to the spin hot spots at zero magnetic field. Chakraborty, *et al* (2002) presented the transition energies of a single electron in a vertically coupled parabolic quantum dot in the presence of a spin-orbit coupling. Pietilainen (2006) studied that in the quantum dots the electric field can arise from the inversion asymmetry of the potential restricting the motion of the electrons, with charge $e < 0$ and effective mass $m^*$, to a two dimensional plane. Then the electric field would be perpendicular to the plane of the motion. The field to be nearly homogeneous within the range of the electron wave functions it can be replaced to a good approximation with its

* University Department of Physics, Vinoba Bhave University, Hazaribagh, Jharkhand, INDIA.
** Department of Physics, R.B.S. College, Chandi Dhenuki, Vaishali, Bihar, INDIA.
*** Department of Electronics and Communication, Engineering and Technology, Institute, Patna, Bihar, INDIA.

CC-0. In Public Domain. Gurukul Kangri Collection, Haridwar

Digitized by Arya Samaj Foundation Chennai and eGangotri



average value. It is did to collect all the parameters including the average of the electric field into a single coupling constant leading to the Bychkov-Rashba potential for the spin-orbit coupling due to the inversion asymmetry. The electric field in the quantum dot confines the electrons into the dot in the two dimensional plane. Voskoboynikov, *et al* (2001) showed that field lies in the plane of motion, if the confinement is rotationally symmetric it will be parallel to the radius vector.

## RESULTS AND DISCUSSION

We found that coupled dot system is

$$H = \sum_i H_i^0 + \sum_{i<j} \frac{e^2}{(r_{ij}^2 + d^2)^{1/2}}$$

where d is inter dot separation, $H_i^0$ is the Hamiltonian for a single electron in a parabolic quantum dot

Hence - $$H_i^0 = H^0 + H_{S0}^0$$

$$H^0 = \frac{1}{2m^*}(\vec{p} + \frac{e}{c}\vec{A}) + \frac{1}{2}\sigma_z \mu B_g B + \frac{1}{2} m^* \omega_0^2 r^2$$

$\sigma_z$ is the Pauli z matrix. $H_{S0}^0$ is independent of the external magnetic field B.

When B=0, it lifts the spin degeneracy because of the magnetic field starting from the orbital motion of the electron in the presence of electric field coming from the confinement potential. The corresponding electron energy levels are given by

$$E_{n,\lambda\sigma} = \eta\Omega_\sigma(2n + |\lambda| + 1) + \lambda\frac{\eta\omega_c}{2} + \sigma\frac{\mu_B}{2} gB + \lambda\alpha m^* \omega_0^2$$

and $$\Omega_\sigma^2 = \omega_0^2 + \frac{\omega_c^2 B}{4} + \sigma\alpha\frac{m^*\omega_0^2}{\eta}\omega_c$$

where $\omega_c$ is the cyclotron frequency. So spin-orbit coupling influence $\Omega_\sigma$ which increase the energy of the up spin and decrease in down spin.

A graph is plotted between magnetic field and energy as shown in graph (1). In indicates that for two dots each containing one electron and are vertically coupled. It is seen that for large separation of dot the transition energies are same as in a single electron. When the dots are closer the inter dot interaction becomes stronger and optical spectra are unchanged. If $\lambda_{D_1}$, $s_{D_1}$ and $\lambda_{D2}$, $s_{D_2}$ represent the quantum numbers for the first and second dot. In the case of very weak inter dot interaction the two states when $\lambda_{D_1}$=1, $\lambda_{D_2}$=0 and $\lambda_{D_1}$=0, $\lambda_{D_2}$=1 are degenerate. Graph (2) is plotted which shows the transition energy spectrum of two


CC-0. In Public Domain. Gurukul Kangri Collection, Haridwar

Digitized by Arya Samaj Foundation Chennai and eGangotri



vertically coupled dots separated by $0.5l_B$ and $9.5\ l_B$ in the presence of spin orbit coupling. In this case one dot confines a single electron while the other dot contains two interacting electrons. When the separation is large there are four lines as a function of the magnetic field and two lines are found for smaller separation. It was observed that splitting disappears for a dot having two electrons and lifting of degeneracy is seen when B = 0 for two coupled quantum dots. For the two coupled dots one partner dot has two interacting electrons and other has only one electron. The dipole transition energies depend on the inter dot separation.

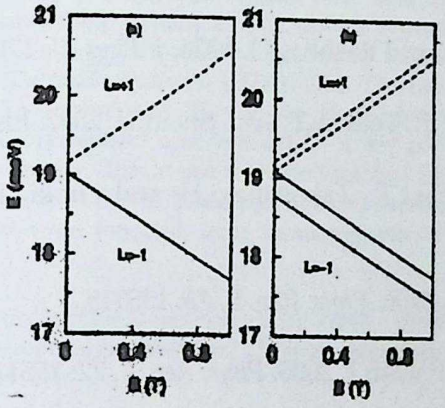


**Graph-1 : The (a) transition energy spectrum and (b) the few low lying energy levels of two vertically coupled dots.**

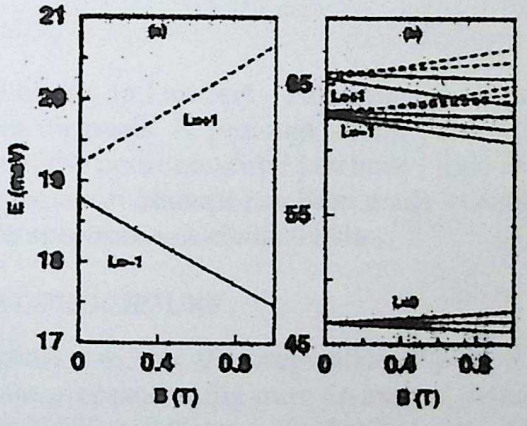


**Graph- 2 : The transition energy spectrum of two vertically coupled dots.**


CC-0. In Public Domain. Gurukul Kangri Collection, Haridwar

Digitized by Arya Samaj Foundation Chennai and eGangotri


## CONCLUSION

A dot having single electron shows the lifting of the degeneracy of dipole transition when B=0 because of spin-orbit coupling and it will disappear for dot having two electrons. The optical spectra is not affected by the coupling for dot having one electron. For two coupled dot remarkable effect is seen.

## REFERENCES

1. Awschalom, D.D., Loss,D. and Samarth,N. 2002. Singer, New York.

2. Bychkov,Y.A. and Rashba,E.I. 1984. *J. Phys.* C, 17: 6039.

3. Chakraborty, T., Peeters,F. and Sivan,U. 2002. Elsevier, New York.

4. Nitta,J., Akazaki,T., Takayanagi,H. and Enoki, T.1997. *Phys. Rev. Lett.* 78: 1335.

5. Pietilainen,P. 2006. *Phys. Rev.* B, 73: 155315.

6. Stano,P. and Fabian,J. 2005. *Phys. Rev.* B, 72: 155410.

7. Voskoboynikov, O., Lee, C.P. and Tretyak, O. 2001. *Phys. Rev.* B, 63: 165306.


CC-0. In Public Domain. Gurukul Kangri Collection, Haridwar

Digitized by Arya Samaj Foundation Chennai and eGangotri

ISSN-0970-6569
*Bulletin of Pure and Applied Sciences. Vol.28D(No.2)2009:P.121-125*

# SYNTHESIS AND CHARACTERIZATION OF TETRAKIS (4 AMINOPYRIDINE – $\kappa N^1$) – DICHLORIDOCOPPER (II) MONOHYDRATE

**S. Alfred Cecil Raj[a*], A. Sinthiya[b], Samuel Robinson Jebas[c], and S.R. Bheeter[d]**
[a*] Department of Physics, St. Joseph's College, Trichy 620 002, (T. N.), India,

**ABSTRACT**

The blue $[CuCl_2 (C_5H_6N_2)_4] H_2O$ crystals have been synthesized by the slow evaporation technique. The grown crystals have been characterized using UV-visible spectrum, FTIR spectrum, Differential Thermal Analysis (DTA) and Thermo Gravimetric Analysis (TGA) techniques. The results show that the as-grown crystals were crystallized and indexed in a triclinic system with octahedral geometry. The crystal is in good stability upto 210°C and melts congruently at 245°C. The frequencies of the vibration modes of the crystal were reported from measurements of the infrared spectrum.

**Key words :** Crystal Growth; Tetrakis (4-aminopyridine – $\kappa N^1$) – dichloridocopper (11) monohydrate; optical transmission; Thermal properties.

## 1. INTRODUCTION

Fampyridine, a new sustained release oral tablet of 4-AP is currently under phase III clinic trial for its therapeutic efficacy in patients with multiple sclerosis (MS) and Chronic spinal cord injury. Low concentration of 4-AP are considered to block transient, voltage activated, outward $K^+$ currents ( Taccola and Nistri 2005).

It is used clinically in Lambert – Eaton myasthenic syndrome because by blocking potassium channels. It prolongs action potentials thereby increasing transmitter release at the neuromuscular junctions ( Jude and Bever 2006, Strupp *et al* 2004 ).In this paper an attempt has been made to analyze 4-aminopyridine with reference to its spectroscopic characteristics

## 2. EXPERIMENTAL PROCEDURE

All the reagents used for the preparation of sample are analytical grade and the solutions are prepared using pure de-ionized distilled water. A solution of 4-aminopyridine (0.376g) in 99.9% pure distilled water (20ml) was added to a solution of $CuCl_2$. $2H_2O$ (0.170g) in 99.9% pure distilled water (20ml) to form 4:1 ratio mixture and the mixture was stirred at 30°C for 6 hours. The clear blue

Tel: +0 9994977210, Fax: +0 431 2701501, sac63raj@gmail.com
[b] Department of Electronics, St. Joseph's College, Trichy 620 002, Tamil Nadu, India.
[c] Department of Physics, Karunya University, Karanya Nagar, Coimbatore 641 114, TN, India.
[d] Department of Chemistry, St. Joseph's College, Trichy 620 002, Tamil Nadu, India.

CC-0. In Public Domain. Gurukul Kangri Collection, Haridwar

Digitized by Arya Samaj Foundation Chennai and eGangotri



solution obtained was double filtered and allowed to evaporate slowly. The chemical reaction taking place in the growth process is:

$$CuCl_2.\ 2H_2O + 4C_5H_6N_2 \rightarrow [CuCl_2\ (C_5H_6N_2)_4].\ H_2O + H_2O\uparrow$$

Blue $[CuCl_2\ (C_5H_6N_2)_4]\ H_2O$ single crystals of titled compound were obtained after a month. FTIR spectrum was measured using Perkin – Elmer FTIR spectrophoto meter over the range of ± 400 $cm^{-1}$ – 4000 $cm^{-1}$ at room temperature. UV spectrum was measured using Perkin – Elmer Lambda 35uv spectrophoto meter over the range of 190 nm – 1100 nm at room temperature. Differential Thermal Analysis (DTA) and Thermo Gravimetric Analysis (TGA) were recorded using a thermal analyzer [NET2SCH STA 409 C/CD] over the range of 20 / 10.0 (K/min) / 1200.

## 3. RESULTS AND DISCUSSION

After 30 days of slow evaporation, blue coloured crystals were harvested. Some typical as-grown crystals are shown in Figure 1, the maximum size being 3 × 1 × 1 = 3$mm^3$. The crystal belongs to triclinic structure and its lattice parameters were reported (Sinthiya *et al* 2008). From the single crystal data [APE X2 (Bruker, 2005)], it confirms that the as-grown crystals were well crystallized.

**Figure-1 :** Photograph of the as-grown $[CuCl_2(C_5H_6N_2)_4]H_2O$ crystals

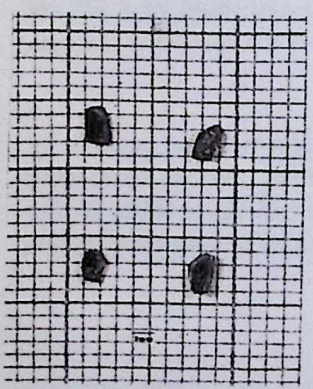


CC-0. In Public Domain. Gurukul Kangri Collection, Haridwar

Digitized by Arya Samaj Foundation Chennai and eGangotri



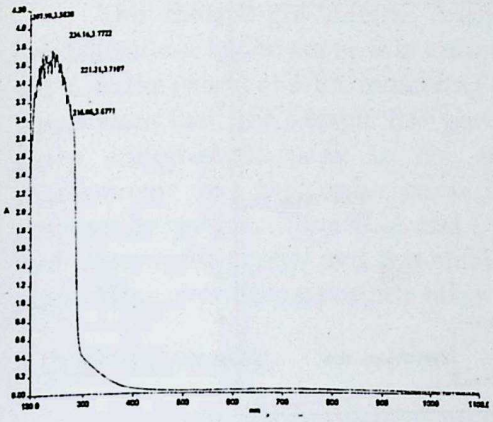

**Figure-2 :** UV spectrum of $[CuCl_2(C_5H_6N_2)_4]H_2O$ (absorbance curve)

Figure.2 shows the UV-visible absorbance characteristics of as-grown $[CuCl_2 (C_5H_6N_2)_4] H_2O$ crystals. The minimum absorption between 300 nm to 1100 nm with absence of any overtons or combination modes was observed which is an important requirement for NLO applications ( Toulemonde *et al* 1992).

Figure - 3 shows the IR spectrum of as grown $[CuCl_2 (C_5H_6N_2)_4]H_2O$ crystals. The results are tabulated in Table 1.

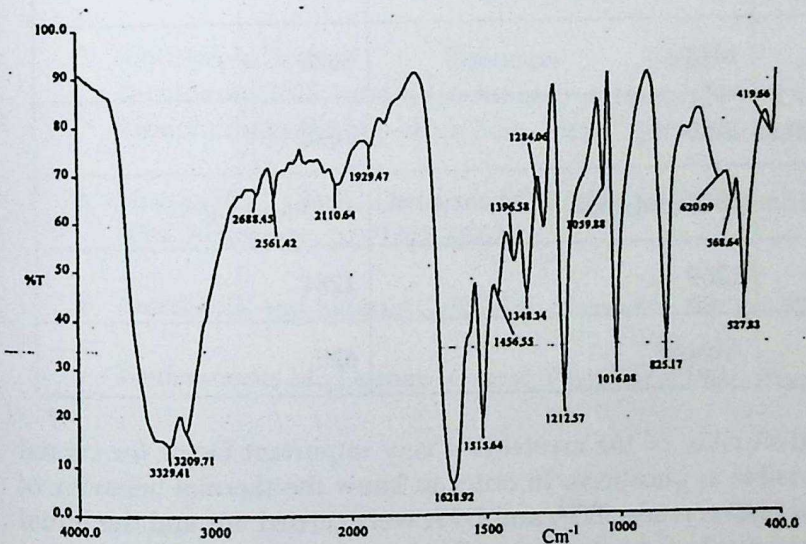


**Figure-3 :** FTIR spectrum of $[CuCl_2(C_5H_6N_2)_4]H_2O$


CC-0.In Public Domain. Gurukul Kangri Collection, Haridwar

Digitized by Arya Samaj Foundation Chennai and eGangotri


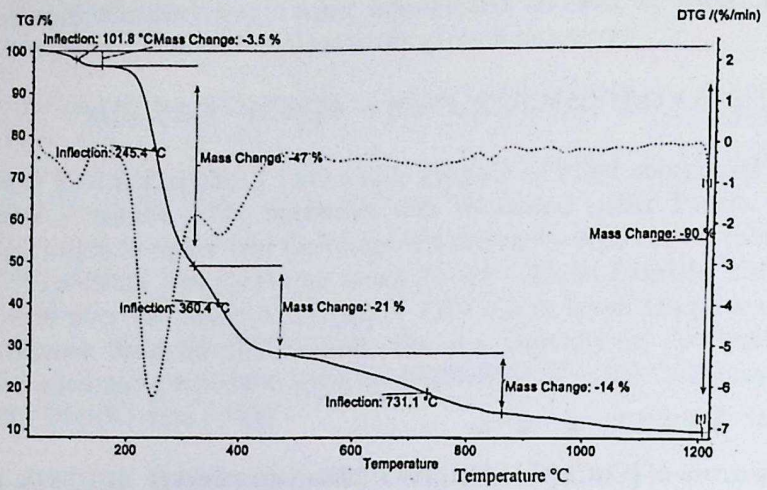


**Figure - 4 :** TGA/DTA curves of $[CuCl_2(C_5H_6N_2)_4]H_2O$

**Table – 1 Assignment of vibration frequency**

| Vibration modes | Frequency ($cm^{-1}$) | |
|---|---|---|
| | Parent Compound $C_5H_6N_2$ | $[CuCl_2(C_5H_6N_2)_4]H_2O$ |
| NH asymmetric | 3432 | 3329 |
| C = N stretch | 1648 | 1628 |
| NH deformation | 1595 | 1628 |
| C = C stretch | 1502 and 1432 | 1515 and 1456 |
| C – N stretch | 1269 | 1284 |
| $C_u$ – N stretch | Absent | 620 |

The thermal stability of the crystal is a very important factor for crystal growth and its possible applications. In order to know the thermal behavior of $[CuCl_2(C_5H_6N_2)_4]H_2O$ crystals, TGA and DTA were carried out and the initial mass of the crystal sample subjected to analysis was 13.600 mg. The recorded curves are shown in Figure 4.


CC-0. In Public Domain. Gurukul Kangri Collection, Haridwar

Digitized by Arya Samaj Foundation Chennai and eGangotri


The thermo-gravimetric analysis shows the presence of water after crystallization. In the curve it is indicated by the presence of weight loss around 101°C to the extent of 3-5% indicating the presence of monohydrate in the crystal. Apart from that, the sample has good stability. The DTA shows that there is a sharp endothermic peak in the temperature range 245°C, which is the characteristic of a first order phase transition and is identified as the melting point of the crystals. Thus TGA and DTA studies reveal that there is one water of hydration in the crystal and it is stable up to 210°C beyond which melting takes place. More over decomposition takes place continuously up to 1200°C.

## 4. CONCLUSIONS

As grown $[CuCl_2 (C_5 H_6 N_2)_4] H_2O$ crystals were crystallized and indexed in a triclinic crystal system. Differential Thermal Analysis and Thermo Gravimetric Analysis show that the crystal is stable in the measurement temperature range up to 210°C and it starts meeting congruently. UV spectrographs show that there are no over tones above 300 nm.

## REFERENCES

1. Jude ,S. and Bever ,C. 2006. *Pharmacol* , 111: 224 – 259.

2. Schwid, S.B., Petrie,M.D., McDermott, M.P., Tierney, D.S., Mason,D.H and Goodman ,A.D. 1997. *Neurology* , 48: 817 – 821.

3. Sinthiya,A.,Samuel Robinson Jebas, and Suganthi Devadasan.2008.Tetrakis (4 Aminopyridine – κN¹) – Dichloridocopper (II) Monohydrate Hoong – Kun Fun, , *Acta Cryst* , E64 : m853 – m854.

4. Strupp,M., Halla,R., Dichgans,M., Fraitinger,T., Glasauer,S. and Brandt ,T. 2004. *Neurology* , 62 : 1623 – 1625.

5. Taccola ,G. and Nistri,A. 2005.*Acta Neurochir* , 93: 151-154.

6. Toulemonde, M., Dufour , C. and Parrmier,E.1992. *Phys. Rev.* ,B4, 14362.


CC-0. In Public Domain. Gurukul Kangri Collection, Haridwar

Digitized by Arya Samaj Foundation Chennai and eGangotri

CC-0. In Public Domain. Gurukul Kangri Collection, Haridwar

Digitized by Arya Samaj Foundation Chennai and eGangotri

*ISSN-0970-6569*
*Bulletin of Pure and Applied Sciences.Vol.28D(No.2)2009:P.127-136*

# STUDY OF HARDNESS OF NaF, NaCl & NaF+NaCl CRYSTALS GROWN BY SOLUTION EVAPORATION METHOD AT AMBIENT TEMPERATURE.

**Ketki A. Mistry, Priyanka Rustagi and I.B.Patel**
Deptt. of Physics, Veer Narmad South Gujarat University,
Surat, Gujarat-395 007,India

**ABSTRACT**

Generally Alkali Halide crystals are ionic crystals which are highly soluble in water. From them NaF and NaCl are most popular materials due to their optical properties. Therefore author have grown these crystals by solution evaporation method at ambient temperature. In this paper, measurement of the mechanical property named hardness of NaCl, NaF and NaCl + NaF-mixed crystals is done in two different ways. First keep the load constant, loading time constant and by varying the temperature hardness was measured. Then keep the temperature constant, loading time constant and by varying the load hardness was measured. The graph of Hardness Vs Load and Hardness Vs Temperature are plotted for all these three crystals. The results and conclusions are reported in this paper.

**Key words :** Crystal growth, Alkali Halide, Mechanical properties, Hardness.

## 1. INTRODUCTION

Among the Alkali Halide crystals, Sodium Floride and Sodium chloride are most famous due to their applications as an optical crystal such as in thin film NaCl is used, NaF is used as radioactive detector in cherencov counter and G.M. counter. The authors have grown NaF, NaF + NaCl and NaCl crystals by solution evaporation method at ambient temperature. Then measured the mechanical property named hardness of these crystals by Vaiseshika Vickers's micro hardness tester whose photograph is shown in the figure-1. Hardness refers to various properties of matters in solid phase that gives it high resistance to various kinds of shape changes when force is applied. It is the standard method for measuring the hardness of metals, particularly those with extremely hard surface,

The surface is subjected to a standard pressure for a standard length of time by means of Pyramid- shaped diamond. The diagonal of the resulting indention was measured under a microscope and the Vickers hardness value read from a conversion table. Vickers Hardness is a measure of the hardness of a

CC-0. In Public Domain. Gurukul Kangri Collection, Haridwar

Digitized by Arya Samaj Foundation Chennai and eGangotri


material, calculated from the size of an impression produced under load by a pyramid shaped diamond indenter as shown in the figure-3. The Vickers number (HV) is calculated using the following formula:

$$HV=1.854\ (P/d^2)$$

Where,

P= the applied load (measured in kg. force)

$d^2$= the area of the indentation

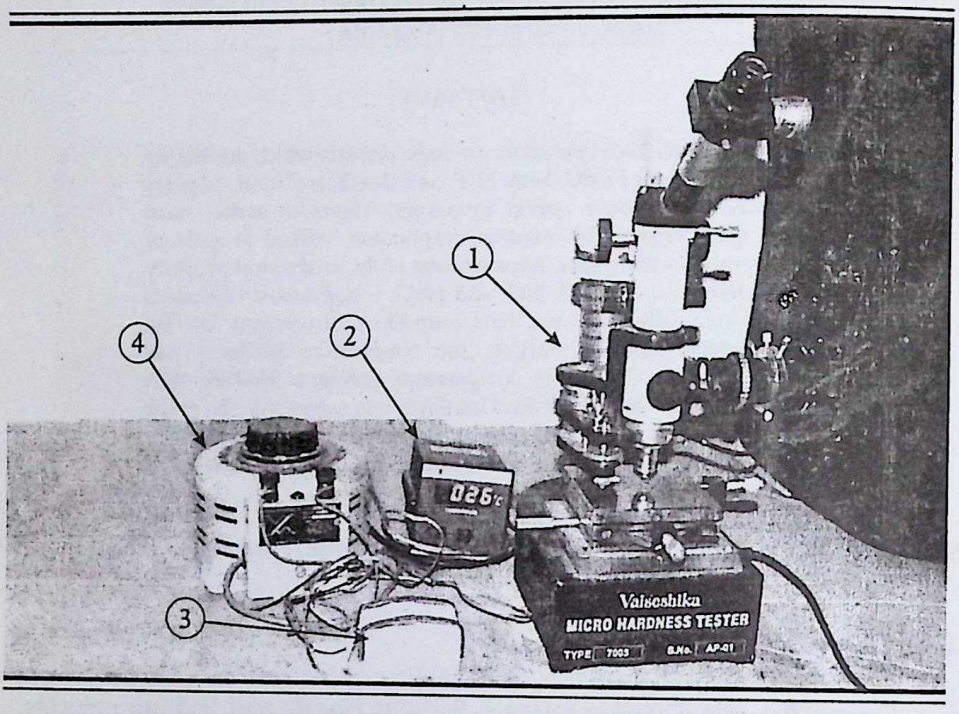


**Figure-1:** Vaiseshika Vickers's micro hardness tester

1. Micro hardness tester
2. Temperature sensor
3. Heating coil
4. Variance

## 2. EXPERIMENTAL PROCEDURE

The author has grown NaF, NaCl and NaCl + NaF crystals by solution evaporation method at ambient temperature. First of all to grow a seed crystal, the basic requirement is to make a saturated solution. In order to grow a crystal, first make a solution which maximizes the chances for the solute particles to come together and form a nucleus, which will grow into our crystal. This means author wants a concentrated solution with as much solute as they can dissolve


CC-0. In Public Domain. Gurukul Kangri Collection, Haridwar

Digitized by Arya Samaj Foundation Chennai and eGangotri

(saturated solution).So they have made the saturated solution of NaCl and NaF in distilled water. Then they gave the heat and also stirred the solution. So they got the super-saturated solution and they have filtered it and filled them in two sets of Petri dishes. For NaCl+NaF mixed crystal, they made a saturated solution of NaCl and NaF in equal quantities then mixed them. Then added some amount of both NaCl and NaF powder in that mixed solution and again gave heat and stirred it. The process continued until the NaCl+ NaF super saturated solution was made. The photographs of these crystals are shown in figure-2(a), figure2(b), figure-2(c).

Fig-2-(a)

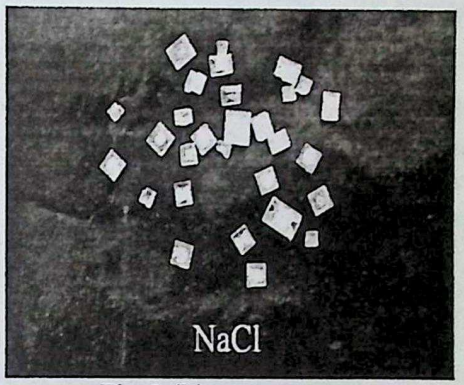


Fig-2-(b)

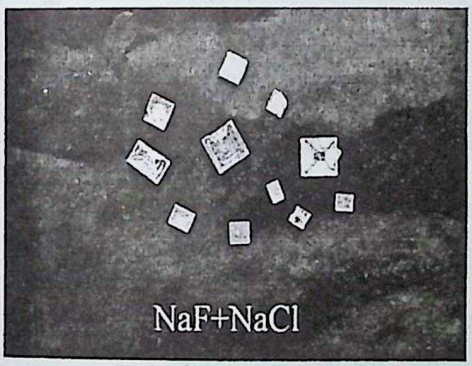


Fig-2-(c)

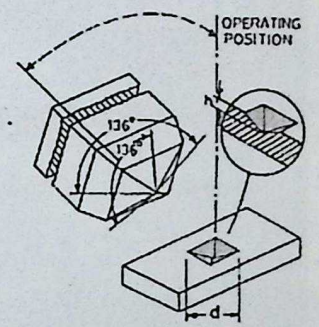


Fig-3

**Figure- 2(a, b, c):** Photograph of the crystals

After growing the crystal, the effect of temperature on the hardness of these crystals was done. For this purpose, the author used heating coil. The line diagram of the coil is 0.5 cm with 6 cm in length. In order to determine the effect of temperature on the micro-hardness of NaF, NaCl and NaF+ NaCl crystals,


CC-0. In Public Domain. Gurukul Kangri Collection, Haridwar

Digitized by Arya Samaj Foundation Chennai and eGangotri


they were carried out at the room temp and 303 K to 353 K at an interval of 5 K by keeping the load of 0.010 kg, loading time of 10 seconds. The important results are discussed in the first three tables and graph of hardness Vs temperature is plotted for all these crystals. Then the effect of different load from 0.010 kg to 0.035 kg at the interval of 0.005 kg by keeping temperature constant and loading time of 10 seconds, was done. The pyramid shape, on grown NaF,NaF+NaCl and NaCl crystal's surface ,shown in Figure-4(a) and Figure-4(b), measured the area of the indentation (d) and calculated hardness by using equation (1).The results are discussed in the tables and a graph of Hardness Vs Load is plotted for all these crystals. The nature of these graphs is also discussed in results.

## 3. RESULTS

The author has grown the crystals successfully. The photographs of Pyramid- shaped diamond on the crystal's surface are shown. The important observation tables for NaF, NaCl and NaF+NaCl are given bellow. The graph of hardness Vs temperature and Hardness Vs Load is plotted for all these crystals, figure 5(a) and figure 5(b)

**Figure-4(a):** the photographs of Pyramid- shaped on grown crystal's surface


CC-0. In Public Domain. Gurukul Kangri Collection, Haridwar

Digitized by Arya Samaj Foundation Chennai and eGangotri

**Figure-4(b):** the photographs of Pyramid- shaped on grown crystal's surface

**Table 1 :** HARDNESS OF NaF Crystal

| Sr. No. | Temperature in K | Width a in mm | Length b in mm | d=(a+b)/2 mm | $d^2$ $mm^2$ | H=(1.854*p)/$d^2$ HV |
|---|---|---|---|---|---|---|
| | | | | | | |
| 1 | 303 | 0.0150 | 0.0188 | 0.0169 | 0.00028 | 64.9136 |
| 2 | 308 | 0.0163 | 0.0181 | 0.0172 | 0.00029 | 62.6690 |
| 3 | 313 | 0.0188 | 0.0200 | 0.0194 | 0.00037 | 49.2613 |
| 4 | 318 | 0.0203 | 0.0193 | 0.0198 | 0.00039 | 47.2910 |
| 5 | 323 | 0.0250 | 0.0213 | 0.0232 | 0.00053 | 34.5945 |
| 6 | 328 | 0.0263 | 0.0250 | 0.0257 | 0.00065 | 28.1796 |
| 7 | 333 | 0.0269 | 0.0275 | 0.0272 | 0.00073 | 25.0594 |

P= Load in kg=0.010kg Constant Time = 10 Sec.


CC-0. In Public Domain. Gurukul Kangri Collection, Haridwar

**Table 2** HARDNESS OF NaCl Crystal
P= Load in kg=0.010kg Constant Time = 10 Sec.

| Sr. No. | Temperature in K | Width a in mm | Length b in mm | d=(a+b)/2 mm | $d^2$ $mm^2$ | $H=(1.854*p)/d^2$ HV |
|---|---|---|---|---|---|---|
| 1 | 303 | 0.0268 | 0.0288 | 0.0278 | 0.00077 | 23.9894 |
| 2 | 308 | 0.0313 | 0.0294 | 0.0303 | 0.00092 | 20.1276 |
| 3 | 313 | 0.0319 | 0.0331 | 0.0325 | 0.00105 | 17.5526 |
| 4 | 318 | 0.0338 | 0.0350 | 0.0344 | 0.00118 | 15.6672 |
| 5 | 323 | 0.0348 | 0.0363 | 0.0355 | 0.00126 | 14.6700 |
| 6 | 328 | 0.0375 | 0.0394 | 0.0384 | 0.00147 | 12.5405 |
| 7 | 333 | 0.0413 | 0.0431 | 0.0422 | 0.00178 | 10.4108 |

**Table 3** HARDNESS OF NaF+NaCl Crystal
P= Load in kg=0.010kg Constant Time = 10 Sec.

| Sr. No. | Temperature in K | Width a in mm | Length b in mm | d=(a+b)/2 mm | $d^2$ $mm^2$ | $H=(1.854*p)/d^2$ HV |
|---|---|---|---|---|---|---|
| 1 | 303 | 0.0431 | 0.0413 | 0.04220 | 0.00178 | 10.4108 |
| 2 | 308 | 0.0450 | 0.0463 | 0.04565 | 0.00208 | 8.89668 |
| 3 | 313 | 0.0483 | 0.0474 | 0.04785 | 0.00228 | 8.09740 |
| 4 | 318 | 0.0469 | 0.0495 | 0.04820 | 0.00232 | 7.98023 |
| 5 | 323 | 0.0513 | 0.0519 | 0.05160 | 0.00266 | 6.96322 |
| 6 | 328 | 0.0506 | 0.0538 | 0.05220 | 0.00272 | 6.80406 |
| 7 | 333 | 0.0520 | 0.0531 | 0.05255 | 0.00276 | 6.71373 |


Digitized by Arya Samaj Foundation Chennai and eGangotri
CC-0. In Public Domain. Gurukul Kangri Collection, Haridwar

Digitized by Arya Samaj Foundation Chennai and eGangotri

# STUDY OF HARDNESS OF NaF, NaCl & NaF+NaCl CRYSTALS GROWN BY SOLUTION EVAPORATION METHOD AT AMBIENT TEMPERATURE.

**Table 4** HARDNESS OF NaF Crystal
Temperature = Room Temperature Time = 10 Sec.

| Sr. No. | Load in kg | Width a in mm | Length b in mm | d=(a+b)/2 mm | $d^2$ $mm^2$ | $H=(1.854*p)/d^2$ HV |
|---|---|---|---|---|---|---|
| 1 | 0.010 | 0.0181 | 0.0163 | 0.0172 | 0.00029 | 62.6690 |
| 2 | 0.015 | 0.0194 | 0.0206 | 0.0200 | 0.00040 | 69.5250 |
| 3 | 0.020 | 0.0224 | 0.0234 | 0.0229 | 0.00052 | 70.7080 |
| 4 | 0.025 | 0.0244 | 0.0258 | 0.0251 | 0.00063 | 73.5702 |
| 5 | 0.030 | 0.0258 | 0.0268 | 0.0263 | 0.00069 | 80.4117 |
| 6 | 0.035 | 0.0281 | 0.0280 | 0.0280 | 0.00078 | 82.4730 |

**Table 5** HARDNESS OF NaCl Crystal
Temperature = Room Temperature Time = 10 Sec.

| Sr. No. | Load in kg | Width a in mm | Length b in mm | d=(a+b)/2 mm | $d^2$ $mm^2$ | $H=(1.854*p)/d^2$ HV |
|---|---|---|---|---|---|---|
| 1 | 0.010 | 0.0325 | 0.0363 | 0.0344 | 0.00118 | 15.6672 |
| 2 | 0.015 | 0.0338 | 0.0375 | 0.0356 | 0.00127 | 21.8817 |
| 3 | 0.020 | 0.0413 | 0.0406 | 0.0409 | 0.00167 | 22.1121 |
| 4 | 0.025 | 0.0425 | 0.0431 | 0.0428 | 0.00183 | 25.3024 |
| 5 | 0.030 | 0.0434 | 0.0444 | 0.0439 | 0.00192 | 28.8603 |
| 6 | 0.035 | 0.0450 | 0.0457 | 0.0453 | 0.00205 | 31.5517 |


CC-0. In Public Domain. Gurukul Kangri Collection, Haridwar

Digitized by Arya Samaj Foundation Chennai and eGangotri


Table 6 HARDNESS OF NaCl+NaF Crystal
Temperature = Room Temperature Time = 10 Sec.

| Sr. No. | Load in kg | Width a in mm | Length b in mm | d=(a+b)/2 mm | $d^2$ $mm^2$ | $H=(1.854*p)/d^2$ HV |
|---|---|---|---|---|---|---|
| 1 | 0.010 | 0.0500 | 0.0508 | 0.0504 | 0.00254 | 7.2987 |
| 2 | 0.015 | 0.0513 | 0.0525 | 0.0519 | 0.00269 | 10.3244 |
| 3 | 0.020 | 0.0538 | 0.0531 | 0.05345 | 0.00285 | 12.9790 |
| 4 | 0.025 | 0.0569 | 0.0558 | 0.0563 | 0.00317 | 14.5969 |
| 5 | 0.030 | 0.0575 | 0.0573 | 0.0574 | 0.00329 | 16.8813 |
| 6 | 0.035 | 0.0573 | 0.0588 | 0.0580 | 0.00337 | 19.2563 |


CC-0. In Public Domain. Gurukul Kangri Collection, Haridwar

Digitized by Arya Samaj Foundation Chennai and eGangotri

# STUDY OF HARDNESS OF NaF, NaCl & NaF+NaCl CRYSTALS GROWN BY SOLUTION EVAPORATION METHOD AT AMBIENT TEMPERATURE.

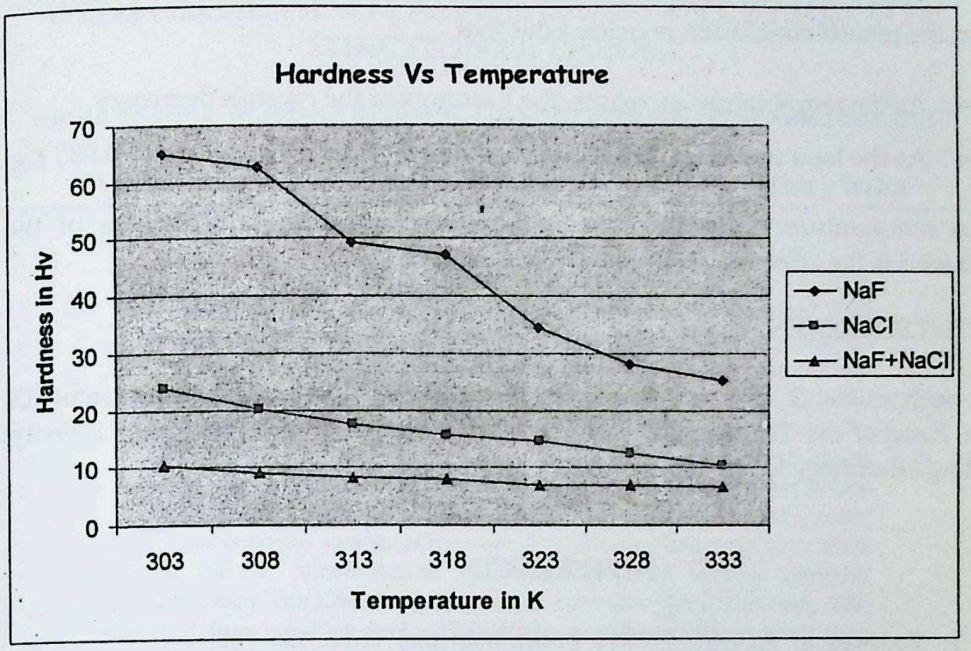


**Figure-5(a):** A graph of Hardness Vs Temperature

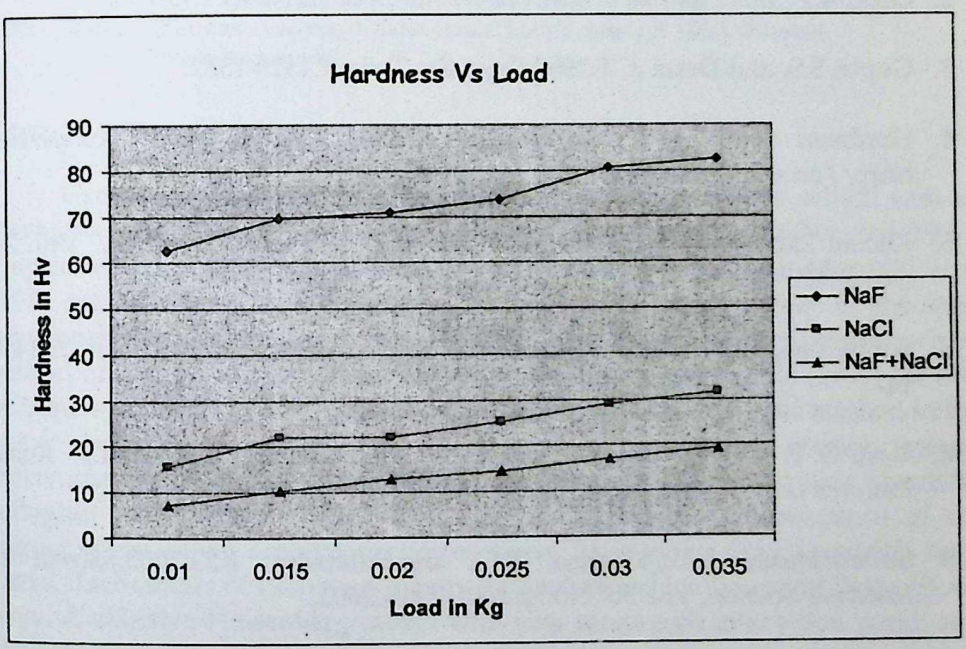


**Figure-5(b):** A graph of Hardness Vs Load


CC-0. In Public Domain. Gurukul Kangri Collection, Haridwar

Digitized by Arya Samaj Foundation Chennai and eGangotri


## 4. CONCLUSITION

From the results conclusion is carried out that

- As the temperature increases, the hardness of the crystals decreases.
- As the load increases, the hardness of the crystals increases up to 0.035 Kg.

Thus temperature is the effective parameter of growth and hardness of the crystal and load is the effective parameter of hardness of the crystal

## 5. ACKNOWLEDGEMENT

The authors thank to Dr. I.B.Patel for his guidance and his encouragement, Dr K.C. Poria, Head of the department of Physics, Veer Narmed South Gujarat University, for providing laboratory facilities.

## REFERENCES

1. Brookes, C. A. 1975. *J. Phys. E: Sci. Instrum.*, Vol.8: 456-460.
2. Gerk, A.P. 1977. *Journal of Material Science* .,Vol 12(No.4): 735-738.
3. Gupte, S.S. and Desai ,C.F.1999.*Cryst.Res.Technol*:1329-1332.
4. Hardness From Wikipedia, the free encyclopedia; http://en.wikipedia.org/wiki/Hardness
5. Kishan Rao,K. and Sirdeshmukh, D B. 1985. *Journal of Pramana.*, Vol. 24 (No.6): 887-893.
6. Subba Rao, U. V. and Hari Babu,V. 1978. *Journal of Pramana.*, Vol. 2: 149-147.
7. Upit, G. P. and Varchenya, S. A. 1966 . *Physica status solidi (RRL) - Rapid Research Letters*.Vol.17( No.2): 831 – 835.
8. Sirdeshmukh, D.B., Krishna, P.G. and Subhadra, K.G.2003.*Journal of Materials Science.*, Vol. 38 (No.9): 2001-2006 ,2003.


CC-0. In Public Domain. Gurukul Kangri Collection, Haridwar

ISSN-0970-6569 Digitized by Arya Samaj Foundation Chennai and eGangotri
*Bulletin of Pure and Applied Sciences.Vol.28D(No.2)2009:P.137-140*

# STUDY OF THE CHANGE OF THE SPIN WAVE SPECTRUM WITH DECREASING LATTICE CONSTANT BY DENSITY FUNCTIONAL THEORY

**Amita Sharma, Maqbool Hussain, Girijesh Sharma*, Bishwambhar Roy** and Veena Kumari*****

Department of Physics, R.D.S. College, Muzaffarpur, (Bihar), India

**ABSTRACT**

We calculated spin wave spectra for different lattice constant. The results for the spin wave spectra along the high symmetry lines in the Brillouin zone were observed for reduced lattice constant (a) and for an extended lattice constant. The spin wave energies increase when the lattice constant decreases. The Kohn anomalies especially around the H point were clearly visible for all considered lattice constants. The spin wave stiffness increases with decreasing lattice constant and there was an indication that the influence of the quartic terms becomes smaller at the same line. All coupling were accounted for in the calculation of spin wave energies because periodic boundary conditions based on the extended Bloch theorem. The exchange parameters of a Heisenberg model were determined also. The computed pressure dependence of critical temperature is also affected.

**Key words :** Spin wave spectra, Brillouin zone, Lattice constant, Bloch theorem, Heisenberg model.

## INTRODUCTION

Grotheer *et al* (2001) determined the spin wave spectra which was an alternative of so called frozen-magnon method introduced by Halilov *et al* (1997). A spiral external field was applied for a monoatomic unit cell. Muruzzi, *et al* (1978) calculated magnon frequency by density functional theory in the local spin-density approximation in the paramagnetisation and by recently develped method of Liebs and Hummler (1995) and Grotheer and Fahnle (1999) for non collinear spin systems of the tight binding linear muffin-tin orbital method in the atomic sphere approximation. We have also applied atomic sphere approximation of Kubler, *et al* (1988) to the structure and to the spin direction. Gallagher and Willard (1999) explained the temperature dependence of the magnetisation of an amorphous ferromagnet by a mean field approach with spatial fluctuations of exchange parameter *J* estimated by the use of Bethe-Slater curve. A effective Heisenberg model with long range pair interaction parameter *Jij* is proposed

* Department of Physics, C.N. College, Sahebgang, Bihar, INDIA.
** Department of Physics, R.N.A.M. College, Samastipur, Bihar, INDIA.
*** Department of Chemistry, Samta College, Jandaha, Vaishali, Bihar, INDIA.

CC-0. In Public Domain. Gurukul Kangri Collection, Haridwar

Digitized by Arya Samaj Foundation Chennai and eGangotri


$$H = -\frac{1}{2}\sum_{\substack{ij \\ i \neq j}} J_{ij}\underline{e_i}\underline{e_j}$$

where $e_i$ and $e_j$ are the unit vectors in direction of local magnetic moments at sites (i,j). Then we obtain related modifications of $J_{ij}$ and predictions of the mean field theory and random phase approximation for the pressure dependence of critical temperature. The calculations were made by density functional theory in the local spin density approximation.

## RESULTS AND DISCUSSION

### Graphs

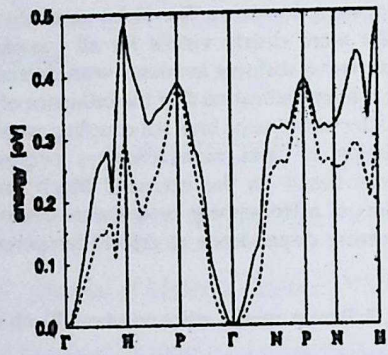


**Graph-1 : The Calculated spin-wave spectra along high-symmetry directions of the Brillouin zone.**

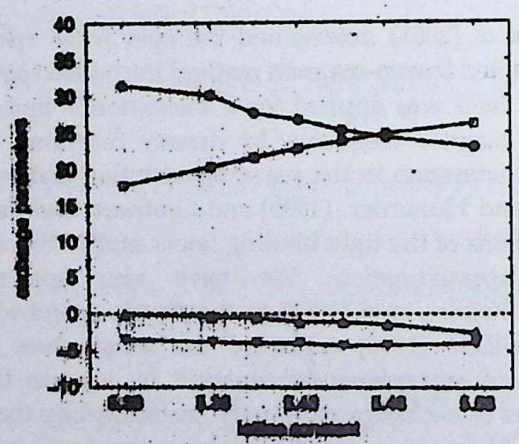


**Graph- 2 : The exchange parameters $J_1$ (in meV) for the four closest near-neighbour pairs as function of the lattice constant a.**


CC-0. In Public Domain. Gurukul Kangri Collection, Haridwar

Digitized by Arya Samaj Foundation Chennai and eGangotri

## STUDY OF THE CHANGE OF THE SPIN WAVE SPECTRUM WITH DECREASING LATTICE CONSTANT BY DENSITY FUNCTIONAL THEORY

The spin wave spectra were calculated for the lattice constant $a_1=5.53a_0$, $a_2=5.48a_0$, $a_3=5.45a_0$, $a_4=5.43a_0$, $a_5=5.405a_0$, $a_6=5.38a_0$, and $a_7=5.33a_0$, $a_0$ is the Bohr's radius. The spin wave spectra along the high symmetry lines in the Brillouin zone are shown in Graph (1), for a reduced lattice constant $a_1$ and for an extended lattice constant $a_7$. Graph (1) shows that the spin wave energies increase when the lattice constant decrease. We also determined real space couplings. We have represented the exchange parameters related to the real space coupling for the four closest near neighbour pairs, because they are numerically stable with respect to the details of the inversion. Our method is able to determine explicity only a limited number of real space couplings, all couplings are accounted for in the calculation of the spin wave energies. Graph (2) shows the exchange parameters for the four closest near neighbour pairs as a function of lattice constant a. The parameter $J_1 > 0$ for the nearest-neighbour pair is the largest for small lattice constant and decreases monotonically with increasing lattice constant. The next nearest-neighbour parameter $J_2 > 0$ increases with increasing lattice constant and exceeds $J_1$ for large lattice constant. In this study one single atom is displaced toward or away from one of the nearest neighbour atoms or toward or away from one of the next-nearest neighbour atoms, whereas the position of all the other atoms are fixed. In that situation both $J_1$ and $J_2$ decrease monotonically with increasing interatomic distance.

## CONCLUSION

We calculated spin wave spectra for various lattice constant using density functional electron theory and exchange parameters. For the explanation of exchange parameter behaviour the Bethe-Slater curve was used. It was also observed that spin wave energies increase with decreasing lattice constants.

## REFERENCES

1. Gallagher, K.A., and Willard,M.A. 1999. *J. Appl. Phys.* 85: 5130.

2. Grotheer, O., Ederer ,C. and Fahnle,M. 2001, *Phys. Rev.* B, 63: 100401.

3. Grotheer,O. and Fahnle,M. 1999, *Phys. Rev.* B, 59:13965.

4. Halilov,S.V., Perlov, A.Y., Oppeneer,P.M. and Eschring, H.1997. *Euro Phys. Lett.* 39: 91.


CC-0. In Public Domain. Gurukul Kangri Collection, Haridwar

Digitized by Arya Samaj Foundation Chennai and eGangotri


5. Kubler, J., Hock, K.H., Sticht,J. and Williams,A.R. 1988. *J. Phys. F. Met. Phys.* 18: 469.

6. Liebs,M. and Hummler,K. 1995, *Phys. Rev.* B, 51: 8664.

7. Muruzzi,V.L., Janak,J.F. and Williams,A.R. 1978. Calculated Electron properties of metals, Pergamon, Press Oxford.


CC-0. In Public Domain. Gurukul Kangri Collection, Haridwar

Digitized by Arya Samaj Foundation Chennai and eGangotri

2010

# Bulletin of Pure and Applied Sciences

115-RPS- D.D.A.Flat, Mansarover Park, Post Box No.9043, Shahdara, Delhi-110032 (India)
(ajaykumarsharma1955@yahoo.com,ajay_shrm@yahoo.com,editorbulletin@yahoo.co.in
,subscriptionbulletin@yahoo.com,draksharma2009@hotmail.com),*www.bpas.in* ; Phone:(011) 22138726

**Ref. No. : Bull/Subs/2010/** **Dated :**

**Dear Sir/Madam,**

We are herewith submitting the annual subscription bills in duplicate for **"January to December" 2010** as under and request you, kindly arrange an early payment by **Bank Demand Draft** drawn in favour of ***BPAS RESEARCH*** payable at ***Delhi***, send to us alongwith a copy of the bill & oblige.

| S.No. | Name of the Journal & its annual subscription rates | Volume | Amount |
|---|---|---|---|
| 1. | **Bulletin of Pure and Applied Science Sec.A-Zoology ISSN-0970-0765** *(Rs. 1000 US $ 60 U.K. £ 30)* | 29A | |
| 2. | **Bulletin of Pure and Applied Sciences Sec. B – Botany ISSN-0970-4612** *(Rs. 1000 US $ 60 U.K. £ 30)* | 29B | |
| 3. | **Bulletin of Pure and Applied Sciences Sec. C – Chemistry ISSN-0970-4620** *(Rs. 1000 US $ 60 U.K. £ 30)* | 29C | |
| 4. | **Bulletin of Pure and Applied Sciences Sec. D – Physics ISSN-0970-6569** *(Rs. 1000 US $ 60 U.K. £ 30)* | 29D | |
| 5. | **Bulletin of Pure and Applied Sciences Sec. E – Math & Stat. ISSN-0970-6577** *(Rs. 1000 US $ 60 U.K. £ 30)* | 29E | |
| 6. | **Bulletin of Pure and Applied Sciences Sec. F – Geology ISSN-0970-4639** *(Rs. 1000 US $ 60 U.K. £ 30)* | 29F | |
| 7. | **Bio-Science Research Bulletin (Micro-biology & Bio-tech.)ISSN-0970-0889** *(Rs. 1000 US $ 60 U.K. £ 30)* | 26 | |
| 8. | **Library Progress (International) (For Library,Information & Computer Sc.) ISSN-0970-1052** *(Rs. 1000 US $ 60 U.K. £ 30)* | 30 | |
| | **Total** | | **Rs.** |

Central Library
Gurukul Kangri University
Haridwar-249404 (U.A.)

CC-0. In Public Domain. Gurukul Kangri Collection, Haridwar

**Managing Editor**

Digitized by Arya Samaj Foundation Chennai and eGangotri

**Managing Editor,**
**BPAS RESEARCH**
Bulletin of Pure & Applied Sciences
115-RPS- DDA Flat, M.S.Park, Post Box-9043
Shahdara,Delhi-110032, India

**SUBJECT:-** Annual Subscription request for January-December 2010

**Dear Sir/Madam**

With reference to your valuable Research Journals, we invite your kind attention on the following ticked (√) Journals,

(A) Please arrange bill in duplicate /triplicate towards the annual subscription for the following ticked (√) Research Journals for January – December 2010 ( complete volume). *(www.bpas.in)*

| S.No. | Name of the Journal | Volume | No. of Copies | Annual Subscription |
|---|---|---|---|---|
| 1. | Bulletin of Pure and Applied Sciences *Section-A-Zoology ISSN 09 70-0765* | 29 A | 1 | Rs.1000 /US$60/UK£30 |
| 2. | Bulletin of Pure and Applied Sciences *Section-A-Botany ISSN09 70-4612* | 29 B | 1 | Rs.1000 /US$60/UK£30 |
| 3. | Bulletin of Pure and Applied Sciences *Section-C-Chemistry ISSN 09 70-4620* | 29 C | 1 | Rs.1000 /US$60/UK£30 |
| 4. | Bulletin of Pure and Applied Sciences *Section-D-Physics ISSN 09 70-6569* | 29D | 1 | Rs.1000 /US$60/UK£30 |
| 5. | Bulletin of Pure and Applied nces *Section-E-Math. & Stat. ISSN 09 70-6577* | 29 E | 1 | Rs.1000 /US$60/UK£30 |
| 6. | Bulletin of Pure and Applied Sciences *Section-F-Geology ISSN 09 70-4639* | 29 F | 1 | Rs.1000 /US$60/UK£30 |
| 7. | Bio-Science Research Bulletin *(Microbiology & Bio-technology) ISSN-0970-0889* | 26 | 1 | Rs.1000 /US$60/UK£30 |
| 8. | Library Progress(International) *(Library,Information & Computer Applications) ISSN-0970-1052* | 30 | 1 | Rs.1000 /US$60/UK£30 |

(B)We are herewith enclosing a Bank Demand Draft of (name of the Bank).....
No.....dated.....for an amount of Rs.....drawn infavour of ***"BPAS RESEARCH "*** payable at **"Delhi"** towards the annual subscription of the above ticked (√) Journals. Please send the Journals at the following address, when published :

.....
.....
.....
Postal Pin code.....Telephone.....Mobile.....

(Limited back volumes are available at the same rates)

**(Seal & Sign. of the Head of Institute)**

CC-0. In Public Domain. Gurukul Kangri Collection, Haridwar

Digitized by Arya Samaj Foundation Chennai and eGangotri

CC-0. In Public Domain. Gurukul Kangri Collection, Haridwar

Digitized by Arya Samaj Foundation Chennai and eGangotri

Entered in Database
Signature with Date

CC-0. In Public Domain. Gurukul Kangri Collection, Haridwar

Digitized by Arya Samaj Foundation Chennai and eGangotri

CC-0. In Public Domain. Gurukul Kangri Collection, Haridwar